# Juno Telecommunications

*Ryan Mukai, David Hansen, Anthony Mittskus, Jim Taylor, Monika Danos, and Andrew Kwok*

*August 2017*

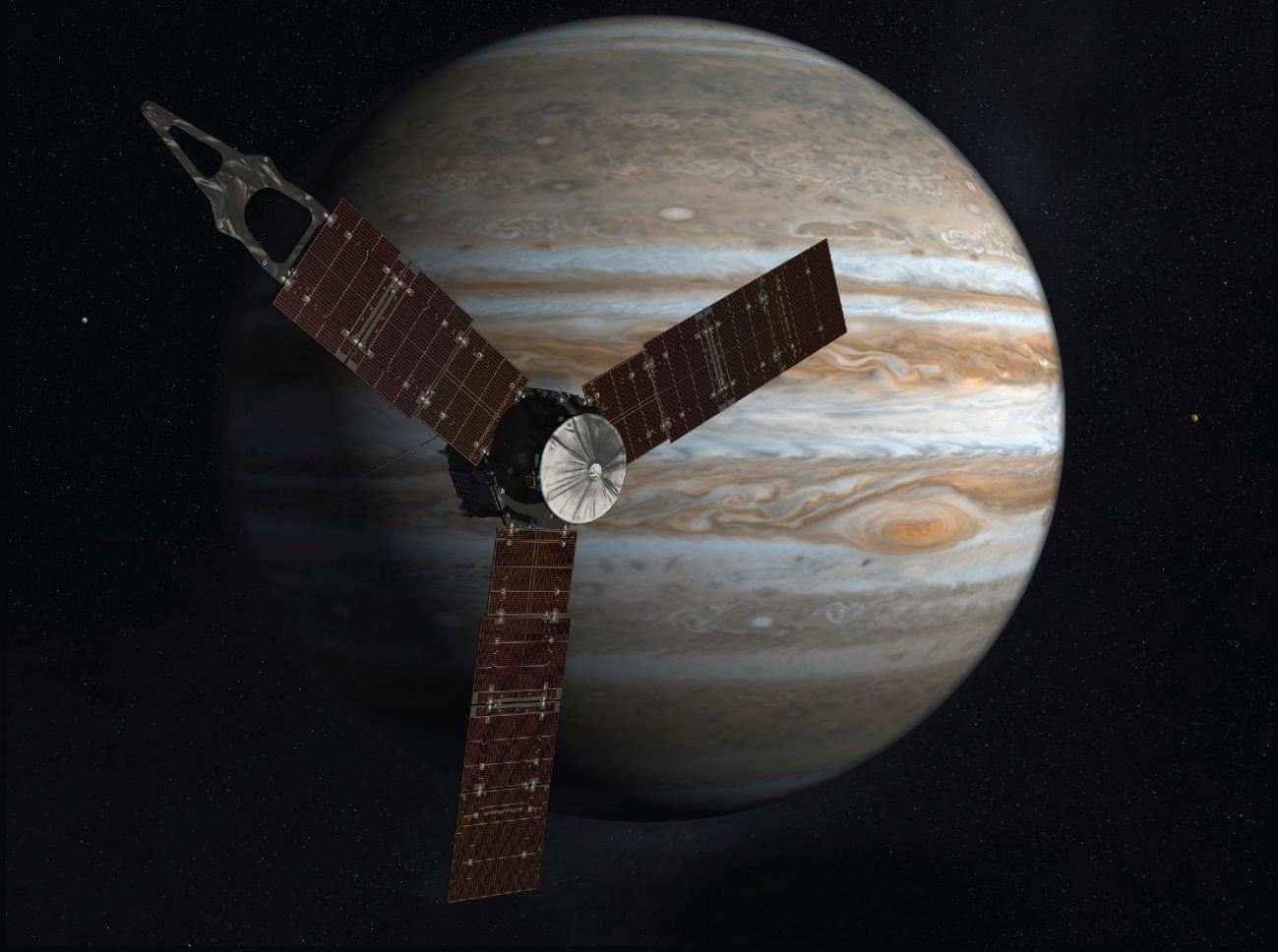

**Revision A: Addition of Operations from Early Cruise through First Months of Operation, Five Science Orbits (September 2012 – May 2017)**

**Jet Propulsion Laboratory**
California Institute of Technology

DESCANSO
Deep Space Communications and Navigation Systems Center of Excellence
**Design and Performance Summary Series**

## The Cover

The cover is an artist's conception of Juno in orbit around Jupiter.[1] The photovoltaic panels are extended and pointed within a few degrees of the Sun while the high-gain antenna is pointed at the Earth.

[1] The picture is titled Juno Mission to Jupiter. See http://www.jpl.nasa.gov/spaceimages/details.php?id=PIA13087 for the cover art and an accompanying mission overview.

## DESCANSO Design and Performance Summary Series

## Article 16

# Juno Telecommunications

## Revision A: Addition of Operations from Early Cruise through First Months of Operation, Five Science Orbits (Sept. 2012–May 2017)


***Ryan Mukai***
***David Hansen***
***Anthony Mittskus***
***Jim Taylor***
***Monika Danos***
***Andrew Kwok***

***Jet Propulsion Laboratory***
***California Institute of Technology***
***Pasadena, California***



**National Aeronautics and**
**Space Administration**
**Jet Propulsion Laboratory**
**California Institute of Technology**
**Pasadena, California**

August 2017

This research was carried out at the Jet Propulsion Laboratory, California Institute of Technology, under a contract with the National Aeronautics and Space Administration.

Reference herein to any specific commercial product, process, or service by trade name, trademark, manufacturer, or otherwise, does not constitute or imply endorsement by the United States Government or the Jet Propulsion Laboratory, California Institute of Technology.

Copyright 2017 California Institute of Technology. Government sponsorship acknowledged.

# DESCANSO DESIGN AND PERFORMANCE SUMMARY SERIES

Issued by the Deep Space Communications and Navigation Systems
Center of Excellence
Jet Propulsion Laboratory
California Institute of Technology

Jon Hamkins, Editor-in-Chief

## Published Articles in This Series

***Article 1*—"Mars Global Surveyor Telecommunications"**
Jim Taylor, Kar-Ming Cheung, and Chao-Jen Wong

***Article 2*—"Deep Space 1 Telecommunications"**
Jim Taylor, Michela Muñoz Fernández, Ana I. Bolea Alamañac, and Kar-Ming Cheung

***Article 3*—"Cassini Orbiter/Huygens Probe Telecommunications"**
Jim Taylor, Laura Sakamoto, and Chao-Jen Wong

***Article 4*—"Voyager Telecommunications"**
Roger Ludwig and Jim Taylor

***Article 5*—"Galileo Telecommunications"**
Jim Taylor, Kar-Ming Cheung, and Dongae Seo

***Article 6*—"Odyssey Telecommunications"**
Andre Makovsky, Andrea Barbieri, and Ramona Tung

***Article 7*—"Deep Space 1 Navigation: Extended Missions"**
Brian Kennedy, Shyam Bhaskaran, J. Edmund Riedel, and Mike Wang

***Article 8*—"Deep Space 1 Navigation: Primary Mission"**
Brian Kennedy, J. Edmund Riedel, Shyam Bhaskaran, Shailen Desai, Don Han, Tim McElrath, George Null, Mark Ryne, Steve Synnott, Mike Wang, and Robert Werner

***Article 9*—"Deep Impact Flyby and Impactor Telecommunications"**
Jim Taylor and David Hansen

***Article 10*—"Mars Exploration Rover Telecommunications"**
Jim Taylor, Andre Makovsky, Andrea Barbieri, Ramona Tung,
Polly Estabrook, and A. Gail Thomas

***Article 11*—" Mars Exploration Rover Navigation"**
Louis A. D'Amario

***Article 12* —"Mars Reconnaissance Orbiter Telecommunications"**
Jim Taylor, Dennis K. Lee, and Shervin Shambayati

***Article 13* —"Dawn Telecommunications"**
Jim Taylor

***Article 14* —"Mars Science Laboratory Telecommunications Systems Design"**
Andre Makovsky, Peter Ilott, and Jim Taylor

***Article 15* —"Phoenix Telecommunications"**
Jim Taylor , Stan Butman, Chad Edwards, Peter Ilott, Richard Kornfeld, Dennis Lee, Scott Shaffer, and Gina Signori

***Article 16* —"Juno Telecommunications**
**"**Ryan Mukai, David Hansen, Anthony Mittskus, Jim Taylor, Monika Danos, and Andrew Kwok
Revision A: Addition of Operations from Early Cruise through First Months of Operation, Five Science Orbits (Sept. 2012–May 2017)

# Foreword

This Design and Performance Summary Series, issued by the Deep Space Communications and Navigation Systems Center of Excellence (DESCANSO), is a companion series to the DESCANSO Monograph Series. Authored by experienced scientists and engineers who participated in and contributed to deep-space missions, each article in this series summarizes the design and performance of major systems, such as communications and navigation, for each mission. In addition, the series illustrates the progression of system design from mission to mission. Lastly, the series collectively provides readers with a broad overview of the mission systems described.

Jon Hamkins

DESCANSO Leader

**Blank**

# Preface

Launched from Earth in 2011, the Juno spacecraft arrived at Jupiter in 2016 to study the giant planet from an elliptical, polar orbit. Juno will repeatedly dive between the planet and its intense belts of charged particle radiation, coming only 5,000 kilometers (about 3,000 miles) from the cloud tops at closest approach.

Juno’s primary goal is to improve our understanding of Jupiter’s formation and evolution. The spacecraft will spend a year investigating the planet's origins, interior structure, deep atmosphere and magnetosphere. Juno’s study of Jupiter will help us to understand the history of our own solar system and provide new insight into how planetary systems form and develop in our galaxy and beyond.

The original issue of this document was current as of September 14, 2012 and carried a publication date of October 2012. At that time, the Juno spacecraft had completed both parts of the Deep Space Maneuver. However, it was still in transit to Jupiter and had performed no Jupiter science observations.

This Revision A is current as of June 1, 2017. As of that date, Juno had completed Jupiter orbit insertion and the first five science orbits of Jupiter. New sections 6–8 make up this 2017 update.

**Blank**

# Acknowledgements

This article is a compilation of data from many sources. Much of the telecom information in this article was directly obtained from the *Juno Mission Plan* [1], the *Juno Project Telecommunications Design Control Docume*nt [2], the *Juno Ka-Band Translator (KaTS) User Manual* [3], the *DSN Telecommunications Link Design Handbook*, 810-005 [4], the *Juno Project Navigation Plan* [5], the *Dawn Telecommunications* article in the DESCANSO series [6], the *Deep Space Network* (DSN) web site [7], the *DSN-Juno Operations Interface Control Document* (OICD) [8], the Juno Launch and Early Orbit Phase (LEOP) Implementing Agreement [9], and the *Small Deep Space Transponder (SDST) Functional Specification and Interface Control Document* [10].

Susan Kurtik, Padma Varanasi, and Wolfgang Heil are the authors of Ref. [9], and large amounts of this document were incorporated into Section 4 directly. Moreover, the Juno OICD is the product of the hard work of many individuals, and we gratefully acknowledge Susan Kurtik and Padma Varanasi again for their efforts here as OICD material has been incorporated into this document as well. Stuart Stephens is the author of Ref. [1], and we have also incorporated a great deal of his material, especially in Section 5 but also in other important parts of this article. We have also used material supplied by Matt Johnson, including his Cruise phase Baseline Reference Mission (BRM) spreadsheet, in the process of writing this article, and his help, knowledge, and materials are gratefully acknowledged. We thank Entry, Descent, and Landing (EDL) Data Analysis (EDA) tones detection engineer Melissa Soriano for her review and for her feedback on this article.

For the 2017 Revision A, the authors appreciate the mission plan and science plan updates provided by Stuart Stephens and Andy Kwok, the Juno lessons learned provided by David Oberhettinger, and a video from Juno flybys provided by the Juno principal investigator Dr. Scott Bolton.

**Blank**

# Table of Contents

**Foreword** ..... **vii**
**Preface** ..... **ix**
**Acknowledgements** ..... **xi**
**1 Mission Phases and Orbit Summary** ..... **1**
1.1 Mission Overview ..... 1
1.2 The Juno Spacecraft ..... 2
1.3 Mission Phases ..... 5
1.3.1 Launch Phase ..... 5
1.3.2 Cruise Phase ..... 6
1.3.3 JOI and PRM Phase ..... 11
1.3.4 Orbital Phase ..... 11
**2 Telecommunications Subsystem Overview** ..... **15**
2.1 X-Band ..... 15
2.1.1 Interfaces ..... 19
2.1.2 Small Deep Space Transponder (SDST) ..... 20
2.1.3 Traveling Wave Tube Amplifier ..... 22
2.1.4 Antennas ..... 23
*2.1.4.1 High-Gain Antenna (HGA)* ..... *23*
*2.1.4.2 Toroidal Low-Gain Antenna (TLGA)* ..... *27*
*2.1.4.3 Medium-Gain Antenna (MGA)* ..... *30*
*2.1.4.4 Forward Low-Gain Antenna and Aft Low-Gain Antenna* ..... *32*
2.1.5 Waveguide Transfer Switch ..... 35
2.1.6 X-Band Diplexer ..... 36
2.2 Ka-Band Radio Science ..... 37
2.2.1 Ka-Band Translator – KaTS ..... 37
2.3 Subsystem Power and Mass Estimates ..... 41
**3 Link Performance** ..... **43**
3.1 Summary of Link Performance ..... 43
3.2 Detailed Link Performance ..... 45
3.2.1 Link Performance Assumptions ..... 45
*3.2.1.1 Pointing Errors Assumptions* ..... *48*
*3.2.1.2 Downlink Performance Assumptions* ..... *48*
*3.2.1.3 Uplink Performance Assumptions* ..... *48*
*3.2.1.4 Ranging Performance Assumptions* ..... *48*
*3.2.1.5 Differential One-way Ranging* ..... *49*
3.2.2 Ka-Band Assumptions ..... 49
3.2.3 Link Analysis ..... 49
*3.2.3.1 Cruise Phase* ..... *49*
*3.2.3.2 Orbital Phase* ..... *56*
*3.2.3.3 Telecom during Main Engine Burns* ..... *64*
*3.2.3.4 Safe Mode* ..... *65*
**4 Ground Systems** ..... **69**
4.1 Deep Space Network ..... 69

4.2 Initial Acquisition Support from the European Space Agency .....70
**5 Gravity Science Operations ..... 77**
5.1 Gravity Science Overview.....77
5.2 Science Orbits .....78
**6 Mission and Science Plans for a 53-day Orbit Period ..... 87**
6.1 Entry into Safe Mode Just Prior to Second Jupiter Flyby .....87
6.2 Third Jupiter Flyby: Weighing a Decision to Remain in 53-day Orbit.....87
6.3 "Juno to Remain in Current Orbit at Jupiter" .....88
**7 Mission and Science Activities ..... 93**
7.1 Science Objectives and Plan Overview .....93
7.2 Overview of Science Activities (as of May 2017).....93
7.3 Earth Flyby (Oct. 9, 2013).....94
7.4 Pre-JOI Trajectory Correction Maneuvers (Feb. 3, 2016 – May 31, 2016) .....95
7.5 Juno's Entry into Jupiter's Magnetic Field (June 25, 2016) .....95
7.6 Jupiter Orbit Insertion (July 5, 2016 Universal Time) .....96
7.7 Instrument Turn-On (July 6 – 31, 2016) .....97
7.8 First Jupiter Flybys (Aug. 27, 2016 – May 19, 2017).....97
7.9 JunoCam Images .....98
7.10 Early Science Results (from Data-Collection Pass Aug. 27, 2016) .....100
**8 Lessons Learned ..... 105**
**9 References ..... 107**
**10 Abbreviations and Acronyms ..... 111**

# List of Figures

Figure 1-1: Juno science instruments..... 3
Figure 1-2: Juno spacecraft..... 4
Figure 1-3: Juno spacecraft coordinate system. ..... 4
Figure 1-4: Juno launch ground track for 8/5/11 launch..... 7
Figure 1-5: Juno ground station coverage following launch on 8/5/11 launch. ..... 7
Figure 1-6: Spacecraft range from Earth vs. time after launch..... 8
Figure 1-7: SEP and SPE angle vs. time. ..... 9
Figure 1-8: Planned activities from launch to Jupiter Orbit Insertion. .....10
Figure 1-9 *superseded: Juno during JOI, 107-day capture orbit and orbital operations.....12
Figure 1-10 *superseded: Gravity Science Orbit. .....13
Figure 1-11 *superseded: MWR orbit. .....13
Figure 2-1: Juno telecom components (Radio Frequency Instrument Subsystem, RFIS) mounted in the S/C vault. .....16
Figure 2-2: Juno X-band and Ka-band block diagram. .....18
Figure 2-3: LVDS and 1553B cross-strapping to flight system.....19
Figure 2-4: Juno TWT with electronic power converter.....22
Figure 2-5: Location of antennas on the Juno spacecraft. .....23
Figure 2-6: HGA X-band downlink pattern.....25
Figure 2-7: HGA X-band uplink gain.....25
Figure 2-8: HGA Ka-band downlink gain. .....26
Figure 2-9: HGA Ka-band uplink gain.....26

Figure 2-10: External and internal views of TLGA: (a) side view under dome; (b) biconical horn; (c) bottom and waveguide connector. ....28
Figure 2-11: TLGA transmit gain pattern. ....29
Figure 2-12: TLGA receive gain pattern. ....29
Figure 2-13: Photograph (left) and drawing (right) of the MGA. ....30
Figure 2-14: MGA downlink gain pattern. ....31
Figure 2-15: MGA uplink gain pattern. ....32
Figure 2-16: Forward (left) and Aft (right) LGAs with concept above. ....33
Figure 2-17: LGA downlink gain. ....34
Figure 2-18: LGA uplink gain. ....35
Figure 2-19: Picture of a WTS (quarter provided for scale). ....35
Figure 2-20: Photograph of several MER diplexers. ....36
Figure 2-21: KaTS external view with labeled modules. ....37
Figure 2-22: KaTS architecture block diagram [13]. ....39
Figure 2-23: The KaTS manufacturer's photo. ....40
Figure 2-24: KaTS illustration with modules [3]. ....40
Figure 3-1: Juno predicted downlink performance. ....50
Figure 3-2: Juno predicted uplink performance. ....51
Figure 3-3: Predicted and actual carrier power to noise spectral density ($P_c/N_o$) on July 5, 2012. ....54
Figure 3-4: Predicted and actual data power to noise spectral density ($P_d/N_o$) on July 5, 2012. ....54
Figure 3-5: Predicted and actual symbol SNR on July 5, 2012. ....55
Figure 3-6: Predicted and actual uplink carrier power to noise spectral density ($P_c/N_o$) on July 5, 2012. ....55
Figure 3-7: Predicted Juno Ka-band downlink $P_t/N_o$ during orbit phase. ....64
Figure 3-8: Predicted safe mode downlink $P_t/N_o$ – no attitude change. ....66
Figure 3-9: Predicted safe mode uplink $P_t/N_o$ – no attitude change. ....66
Figure 3-10: Predicted safe mode downlink $P_t/N_o$ – Sun-pointed. ....67
Figure 3-11: Predicted safe mode uplink $P_t/N_o$ – Sun-pointed. ....67
Figure 4-1: The Madrid DSN complex. ....69
Figure 4-2: Juno ground track after separation (launch on August 5, 2011). ....71
Figure 4-3: Juno ground track after separation (launch on August 26, 2011). ....71
Figure 4-4: Elevation at the LEOP stations (launch on August 5, 2011). ....72
Figure 4-5: Elevation at the LEOP stations (launch on August 26, 2011). ....73
Figure 4-6: Slant range from the LEOP stations (launch on August 5, 2011). ....73
Figure 4-7: Slant range from the LEOP stations (Launch on August 26). ....74
Figure 4-8: ESA ESTRACK station block diagram. ....75
Figure 4-9: Key events after separation [9]. ....76
Figure 5-1: The Gravity Science instrument. ....78
Figure 5-2 *Superseded: Juno orbital trajectory. ....79
Figure 5-3 *Superseded : Juno orbital radiation environment. ....80
Figure 5-4 *Representative: Orbital radiation accumulation (vault total dose vs. orbit). ....80
Figure 5-5 *Superseded: Global coverage resulting from a net of perijove science passes. ....81
Figure 5-6 *Representative: Science orbits geometry. ....82
Figure 5-7: Spacecraft attitude during MWR and GRAV perijove passes. ....83
Figure 5-8 *Superseded: Timing of perijove events over DSS-25. ....85
Figure 6-1: Orbital trajectories for 53-day orbits (view from Jupiter's North Pole). ....89
Figure 6-2: Orbital trajectories for 53-day orbits (view from the Sun). ....89
Figure 6-3: Radiation environment for 53-day orbit periods viewed from perpendicular to orbit plane. ....91

Figure 7-1: Waves electric field profile on magnetic field entry. .....96
Figure 7-2: “Jovian Cloud Tops” [34] processed from JunoCam data. .....99
Figure 7-3: Jupiter's South Pole from an altitude of 32,000 miles (51,000 km) [36]. .....101
Figure 7-4: Infrared images and spectra of Jupiter’s thermal emission from the Jovian Infrared Auroral Mapper [39]. .....102
Figure 7-5: “Approaching Jupiter” by "citizen scientist" from JunoCam data [41]. .....103

# List of Tables

Table 1-1: *Superseded: Juno Mission phases. ..... 6
Table 2-1: SDST receive functional specifications. .....21
Table 2-2: SDST 880f1 exciter functional specifications. .....21
Table 2-3: HGA parameters. .....24
Table 2-4: TLGA parameters. .....27
Table 2-5: MGA parameters. .....31
Table 2-6: LGA parameters. .....34
Table 2-7: WTS parameters. .....35
Table 2-8: X-band diplexer parameters. .....36
Table 2-9: KaTS parameters [3]. .....38
Table 2-10: Juno telecommunications power and mass equipment list. .....41
Table 3-1: Uplink thresholds and modulation indices. .....44
Table 3-2: Telemetry modes and thresholds with turnaround ranging on. .....44
Table 3-3: Telemetry modes and thresholds with turnaround ranging off. .....45
Table 3-4 Juno Cruise HGA X-band downlink DCT. .....46
Table 3-5: Juno Cruise HGA X-band uplink DCT. .....52
Table 3-6: Juno X-band downlink DCT at maximum range in 2016. .....57
Table 3-7: Juno X-band uplink DCT at maximum range in 2016. .....59
Table 3-8: Juno HGA Ka-band carrier downlink at maximum range. .....61
Table 3-9: Juno HGA Ka-band carrier uplink at maximum range. .....62
Table 5-1 *Superseded: Trajectory event times (UTC) for reference trajectory. .....84
Table 6-1: Mission dates for 53-day orbit. .....90

# 1 Mission Phases and Orbit Summary

## *1.1 Mission Overview*

The Juno Project has the primary objective of delivering an orbiter with a specific science payload into polar orbit at Jupiter for a nominal duration of one Earth year[2]. Jupiter orbit was achieved on July 5, 2016 UTC (Universal Time Coordinated [Greenwich Mean Time]), and data acquisition has commenced. The incoming data from remote sensing, in situ, and gravity science measurements will help characterize Jupiter's interior, atmosphere, and polar magnetosphere with the primary science goal of understanding Jupiter's origin and evolution. The Juno investigations are studying the present state of Jupiter, not necessarily the time variability of the system, with the exception of the investigation of Jovian dynamics as it applies to understanding Jupiter's atmosphere and polar magnetosphere. The investigations are enabled by observational measurements of the polar region and close perijove vantage points at Jupiter.

The spinning solar-powered spacecraft carries a unique payload consisting of:

1. Microwave Radiometer (MWR) to measure the microwave brightness temperature of Jupiter.
2. Fluxgate Magnetometers (FGMs) to measure the Jovian magnetic field and Advanced Stellar Compass (ASC) to measure the orientation of the magnetometers. The abbreviation (MAG) for magnetometer is used to refer to the complete magnetometer instrument consisting of the ASC and the FGMs.
3. Gravity Science (GRAV), which is part of the Telecom Subsystem as described in Section 2, to perform gravity measurements that enable the mapping of Jupiter's interior structure.
4. Jovian Auroral Distributions Experiment (JADE) to resolve the plasma structure of the Jovian aurora by measuring the angular, energy, and compositional distributions of particles in the polar magnetosphere of Jupiter.[3]
5. Jupiter Energetic-particle Detector Instrument (JEDI) to measure the energy and angular distribution of hydrogen, helium, oxygen, sulfur, and other ions in the polar magnetosphere of Jupiter using the time of flight versus energy technique.
6. Ultraviolet Spectrograph (UVS) to record the wavelength, position, and arrival time of detected ultraviolet photons during the time when the spectrograph slit views Jupiter during each turn of the spacecraft. It provides spectral images of the UV auroral emissions in the polar magnetosphere.
7. The Waves (plasma waves/radio) instrument to use electric and magnetic antennas to identify the regions of auroral currents that define Jovian radio emissions and the acceleration of the auroral particles by measuring the radio and plasma spectra in the auroral region. The name Waves refers to both the Waves investigation and the Waves instrument, and is not an acronym.

---

[2] The planned 1-year duration for the science mission ended July 5, 2017, but the mission continues. See Section 6 for an updated mission plan and duration as of June 1, 2017. See Section 7 for some of the announced (published) science results as of June 1, 2017.

[3] For a fuller description of the instruments *see* Internet Archive, Mission Juno: Juno Spacecraft:Instruments, SwRI, https://readtiger.com/https/web.archive.org/web/20120426062922/http://missionjuno.swri.edu/HTML/junospacecraft_instruments/50. (accessed June 6, 2017)

8. JunoCam to provide visible-light three-color color images to aid education and public outreach. It has already provided the first pictures of Jupiter's poles.[4]
9. Jovian Infrared Auroral Mapper (JIRAM) is an infrared camera that acquires infrared images and spectra to provide atmospheric sounding and observations of the auroral structure and the tropospheric structure.

These instruments are illustrated in Figures 1-1 and 1-2 below.

The observations are obtained through orientation of the spin plane (approximately parallel to the orbit plane) and simple operations (no scan platform or instrument pointing). Gravity science requires that the communication antenna be pointing to Earth, while microwave sounding of the atmosphere requires nadir pointing through the center of Jupiter. These two pointing/spin plane settings (gravity or microwave) will provide for all science measurements as all other experiments utilize ride-along pointing and can work in all orbits.

Primary science observations are obtained within 3 hours of closest approach to Jupiter during each orbit. Calibrations, occasional remote sensing, and magnetospheric science observations are planned throughout the orbits.

## *1.2 The Juno Spacecraft*

The primary systems of the Juno Project consist of a flight system, a launch vehicle, and the terrestrial ground data processing stations. The flight system consists of a spacecraft (S/C) with an integrated instrument package. Figure 1-2 shows a depiction of the spacecraft.

In Figure 1-2, the FLGA, MGA, and HGA are the forward low-gain antenna, the medium-gain antenna, and the high-gain antenna, respectively. The SA is the solar array with its restraint and release mechanisms. The reaction control system (RCS) thrusters for attitude control are installed in reaction engine modules (REMs), each module containing one axial and two lateral engines [11].

Figure 1-3 shows the Juno S/C coordinate system that is used throughout this document. The flight system spins about the +Z axis with a positive rate, in a right-handed sense. In Figure 1-3, the +Z axis is toward the reader, and the high-gain antenna (HGA) is pointing toward the reader.

The Magnetometer (MAG) consists of the FGM and ASC sensors, and it is at the end of Solar Wing 1.

[4] The JunoCam and JIRAM are defined in http://www.lockheedmartin.com/us/products/juno.html.

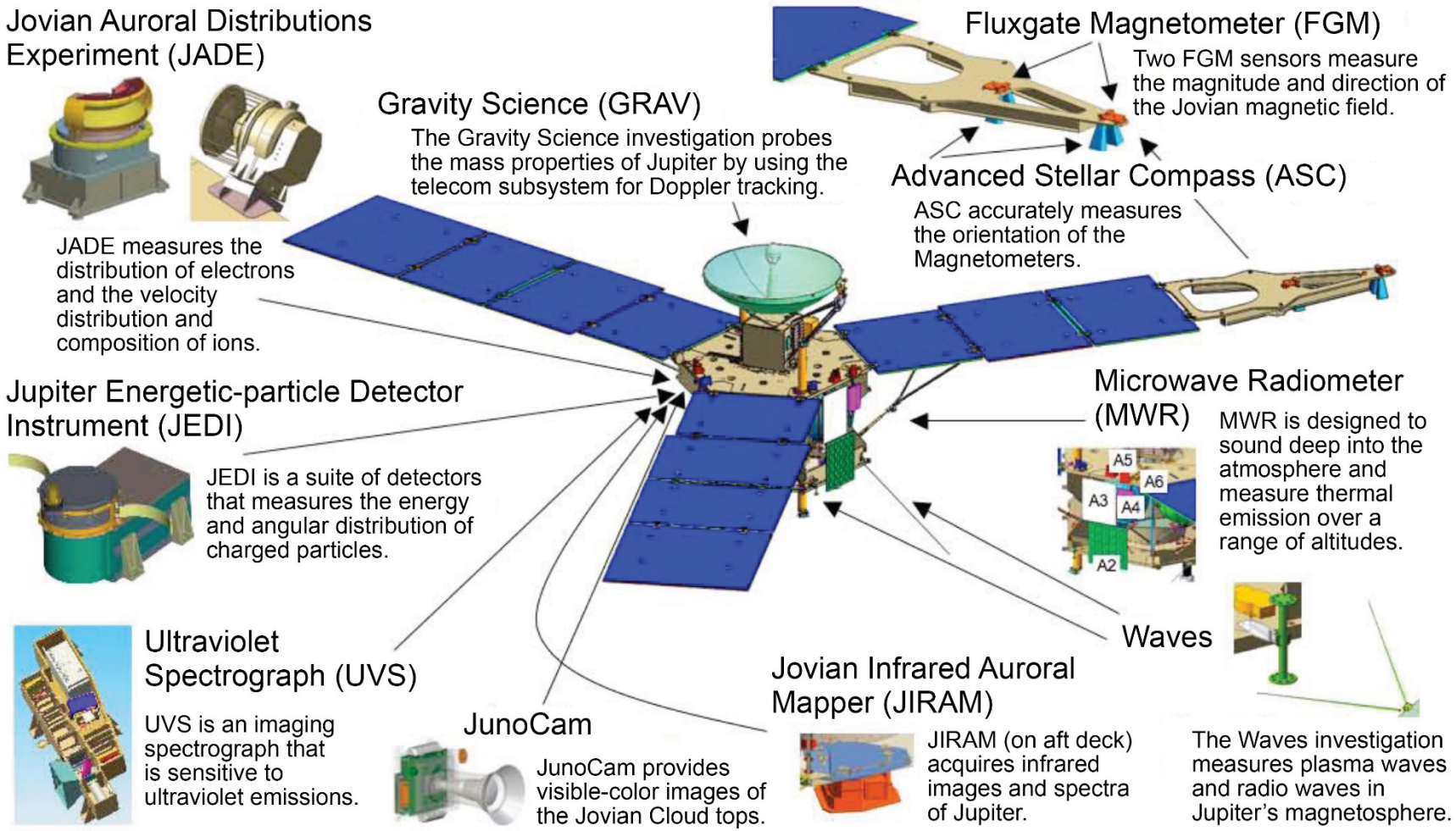


**Figure 1-1: Juno science instruments.**

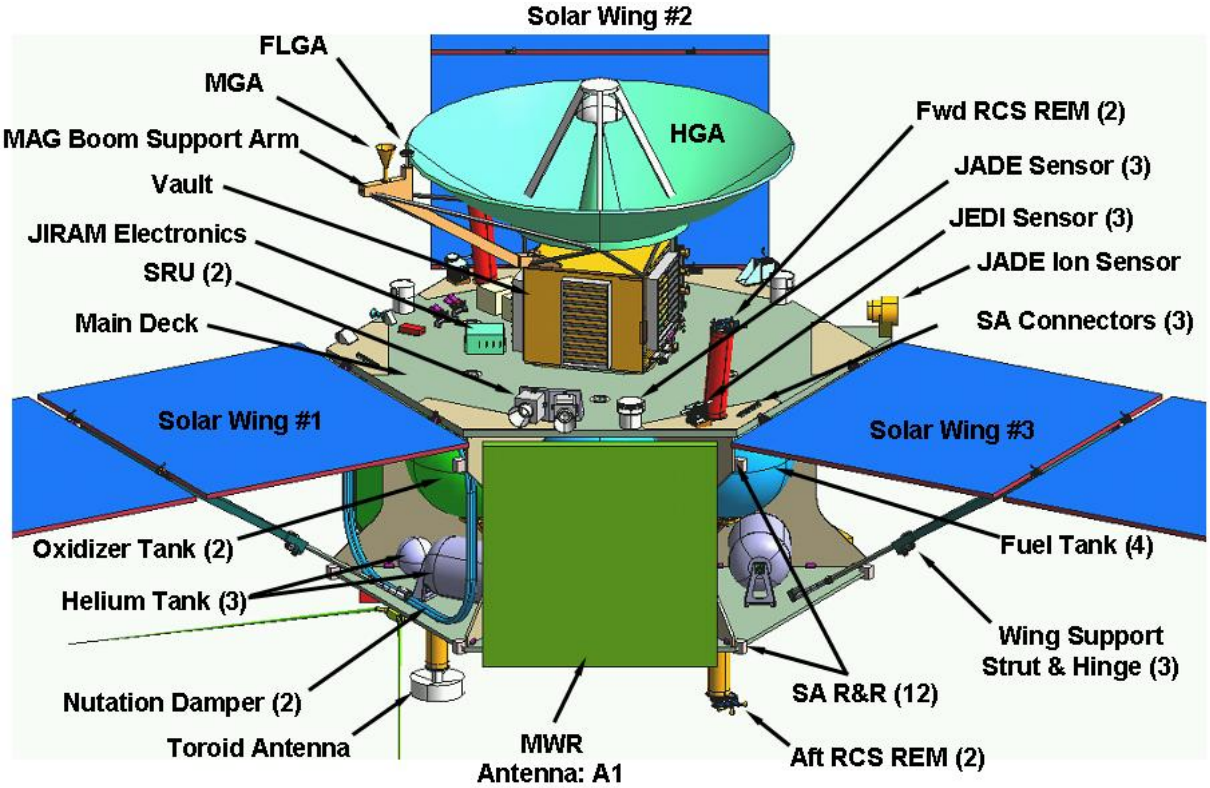


**Figure 1-2: Juno spacecraft.**

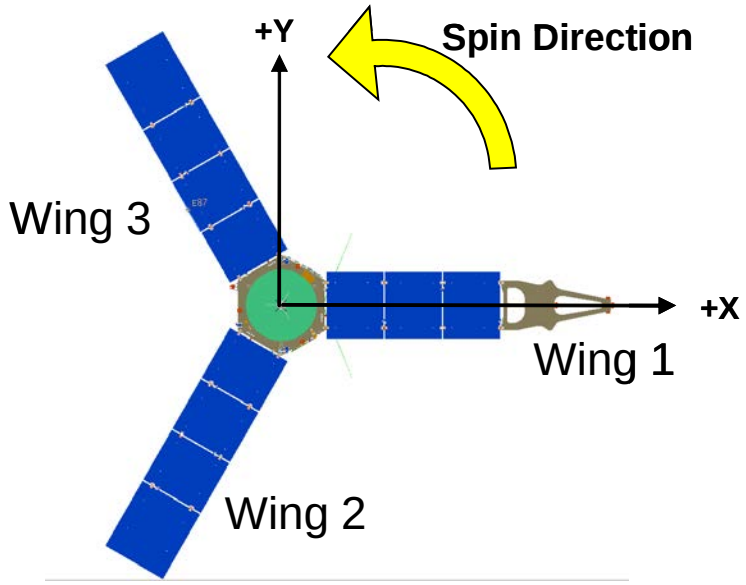


**Figure 1-3: Juno spacecraft coordinate system.**

## 1.3 Mission Phases

### 1.3.1 Launch Phase

The Juno spacecraft was launched on August 5, 2011. The launch vehicle was an Atlas 551. The Launch phase began when the spacecraft transferred to internal power on the launch pad and ended when the spacecraft was declared stable, healthy, and ready to accept commands, and when the launch telemetry had been played back. The major activities in the Launch phase included the liftoff and boost phase of the launch vehicle, insertion into a circular parking orbit, a coast period, followed by additional launch vehicle upper stage burns necessary to inject the spacecraft onto a trajectory away from Earth, separation of the spacecraft from the launch vehicle, initial acquisition by the Deep Space Network (DSN), verification of the initial spacecraft health and operating conditions, and the verified execution of a minimal set of post-launch commands.

Table 1-1 (*) summarizes the phases of the Juno mission[5].

Initial acquisition of the spacecraft used the Perth, Australia (primary) and New Norcia, Australia (backup) European Space Agency (ESA) sites along with the Canberra, Australia DSN site. The use of the ESA stations enabled reception of X-band telemetry from the Juno spacecraft approximately 1.3 minutes earlier than would have been possible using only the Canberra DSN site. This permitted a longer time margin for initial acquisition in order to monitor telemetry during solar array (SA) deployment [9]. The Telecom Subsystem transmitted at X-band shortly after separation through the combined forward and aft low-gain antennas (FLGA and ALGA).

After the launch and initial acquisition phase, Table 1-1 also includes the Cruise phase, the Approach and Jupiter Capture phases, and the Orbit phase described in the next sections. The cruise phase included an Earth Flyby (EFB) in October 2013. The Orbit phase (following JOI) will include an orbit trim maneuver (OTM) after JOI as well as an OTM after the originally planned period reduction maneuver (PRM) and an OTM as part of the third orbit around Jupiter. The orbits are further divided into activity periods (APs) of science and mission operations.

Figure 1-4 shows the ground track of the spacecraft for the August 5, 2011 launch. Figure 1-5 shows initial ground-station coverage for launch on the same day, with "TX ON" showing the time the Canberra transmitter was switched on. In Figure 1-4, CAN, MAD, and GDS refer to the Canberra, Madrid, and Goldstone ground antenna sites, respectively, of the Deep Space Network. MES1 and MES2 indicate main engine start events, and MECO1 and MECO2 indicate main engine cutoff events. Perth refers to both Perth and New Norcia ground sites in Australia.

---

[5] See Section 6, including an update of Table 1-1, for the post-JOI decision to stay in a 53-day orbit for the remainder of the mission by not performing the period reduction maneuver (PRM) shown in Table 1-1.

(*) Table 1-1 and several other Tables and Figures from the pre-JOI mission plan are denoted by *Superseded in the Table or Figure caption and in the List of Tables or List of Figures. These have been retained unchanged from the October 2012 Juno article for historical documentation.

See the JOI Press Kit https://www.jpl.nasa.gov/news/press_kits/juno/ for an earlier post-launch change making the original short orbit 14 days instead of the 11 days shown in Table 1-1.

**Table 1-1: *Superseded: Juno Mission phases.**

| Phase | Begin | Duration (days) | Rationale for Boundaries | Notes<br>Times are in Universal Time, UTS |
|---|---|---|---|---|
| **Pre-Launch** | **L-3d**<br>08/02/11 | 3 | S/C power-up until final config | |
| **Launch** | **L-0.75h**<br>08/05/11 | 2.3 | Until cruise attitude control | Launch = 8/5/11 (16:11), at start of 22-day launch period: 8/5–26. |
| **Inner Cruise 1** | **L+2.3d**<br>08/08/11 | 61 | Until change to Earth-pointing | |
| **Inner Cruise 2** | **L+63d**<br>10/08/11 | 598 | Until change to off-Sun-pointing | DSM 1 = 8/30/12 (22:29), DSM 2 = 9/3/12 (22:29). DSM 1 varies from 6/20 to 8/30 over launch period. |
| **Inner Cruise 3** | **L+661d**<br>05/28/13 | 161 | Until change to Earth-pointing | EFB = 10/9/13 (14:12). Flyby times vary ~8 hours (from 7.14 to 15:08) over launch period. |
| **Quiet Cruise** | **L+822d**<br>11/05/13 | 791 | Until start of Approach science | |
| **Jupiter Approach** | **JOI-182d**<br>01/05/16 | 178 | Until JOI critical sequence | |
| **JOI** | **JOI-4d**<br>07/01/16 | 4 | Until end of critical sequence | JOI start = 7/5/16 (02:29). PJ0 = 7/5/16 (02:44). JOI cleanup OTM at JOI+7.6d. |
| **Capture Orbit** | **JOI+1h**<br>07/05/16 | 106 | Until PRM keepout zone | |
| **PRM** | **PRM-18h**<br>10/19/16 | 1 | Until end of keepout zone | PRM start = 10/19/16 (17:59).<br>PJ1 = 10/19/16 (18:17). |
| **Orbit 1-2** | **PRM+11h**<br>10/20/16 | 20 | Until AP3 start | Orbit 2 includes PRM cleanup OTM 1 at PJ2+1h. Activity Period 2 is first AP (PJ-1d to PJ-1d). |
| **Science Orbits** | **PJ3-1d**<br>11/09/16 | 336 | Until before deorbit burn | Orbits 3-32 + most of (extra) (Orbit 33.<br>Orbit 3 includes PRM cleanup OTM 2 at PJ3+4h. |
| **Deorbit** | **AJ33-1h**<br>10/11/17 | 5.5 | Until impact | Part of Orbit 33 + first half of Orbit 34.<br>Impact = PJ34 = 10/16/17 (19:33). |

### 1.3.2 Cruise Phase

The Cruise phase began after the spacecraft completed the Launch phase.

The Juno spacecraft is spinning at 1 revolution per minute (rpm) during cruise except for the two major engine burns for the Deep Space Maneuver (DSM). Most of the antennas used during Cruise phase (a high-gain antenna [HGA], a medium-gain antenna [MGA], two low-gain antennas (LGAs, forward and aft) have their boresights co-aligned with the spin axis. The toroidal low-gain antenna (TLGA) is also used during Cruise. It is aligned normal to the spin axis on the aft end of the spacecraft.

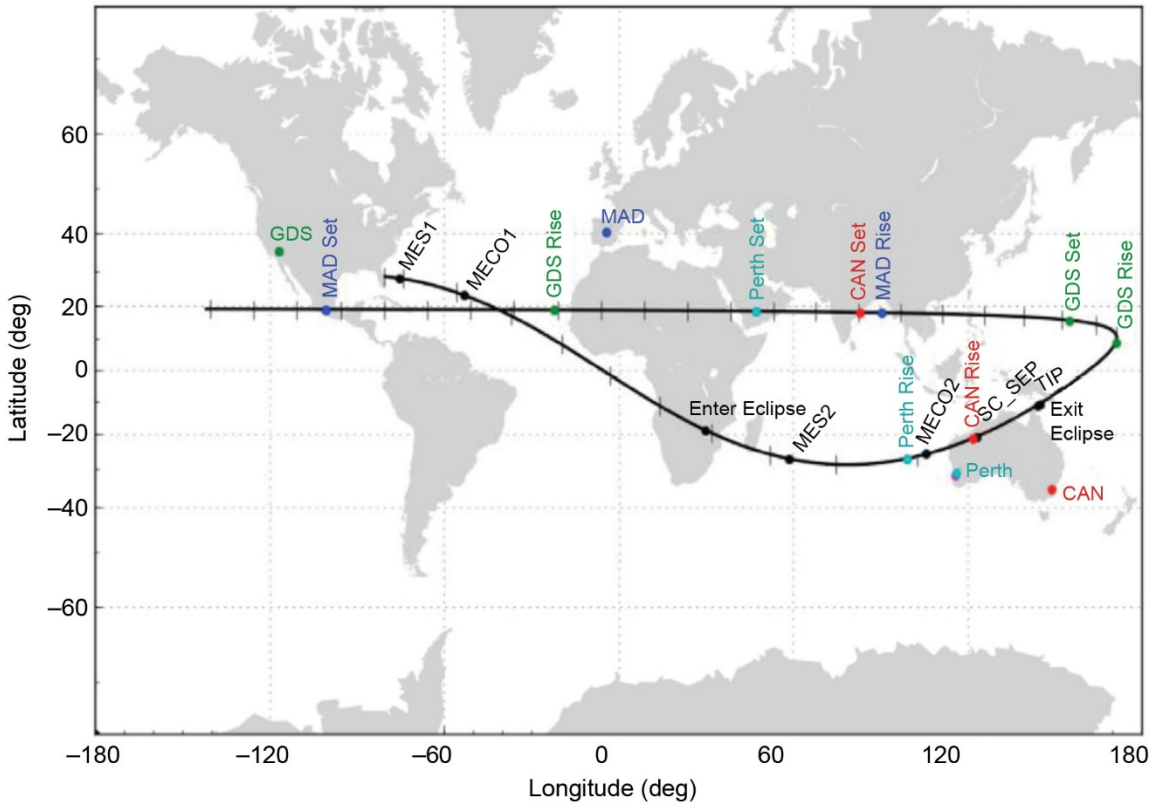


**Figure 1-4: Juno launch ground track for 8/5/11 launch.**

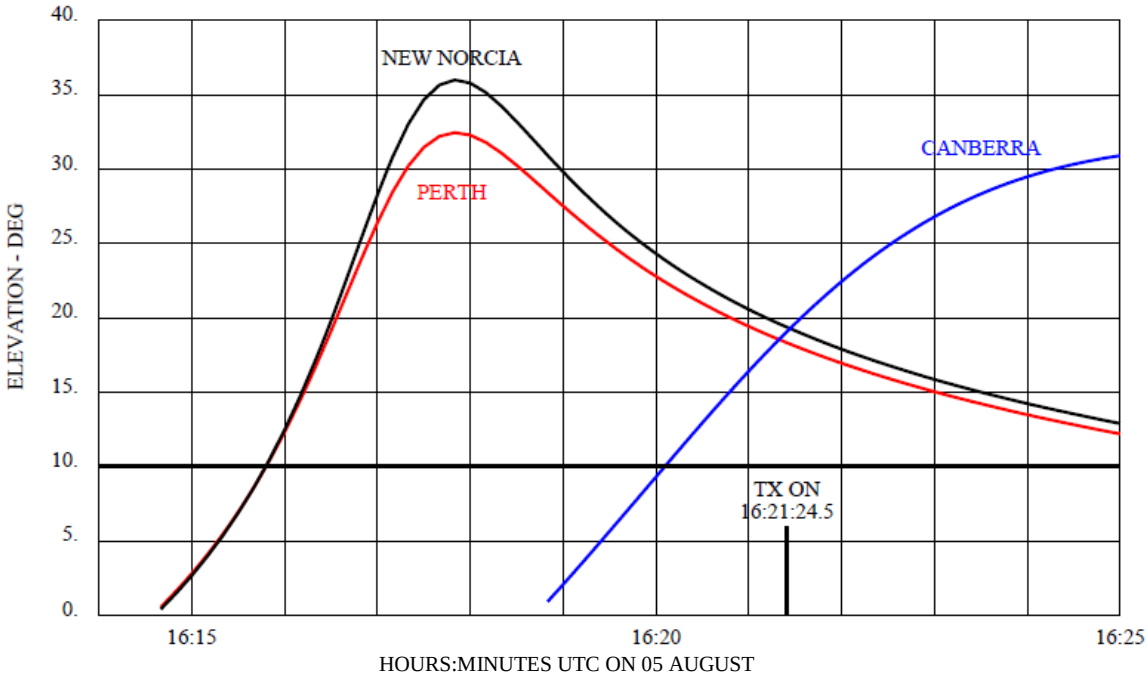


**Figure 1-5: Juno ground station coverage following launch on 8/5/11 launch.**

The major activities in Cruise phase include:

- Checkout and maintenance of the spacecraft in its flight configuration,
- Monitoring and characterization/calibration of the spacecraft and payload subsystems (and associated parameter updates),
- Attitude maintenance turns,
- Navigation activities for determining and correcting the vehicle's flight path,
- Two major engine burns of the DSM,
- Preparations for Jupiter orbit insertion (JOI), Period Reduction Maneuver (PRM), and orbital operations.

The project planned 12 Trajectory Correction Maneuvers (TCMs) leading up to JOI, including the two DSM burns that were successfully executed on August 30 and September 14, 2012.

Figure 1-6 shows the spacecraft range for the 2011 launch opportunity.

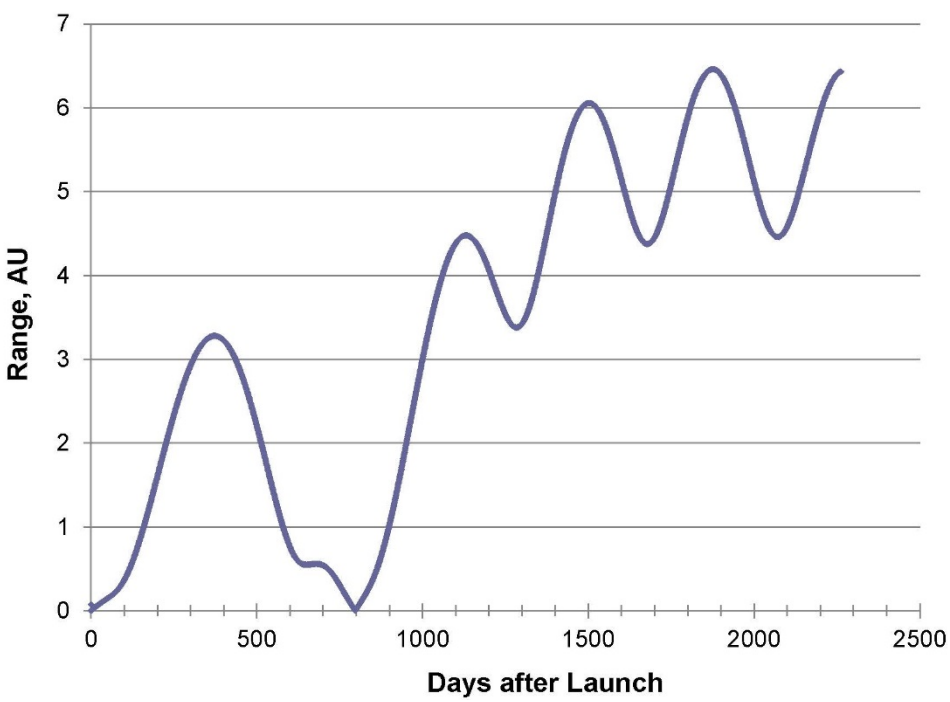


**Figure 1-6: Spacecraft range from Earth vs. time after launch.**

Figure 1-7 shows the Sun–Probe–Earth (SPE) and Sun–Earth–Probe (SEP) angles as a function of time for the full mission.

The spacecraft +Z axis is aligned with the high-gain antenna (HGA), medium-gain antenna (MGA) and forward low-gain antenna (FLGA) boresights. This axis is also normal to the solar arrays. The solar arrays may be slightly adjusted during the mission to realign the spin axis after the main engine burns. The antennas are fixed on the spacecraft body and are not gimbal mounted. Therefore, antenna pointing, particularly with the MGA and with the HGA, is accomplished by orienting the spacecraft +Z-axis.

Note that the SPE angle is the angle from the forward antennas' boresights when the spacecraft is pointed at the Sun. As the spacecraft approached Earth after the Deep Space Maneuver (DSM), the SPE angle exceeded 90 degrees (deg). This required having an antenna on the backside of the spacecraft, i.e., the aft LGA (ALGA).

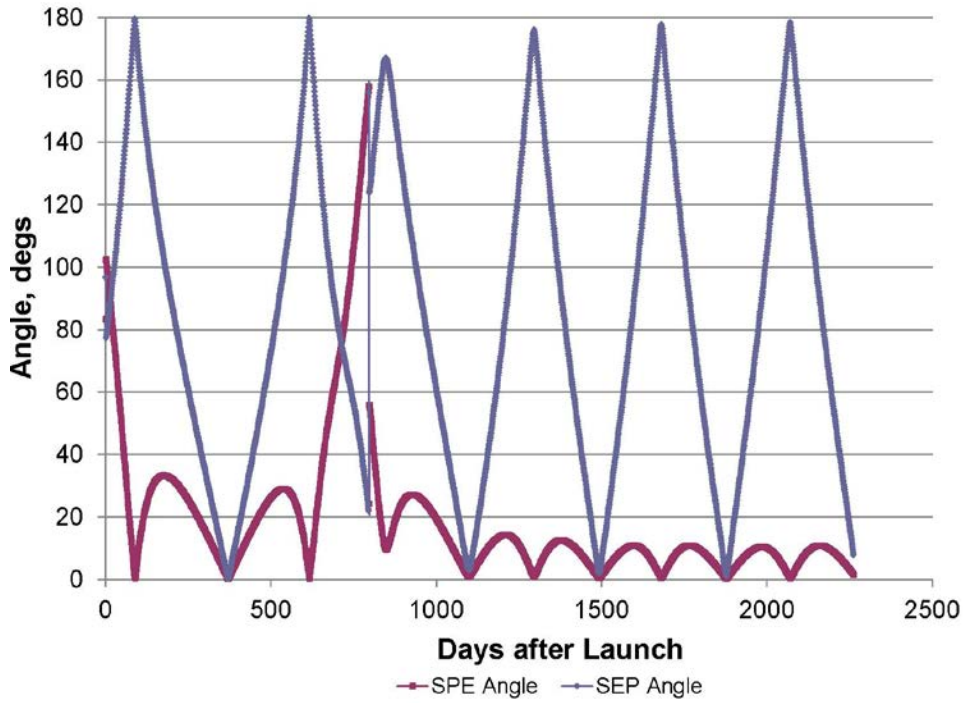


**Figure 1-7: SEP and SPE angle vs. time.**

Figure 1-8 shows the originally planned spacecraft trajectory event dates during Cruise, based on the actual launch date of August 5, 2011. The two parts of the DSM took place on August 30 and September 14, 2012. Note that the second burn on September 14 had been originally planned for September 3, 2012.

Earth Flyby occurred on October 9, 2013 at 19:21 UTC at an altitude of 559 km (*see* Section 7). The mission design target altitude was 500 km [5], with an allowance of about ±100 km of margin to perform hazard avoidance maneuvers.

The Approach phase was defined to begin 182 days prior to JOI and to end 4 days prior to JOI, at which time the JOI phase commences. The principal activities during the Approach phase include the acquisition and processing of navigation data needed to support the development of the final trajectory correction maneuvers (TCMs) and the spacecraft activities leading up to the JOI main engine burn.

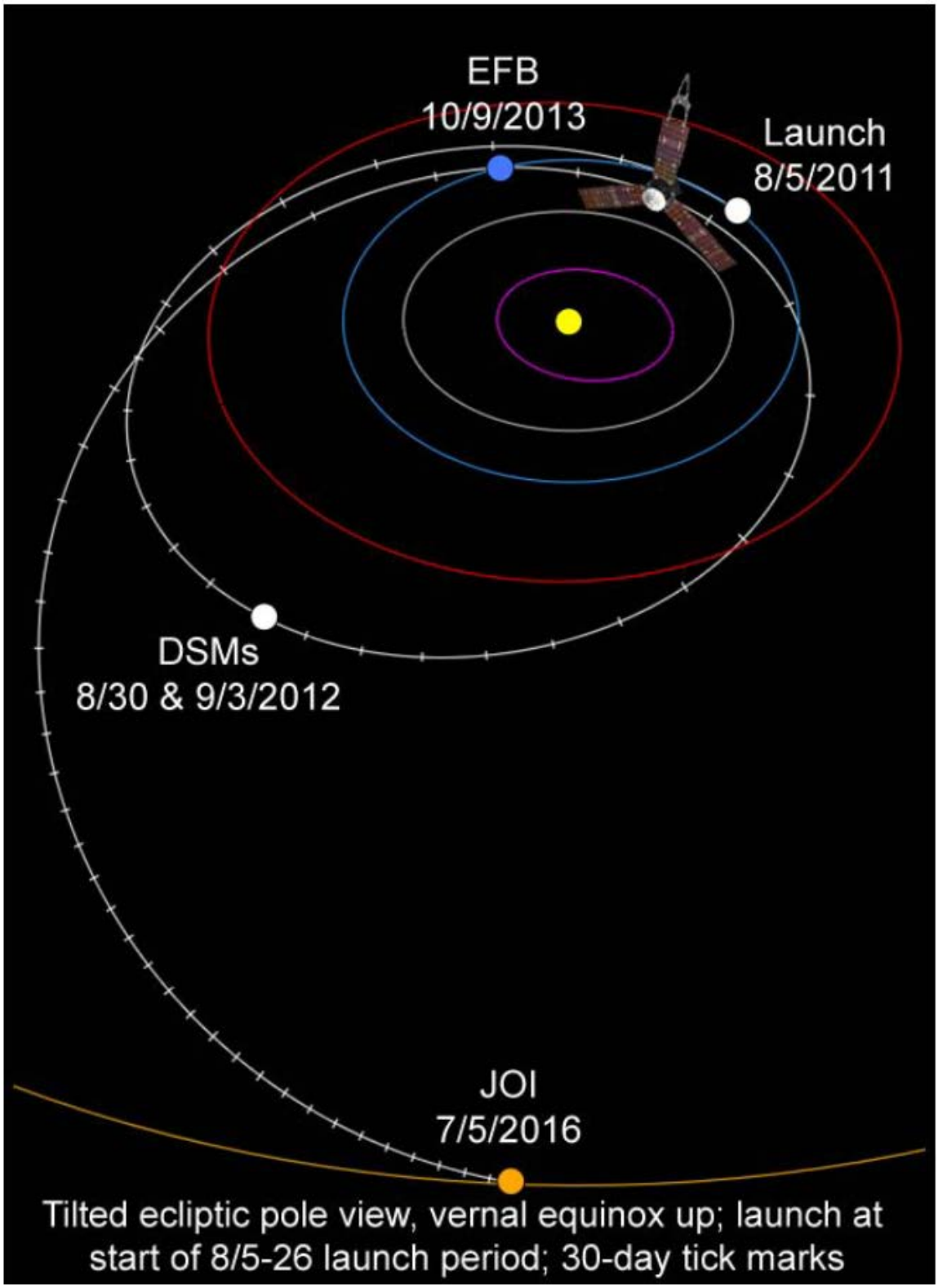


**Figure 1-8: Planned activities from launch to Jupiter Orbit Insertion.**

### 1.3.3 JOI and PRM Phase

Two main engine burns were necessary to achieve the desired Jupiter orbit: Jupiter Orbit Insertion (JOI) and Period Reduction Maneuver (PRM). The JOI burn placed the spacecraft into a 53-day orbit (*see* Section 7). The PRM burn, not executed, was planned to reduce the orbital period from 53 days to ~14 days[6] (*see* Section 6). The 14-day orbit was intended for sequencing perijove over Deep Space Station (DSS) 25 in Goldstone, California for gravity science tracking.

The timing of the JOI burn was planned to reduce the magnetic field effects on spacecraft electronics. Also, the JOI burn was planned with dual 70-m antenna coverage, from the one 70-m antenna each at Goldstone and Canberra. This JOI timing would have resulted in the PRM burn being done just over Goldstone. JOI occurred on July 5, 2016 UTC (July 4 in the USA). PRM had been planned for October 19, 2016. During the JOI burn, the spacecraft turned nearly normal to the Earth line. The spacecraft transmitted tones (subcarriers modulated onto the X-band carrier signal) through the TLGA to the ground for detection.

### 1.3.4 Orbital Phase

The nominal lifetime requirement for Juno is thirty-three 11-day orbits around Jupiter[7].

Figure 1-9 (captioned *superseded) shows the trajectory for the spacecraft before JOI, the 107-day capture orbit, and the 33 science orbits. Figures 1-10 (captioned *superseded) and 1-11 (captioned *superseded) show the two types of science orbits during the science phase—Gravity Science (GRAV) and Microwave Radiometer (MWR). During the GRAV orbits, the spacecraft is performing dual-band Doppler measurements with DSS-25 at Goldstone for 6 hours around perijove. During the MWR orbits, the MWR instrument is pointed at Jupiter during perijove, and there is no communication with Earth. There were six planned Deep Space Network (DSN) passes during each 11-day orbit to return science telemetry and perform navigation updates.

---

[6] The October 2012 version of this article described a planned post-JOI orbit period of 107 days and a final orbit period of 11 days. The as-executed JOI and subsequent orbit trim maneuver resulted in an initial 53-day orbit after JOI, with a plan to reduce it to 14 days. A later decision was to keep the orbit period at 53 days (*see* Section 6).

[7] When the 2012 version of the Juno article was posted, orbits 2-33 were planned to have an 11-day period; these are referred to throughout this update as the "11-day" orbit. The mission plan was changed before JOI to make the orbit period 14 days for orbits 2-11. As described in Section 6.3 of the Revision A article, the mission plan was changed again in February 2017 for the period of the remaining orbits to stay at 53 days. This orbit is referred to throughout the Revision A article as the "53-day" orbit.

With the post-JOI orbit period replan, Figures 1-9, 1-10, and 1-11 for the 11-day orbit became obsolete in detail. They are replaced by figures for the 53-day orbit in Section 6. Table 5-1 summarizes the 11-day orbit plan, and Table 6-1 summarizes the superseding 53-day orbit plan.

(*) These figures remain here for historical purposes as they show events that occur at various parts of the orbit. Each figure is captioned with an *superseded to indicate they are no longer current. See Table 6-1 for an updated Table 1-1 and see Figure 6-1 and Figure 6-2 for representative 53-day orbits as viewed from Jupiter's North Pole and from the Sun, respectively.

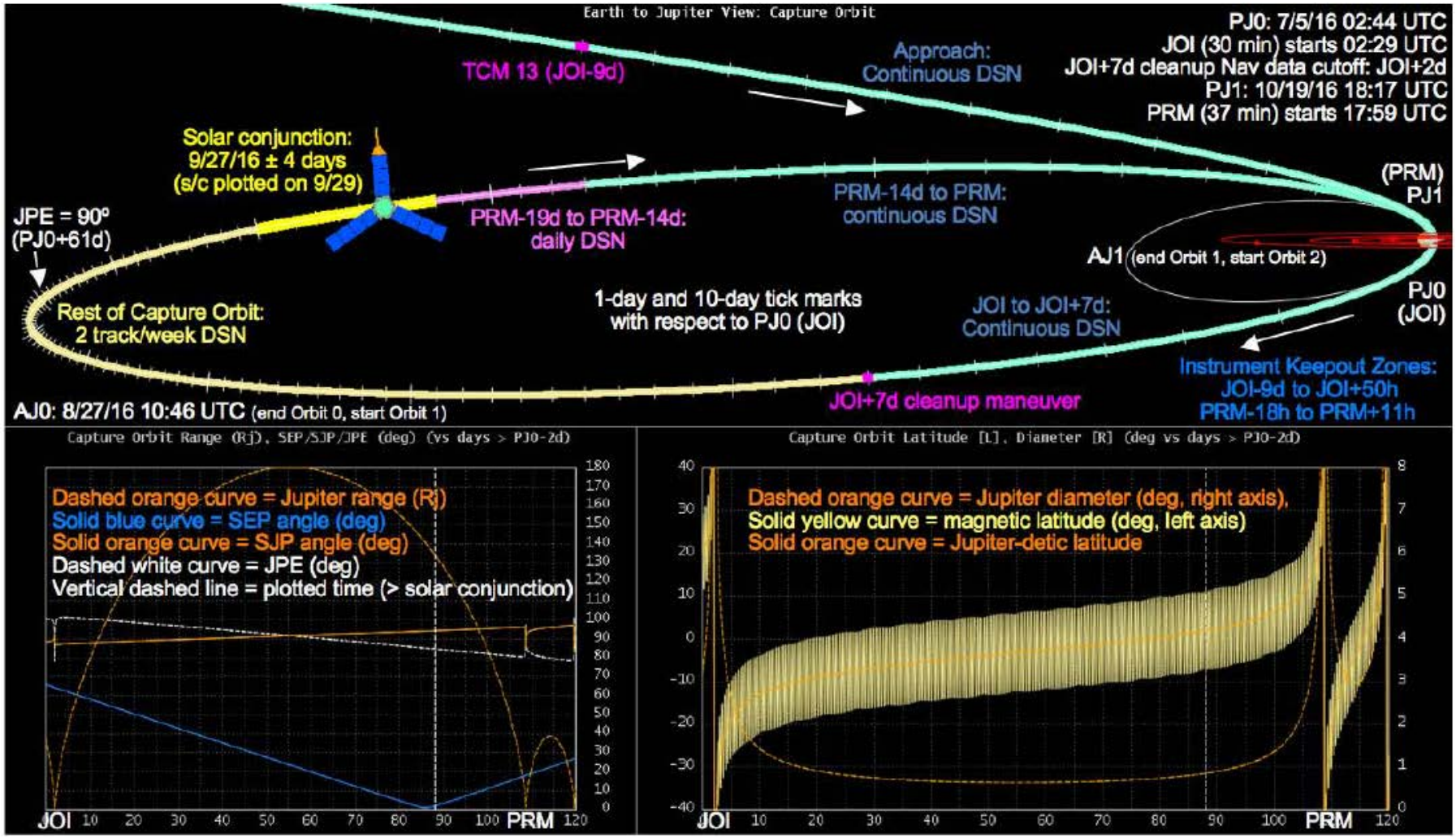


**Figure 1-9 *superseded: Juno during JOI, 107-day capture orbit and orbital operations.**

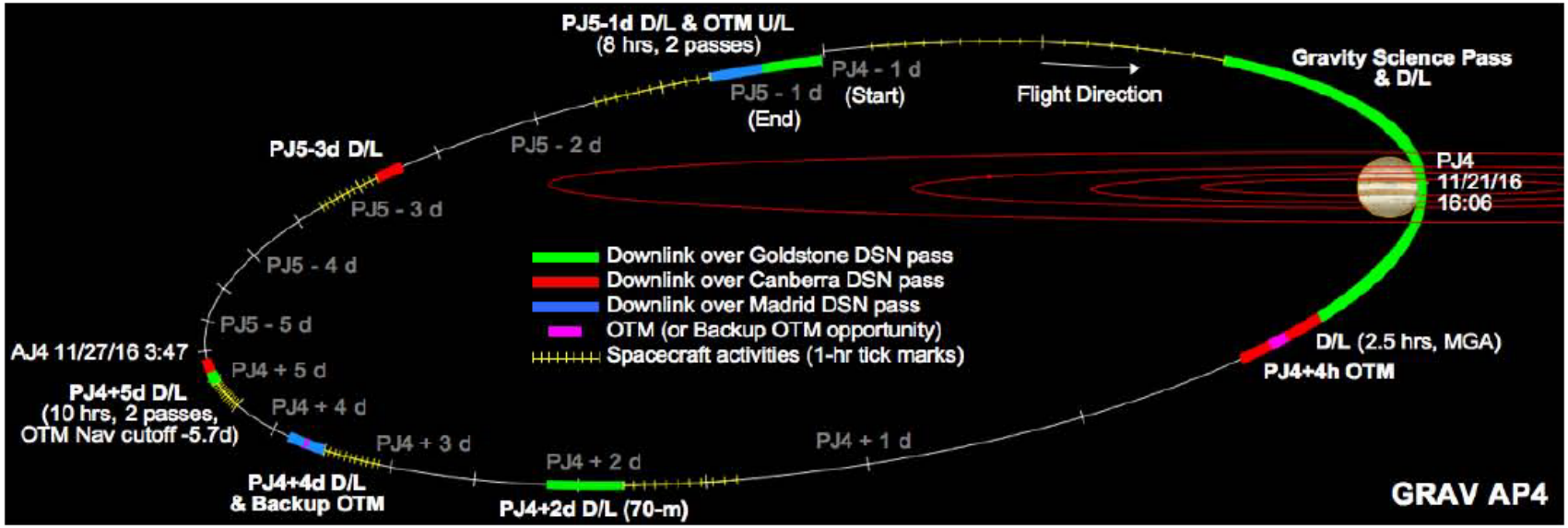


**Figure 1-10 *superseded: Gravity Science Orbit.**

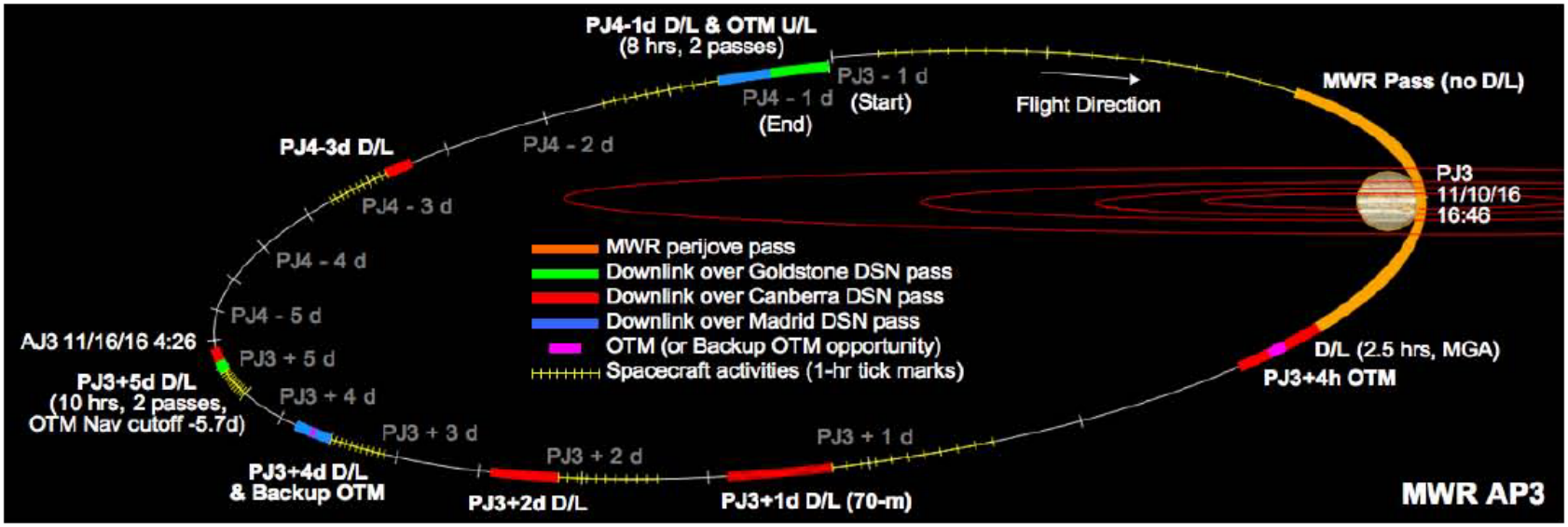


**Figure 1-11 *superseded: MWR orbit.**

The tracking schedule for the 53-day orbit has become more elaborate than what was expected with the 11-day orbit. The tracking schedule template averages a pass at least every 2 or 3 days, and several passes in close succession on the day of periapsis and the following day. The passes are repetitive from orbit to orbit, but within an orbit they differ in purpose, station size, and duration. Excluding set-up time, durations are taken as 8 hours per pass, except for 10 hours for perijove gravity science (DSS-25) and 70-m perijove downlink. From one perijove to the next, the station passes[8] for a typical orbit are grouped as follows:

- **Perijove** (PJ), PJ-6h to PJ+4h, 70m for telemetry and DSS-25 for radio science
- **Post-perijove trim** (OTM), PJ+3h to PJ+11h, 70-m on the MGA, engineering downlink only
- **Science playback**, continuous to ~PJ+2d, at least half of these passes to be 70-m
- **Tracking passes**, 16 hours/day until PJ+7d, spanning ~PJ+2d to BTM-1d
- **Pre-apojove**, AJ-3d to AJ-25h, two passes, 34-m or 70-m, ideally at separate complexes.
- **Apojove trim** (APO), coverage, timing, and duration similar to BTM, nominal start is AJ-4 days. Not needed for all orbits.
- **Radio science**, Ka-band (RS Ka). One pre-PJ GRAV track in each orbit, DSS-25, 8h, starts at ~PJ-16d. Between BPO and STM, add one 34-m tracking pass and two DDORs (N-S and E-W) no later than ~AJ+14d.
- **Statistical OTM** (STM). Coverage similar to BTM, Nominal STM starts at PJ-14d. Not needed for all orbits.
- **8-hr tracking passes**, three per week, spans BTM+14h to PJ-78h. Nominally Monday, Tuesday, Thursday, with two of the three in prime shift. At least one pass weekly is 70-m.
- **PJ-3d**. Two uplink tracks, 34-m or 70-m at different complexes, for background sequence uplinks, PJ-3d to PJ-2d, starting in prime shift.
- **PJ-1d**. Similar to PJ-3d, for tactical uplinks and downlinks to empty buffers (PJ-2d to PJ-13h).
- **Backup trim** (BTM), spanning BTM-26h to BTM+10h, 70-m in BTM prime and second shift and two 34-m uplink passes the day before and one downlink pass the day after[9]. Nominal BTM start is AJ-4d.
- **Backup to APO trim**, coverage similar to APO. Nominal APO starts at AJ+3d. Not needed for all orbits.

As Jupiter and the Earth travel in their orbits around the Sun, the Jupiter–Earth range varies between 4.46 and 6.43 astronomical units (AU) during the Orbit phase of the mission. Jupiter and the Earth are on opposite sides of the Sun as Juno starts and ends its 1-year orbital operations near maximum Earth range. Minimum range occurs with Jupiter and Earth on the same side of the Sun.

At the end of the mission, the spacecraft will perform a deorbit burn and impact Jupiter. This activity is to ensure the spacecraft does not later inadvertently contaminate a Galilean satellite with terrestrial organisms. Impact defines the end of the spacecraft mission. In the pre-JOI mission plan, impact was scheduled October 16, 2017. As shown in Table 6-1, in the 53-day orbit mission, impact is scheduled July 30, 2021.

[8] Specifics are in an internal JPL document, the Juno project spreadsheet entitled "DSN Scheduling Template" [46].
[9] By mid-2017, all required trim maneuvers had been executed properly, thus no backup maneuvers had been necessary.

# 2 Telecommunications Subsystem Overview

The Juno Telecom Subsystem operates at X-band for nominal two-way communications (command [CMD] uplink and telemetry [TLM] downlink), two-way tracking (Doppler and ranging), and changes in differential one-way ranging (delta-DOR), which is always performed in one-way mode. It also includes a Ka-band two-way carrier tracking capability for Gravity Science at Jupiter. These are the high-level functions, with the details explained in the following sections.

- During Cruise, X-band provided uplink, downlink, and radiometric measurements in support of navigation (ranging, Doppler, and delta-DOR).
- During portions of the DSM and JOI, with low signal levels due to antenna off-point, the X-band carrier was modulated with subcarrier tones that could be used for real-time observation and fault reconstruction.
- During the orbital phase of the mission:
    - X-band is used for uplink for commanding and downlink for telemetry return and tracking.
    - X-Band (up and down) and Ka-band (up and down) is used during Gravity Science passes on selected orbits at Jupiter perijove.

Figure 2-1 shows the telecom components mounted in the spacecraft radiation vault.[10] The vault is a titanium box designed to protect the 20+ electronic assemblies inside it against a total integrated dose (TID) of 25 kilorads (krad) or less. The mass of the whole vault is about 200 kg. The wall thicknesses are optimized for the minimum mass needed to attenuate the mix of electrons and protons at Juno over the Orbit phase mission duration.

## *2.1 X-Band*

The Telecom Subsystem block diagram is presented in Figure 2-2.

For the most part, the Juno telecom subsystem operates on DSN X-band channel 6, as defined in Ref. [4]. As defined subsequently in Table 2-9, the KaTS also includes operations on channel 5.

- Receive frequency: 7153.065586 megahertz (MHz)
- Transmit frequency: 8404.135802 MHz

The X-band part of the Telecom Subsystem is designed to perform the following functions:

- Receive an X-band uplink carrier from the DSN. This carrier may be modulated by command data, by a ranging signal, or both. Then the system must demodulate the command data and the ranging signal.

[10] The vault is shown and described https://en.wikipedia.org/wiki/Juno_Radiation_Vault .

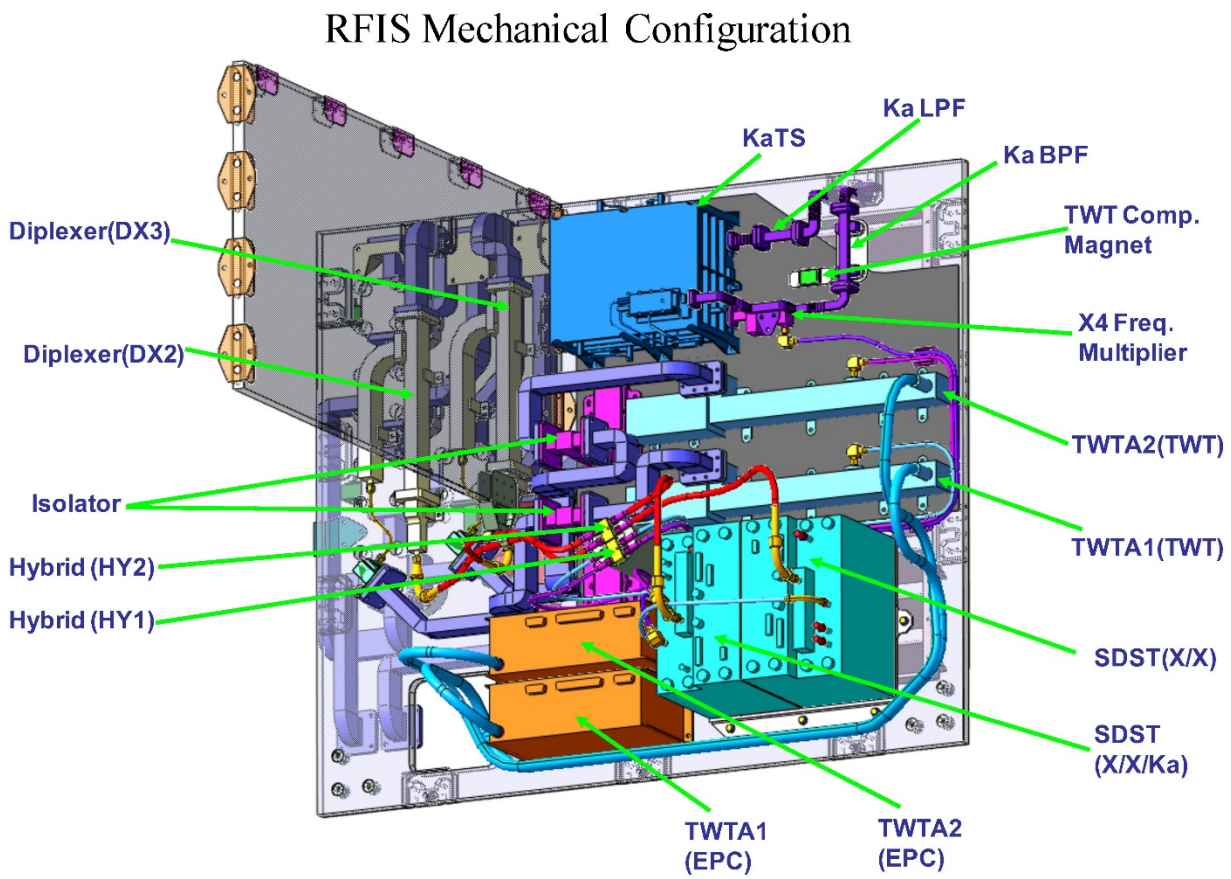


**Figure 2-1: Juno telecom components (Radio Frequency Instrument Subsystem, RFIS) mounted in the S/C vault.**

- Generate an X-band downlink carrier either by coherently multiplying the frequency of the uplink carrier by the turn-around ratio 880/749, or by utilizing an auxiliary crystal oscillator (Aux Osc).
- Phase-modulate the downlink carrier with either of three signals (or a combination of these signals):
    - A composite telemetry binary phase shift keying (BPSK) signal, either direct modulated or data modulated onto a squarewave subcarrier (25p or 281.25 kilohertz, kHz)
    - A tone series, a tone being a telemetry subcarrier frequency with no modulation on the tones
    - Differential one-way ranging (DOR) signal
    - The ranging signal that was demodulated from the uplink (this signal is referred to as two-way or turn-around ranging)

  Note: the planned data downlink configuration includes either telemetry or tones, but not both simultaneously. The radiometric configuration is either the DOR signal or the ranging signal, but not both simultaneously.

- Permit control of the subsystem through commands to select signal routing (i.e., which antenna should be used) and the operational mode of the subsystem (i.e., the configuration of the elements of the subsystem; examples are command data rate, telemetry subcarrier, convolutional code, downlink ranging modulation index). This commanding can be done either directly from the ground (i.e., with real-time commands) or through the initiation of sequences of commands that were previously loaded on the spacecraft.
- Provide status telemetry (to the Avionics Subsystem) for monitoring the operating conditions of the subsystem. Examples are: Aux Osc temperature, Small Deep Space Transponder (SDST) current, subcarrier frequency, state of ranging channel (ON or OFF), coherent/non-coherent operation, and receiver lock state (IN or OUT of lock).
- For all radio frequency (RF) transmitters, provide ON/OFF power control to permit the conservation of power.
- Upon a power-on-reset (POR), the system is placed into a single, well-defined operating mode; this provides a "known baseline state" from which the ground can command the Telecom Subsystem during safe-mode (emergency) operations
- All of the antennas are used during Cruise: They are:
    - FLGA: forward low-gain antenna
    - ALGA: aft low-gain antenna
    - MGA: medium-gain antenna
    - HGA: high-gain antenna
    - TLGA: toroidal low-gain antenna
- The DSM, JOI, and PRM maneuvers include transitions from the HGA to the MGA and then to the TLGA. Times of the switches are based on an internal timeline of maneuver events in flight software (FSW). The FSW switches back to the MGA from the TLGA after the burn. When HGA pointing has been refined after the burn, the spacecraft is sequenced to return to the HGA.
- During the orbital phase, the HGA provides uplink and downlink. (The MGA might be used after post-perijove orbit trim maneuvers (OTMs) depending on the HGA pointing capability.

Other names and acronyms in Figure 2-2 not explained so far are: LPF for low-pass filters, BPF for bandpass filters, HY for hybrid, AT for attenuator, DX for diplexer, WG for waveguide, WTS for waveguide transfer switch, Iso For isolator, and standard waveguide sizes for X-band (WR-112) and Ka-band (WR-28 and WR-34).

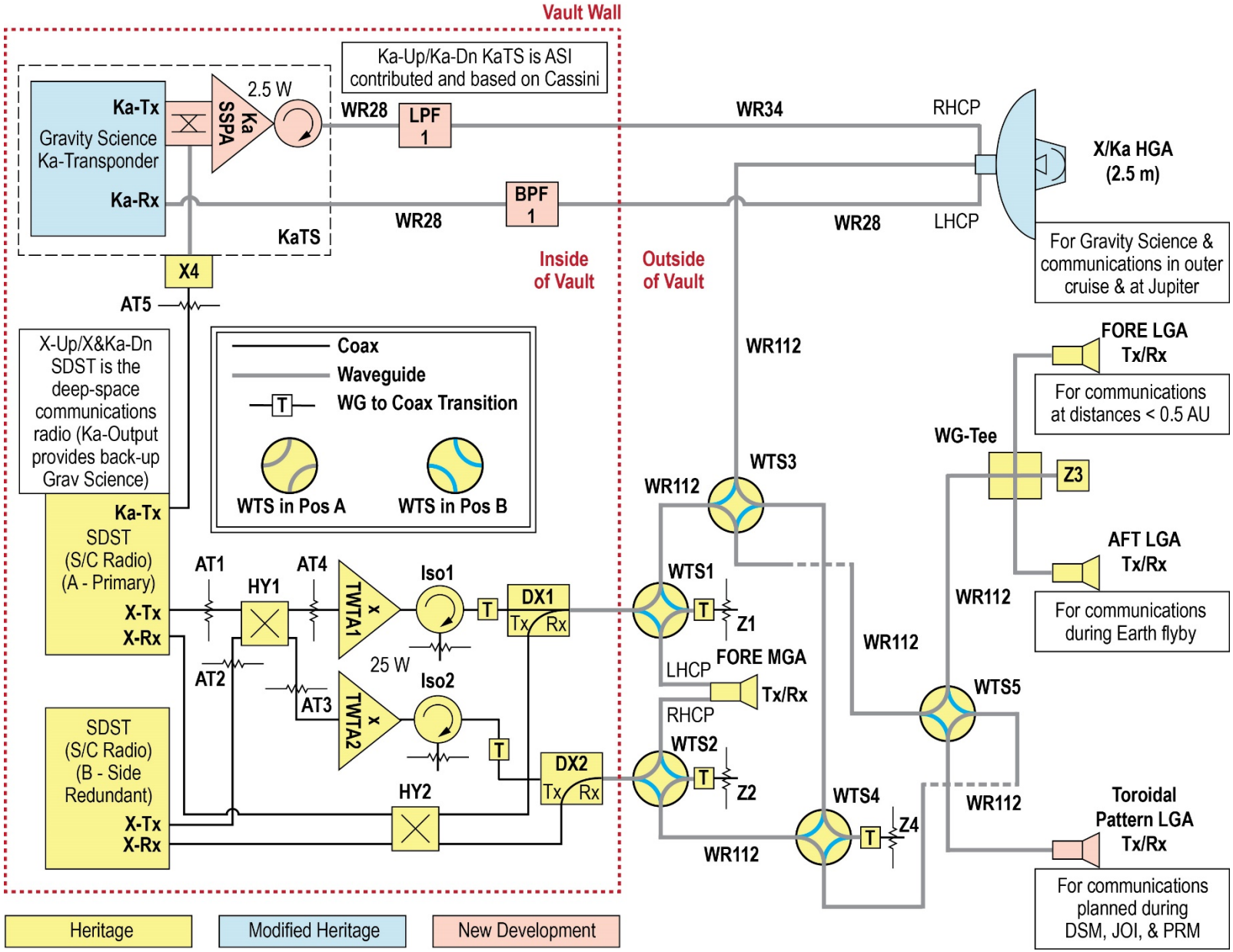


**Figure 2-2: Juno X-band and Ka-band block diagram.**

### 2.1.1 Interfaces

Figure 2-3 shows the interface between the SDSTs and the CD&H. The main interface to the SDST radios is the uplink/downlink (ULDL) card and the Command & Data Handling Subsystem (C&DH). The C&DH provides the following data transfer functions, including:

- Turbo code rate 1/6 with large (8920 bits) frame size, which is the baseline for high rate X-band downlink.
- Reed–Solomon encoding (interleave depth 1) that can be used for X-band downlink (in concatenation with convolutional (7,1/2) performed by the SDST) for low rate X-band downlink at 10 or at 40 bits per second (bps).
- Reed–Solomon encoding (interleave depth 5) that was used for X-band downlink (in concatenation with convolutional (7,1/2) performed by the SDST) at 1745 bps during launch.

The SDSTs provide redundant uplink (command) and downlink (telemetry) low-voltage differential signaling (LVDS) interfaces which are cross-strapped to the two ULDL cards. The active downlink port on the telecom side must be selected by the C&DH by issuing a command on the 1553 bus [12].[11] Both uplink ports in the SDST are always active.

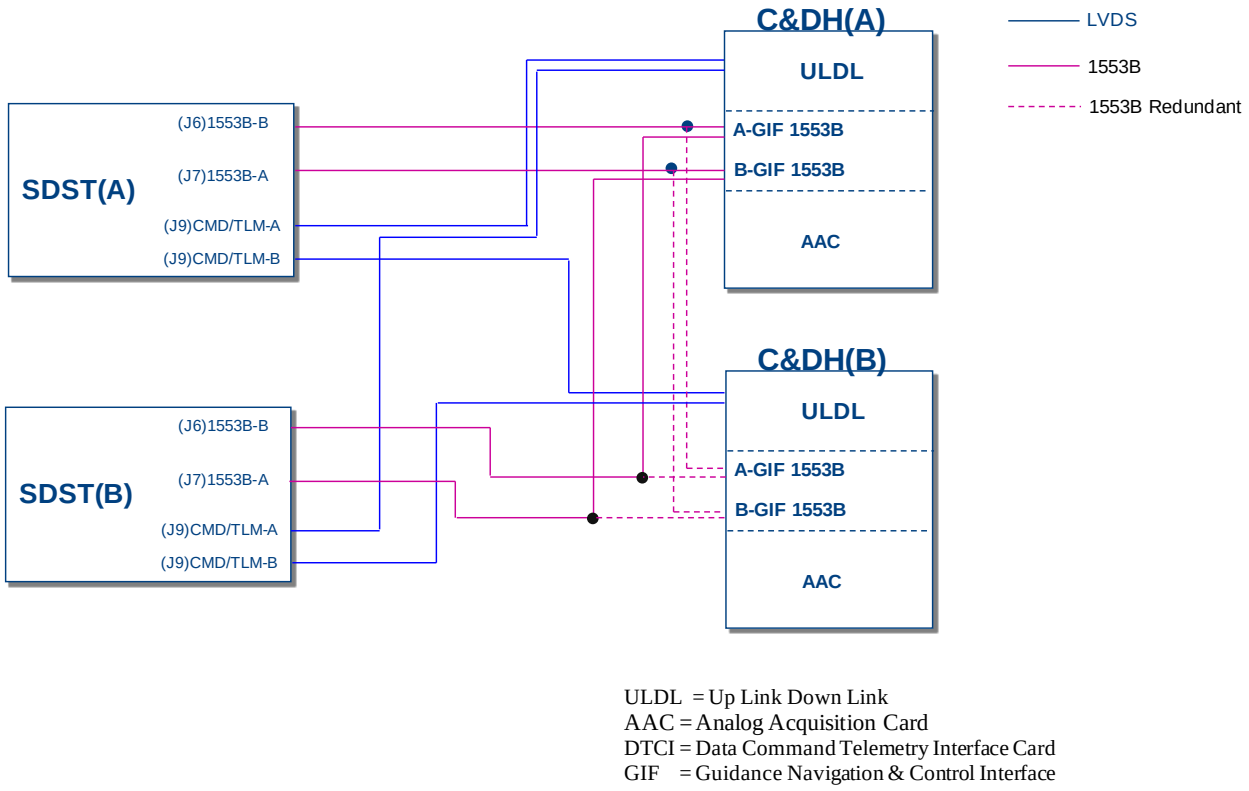


**Figure 2-3: LVDS and 1553B cross-strapping to flight system.**

[11] MIL-STD 1553 is a standard published by the United States Department of Defense that defines the mechanical, electrical and functional characteristics of a serial data bus.

### 2.1.2 Small Deep Space Transponder (SDST)

Juno has two SDSTs, of two different types. The prime unit is an X/X/Ka unit that provides a backup Gravity Science function. The redundant unit is an X/X unit.

The SDST is composed of four different modules: the digital processing module (DPM), the downconverter module, the power converter module, and the exciter module. The DPM is responsible for convolutionally encoding the data, for providing X-band baseband telemetry and ranging signals to the exciter module, and for converting the analog output of the downconverter module into binary data.

The downconverter module takes the 7.153-GHz RF signal received from the ground station and converts it to an intermediate frequency (IF) signal at 4/3 F1. In SDST nomenclature, F1 is the fundamental frequency from which the uplink and downlink frequencies are derived. For example, the X-band downlink is 880F1 and the X-band uplink is 749F1. For Juno, F1 is approximately 9.55 MHz. The voltage-controlled oscillator (VCO) output is at 8 F1. The uplink signal (with command and ranging modulation) gets sampled by an analog-to digital (A/D) converter at the input of the digital processor module. These samples are provided to three “channels” to use the old analog terminology:

a) The command channel

b) The carrier channel (for uplink carrier tracking)

c) The ranging channel

The ranging samples of the baseband uplink are put through a digital-to analog (D/A) converter to get an analog signal (to modulate the downlink with this 'turn-around' ranging).

The exciter module takes any combination of three inputs:

- Telemetry (from the DPM; this is a BPSK-modulated square-wave subcarrier or direct modulated symbol stream);
- DOR (differential one-way ranging; analog, a 2 F1 [~ 19 MHz] sinewave signal; internal to the exciter module) and
- Ranging (analog, from the DPM, after its D/A converter)

and phase-modulates the downlink carrier.

The power converter module is responsible for supplying steady voltages to the other SDST modules.

The SDST functional specifications summarized here are detailed in the *SDST Functional Specification & Interface Control Document* [10]. Tables 2-1 and 2-2 list some of the SDST requirements relevant to the telecom link performance.

**Table 2-1: SDST receive functional specifications.**

| SDST Receive Parameter | Functional Requirement |
|---|---|
| Receive signal maximum power | –70 decibels referenced to milliwatts (dBm) (to meet performance specs)<br>+10 dBm (no damage) |
| Carrier loop threshold bandwidth (BW) | 2 settings:<br>20 ± 2 hertz (Hz) at receiver threshold (varies with carrier loop SNR; max BW is ~ 120 Hz at strong signal, 100 dB SNR)<br>50 Hz ± 5 Hz at receiver threshold |
| Noise | < 3.2 dB over temperature, aging, and radiation, 2.0 dB typical at beginning of life, at 25 ºC |
| Carrier tracking threshold @ best-lock frequency (BLF) and 0 dB loop S/N (20 Hz loop bandwidth) | –157.7 dBm typical<br>–155.0 dBm worst case |
| Command rates | 7.8125 to 4000 bps (SDST capability)<br>7.8125 to 2000 bps used operationally |
| Telemetry modulation index | 0 to 135 deg angle peak (3 deg maximum steps) |

**Table 2-2: SDST 880f1 exciter functional specifications.**

| X-band 880F1 Transmit Parameter | Functional Requirement |
|---|---|
| Output power level<br>Of X-band exciter | 13.0 + 3/–2 dBm over temperature, tolerance, end of life (EOL), radiation |
| Phase Noise | < –20 decibels below carrier (dBc)/Hz @ 1 Hz (Aux Osc mode) |
| Aux Osc short term frequency stability | 0.06 ppm at any constant temp from 10°C to 40°C (1 sec integration measured at 5-minute intervals over a 30 min span) |
| Numerically controlled oscillator (NCO) subcarrier tone short term stability | 30 ppm |
| NCO subcarrier tone long-term stability | 20 ppm |
| Harmonics | < –50 dBc |
| In-band and Out-of-band Spurious | < –50 dBc |
| Minimum symbol rate | 0 sps for subcarrier; 2000 sps for direct modulation |
| Maximum symbol rate | Filtered mode: 10 Msps<br>Wideband (unfiltered) mode: 100 Msps |
| Modulation index accuracy | ± 10% |

| X-band 880F1 Transmit Parameter | Functional Requirement |
|---|---|
| Ranging modulation indices (peak) | 4.375, 8.75, 17.5, 35, 70 deg peak |
| Ranging modulation index accuracy | ± 10% |
| Ranging modulation index stability (over temp., radiation, and EOL) | < ±20% |
| Ranging delay variation over FA temperature range | < 20 ns typical |
| DOR Modulation Index (peak) | 70 deg peak |
| DOR Modulation Index accuracy | ± 10% |
| DOR Modulation Index stability (over temp., radiation, and EOL) | < ±25% |

### 2.1.3 Traveling Wave Tube Amplifier

There are redundant X-Band traveling wave tube amplifiers (TWTAs) on Juno. The TWTAs are 25-W X-band units from Tesat/Thales. The required dc input power is 56 W. The units are fully flight qualified and are based on the design for the Mars Reconnaissance Orbiter (MRO) and Mars Science Laboratory (MSL) X-band TWTAs. The TWTA is comprised of the traveling wave tube (TWT, the RF amplifying element) in the foreground and the electronic power converter (EPC) in the background. A picture of the Juno EPC is shown below in Figure 2-4.

Monika Danos obtained her BSEE from Cornell University (Ithaca, New York) in 1995 and her MSEE with a concentration in communications from the University of Southern California (Los Angeles) in 1998. In 1999 she joined the Jet Propulsion Laboratory where she has worked as a telecommunications systems engineer on various projects including the Mars Exploration Rovers, Juno, and Mars Science Laboratory.

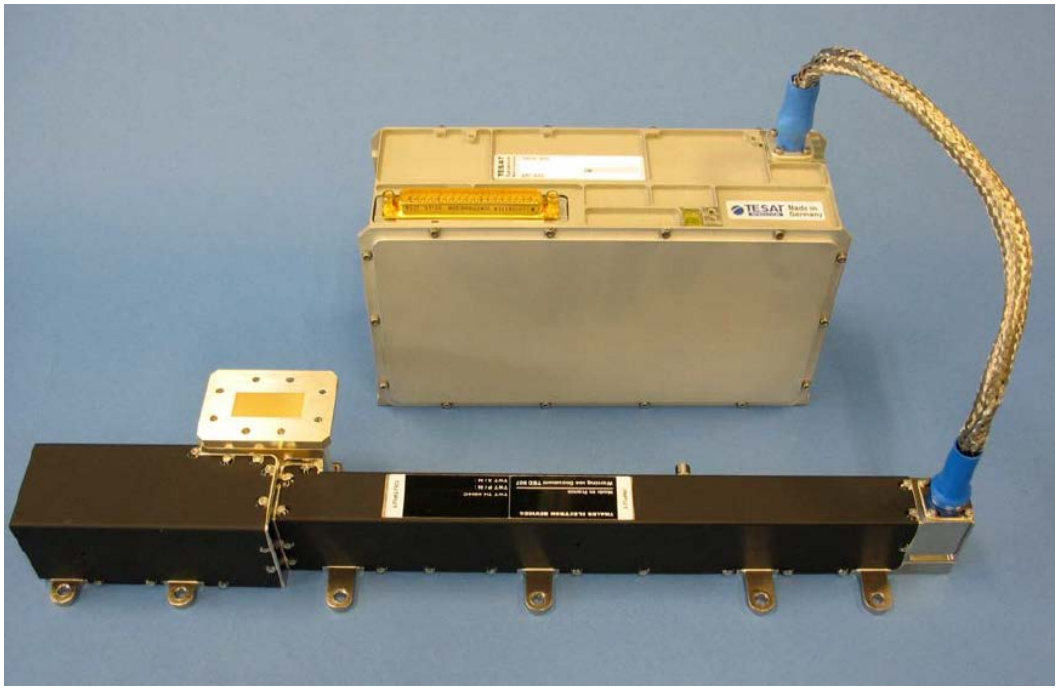


**Figure 2-4: Juno TWT with electronic power converter.**

### 2.1.4 Antennas

There are five telecom antennas on Juno. They are the high-gain antenna (HGA), medium-gain antenna (MGA), toroidal low-gain antenna (LGA) and two low-gain antennas (LGAs), which are the forward LGA (FLGA) and the aft LGA (ALGA). The picture in Figure 2-5 shows the location of the antennas on the spacecraft.

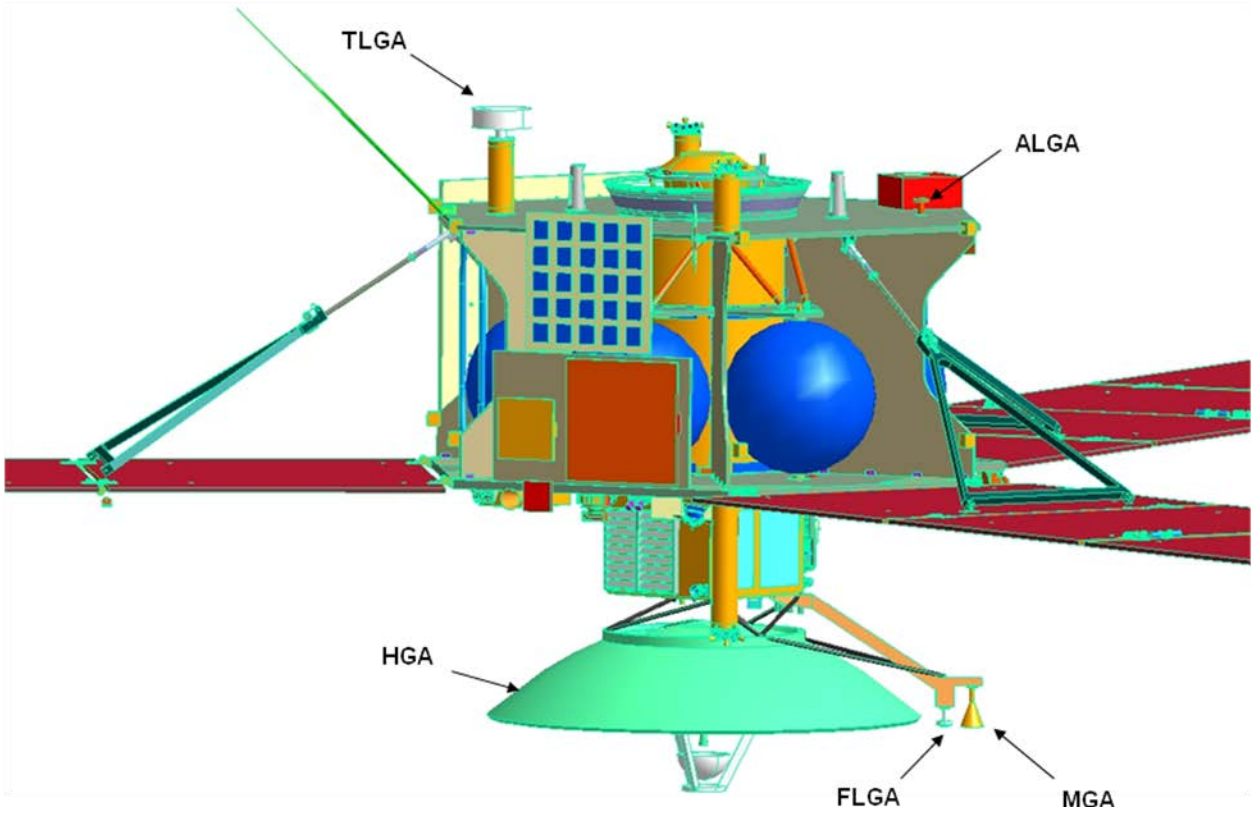


**Figure 2-5: Location of antennas on the Juno spacecraft.**

#### *2.1.4.1 High-Gain Antenna (HGA)*

The HGA is a 2.5-m dual-band (X and Ka) dual reflector. It is a similar design to the 3.0-m MRO HGA. Table 2-3 lists some of the key parameters of the HGA.

**Table 2-3: HGA parameters.**

| Parameter | Value |
|---|---|
| Design | Dual reflector |
| Diameter | 2.5 m |
| Required gain, transmit (X) | 44.5 ± 0.5 dB |
| Required gain, receive (X) | 43.0 ± 0.5 dB |
| Required gain, transmit (Ka) | 47.5± 0.6 dB |
| Required gain, receive (Ka) | 47.0± 0.6 dB |
| Polarization (X) | Right-hand circular polarization (RHCP) (uplink and downlink) |
| Polarization (Ka) | RHCP (downlink) and LHCP (uplink) |
| Axial ratio, receive and transmit (X, Ka) | 2.0 dB |
| Beamwidth, receive and transmit (X) | ± 0.25 deg |
| Beamwidth, receive and transmit (Ka) | ± 0.25 deg |

Figures 2-6 and 2-7 show the HGA gain patterns for downlink and uplink at X-band. Similar patterns for Ka-band are shown in Figures 2-8 and 2-9. The HGA patterns are expressed in dBiL, that is, dB relative to an isotropic linearly polarized antenna.

In these figures, the terms co-pol and cx-pol stand for co-polarization and cross-polarization, respectively. Because the HGA is RHCP, the term co-pol refers to the pattern measured with a test antenna that is also RHCP. The term cx-pol refers to the pattern measured by a LHCP test antenna.

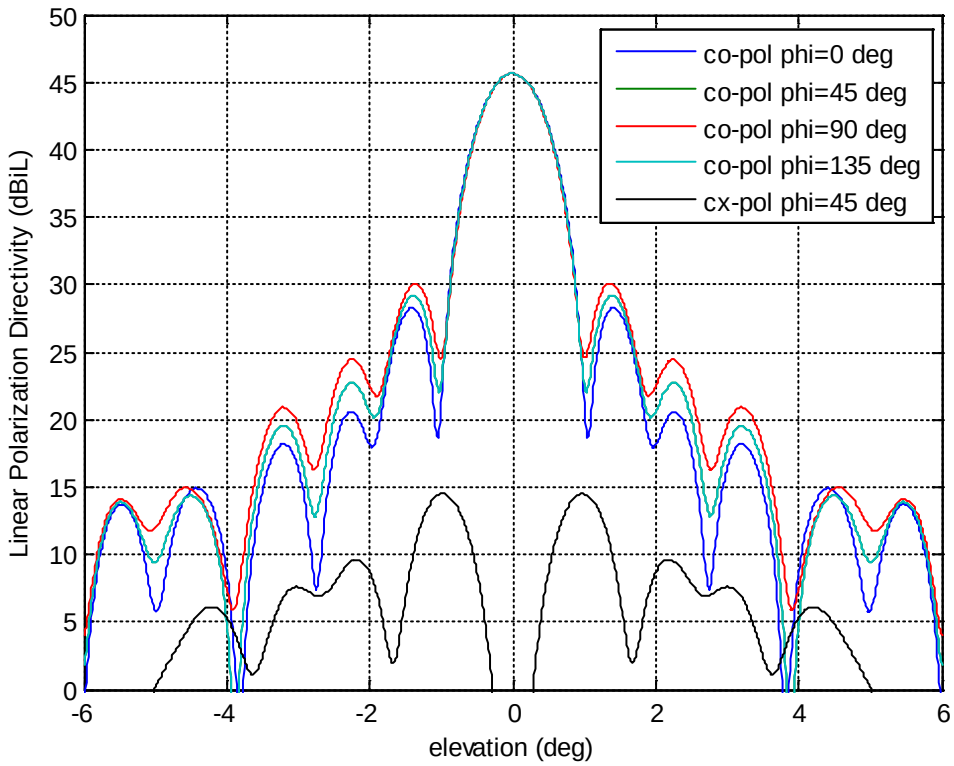


**Figure 2-6: HGA X-band downlink pattern.**

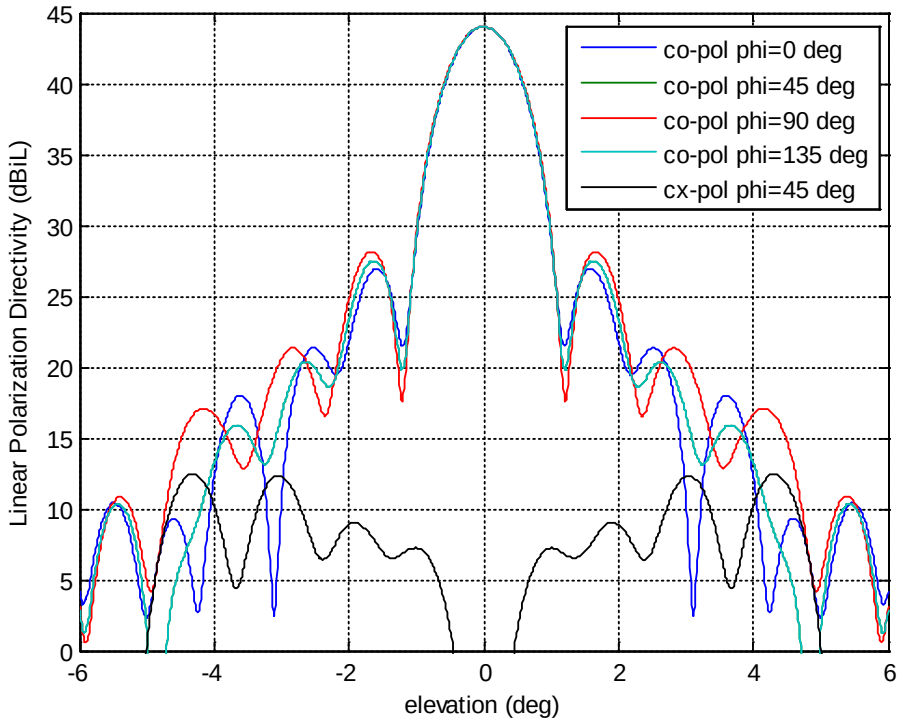


**Figure 2-7: HGA X-band uplink gain.**

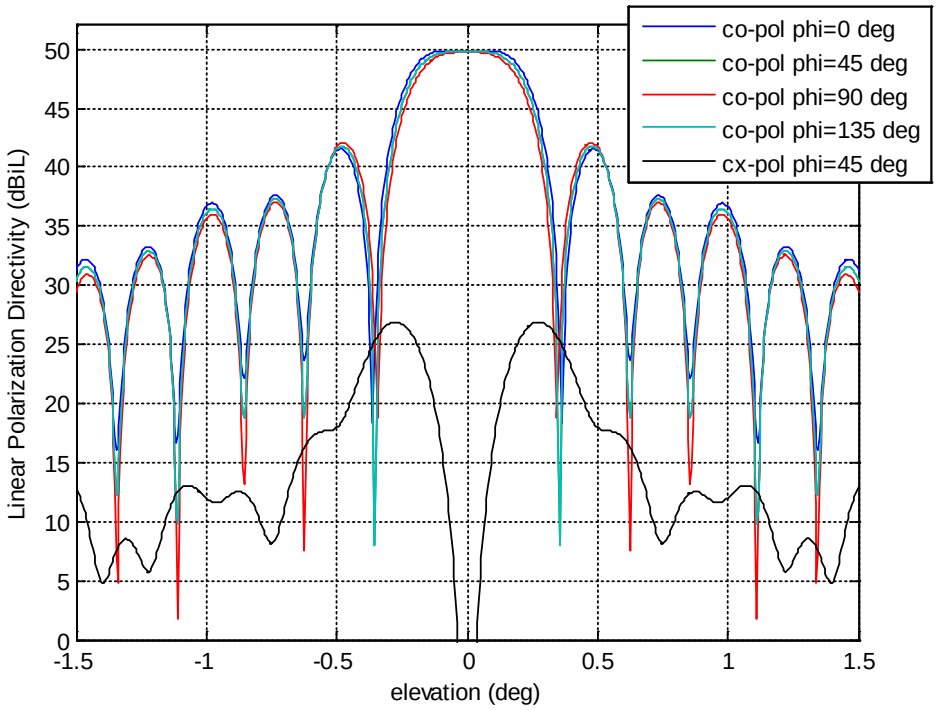


**Figure 2-8: HGA Ka-band downlink gain.**

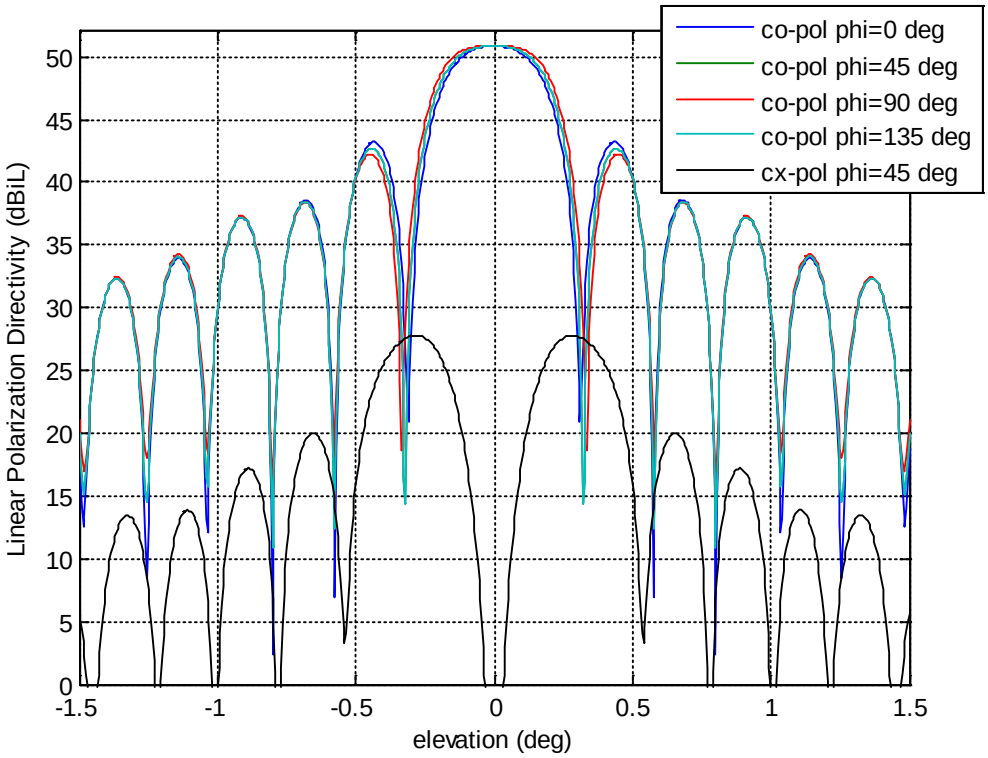


**Figure 2-9: HGA Ka-band uplink gain.**

#### *2.1.4.2 Toroidal Low-Gain Antenna (TLGA)*

The toroidal LGA (TLGA) is a biconical design. It produces an RHCP pattern that is symmetrical about the spin axis. This antenna was added to the design for critical event coverage—the main engine burns for the two DSM burns, JOI and PRM. The antenna is located on the aft deck of the spacecraft. The uplink and downlink gain values will not vary by much. This is a broadband design and easily covers both the uplink and downlink frequency bands.

Table 2-4 lists some key parameters of the TLGA. Figure 2-10 shows three views of the antenna. Part (a) of the figure is a side view of the antenna covered with its protective radome; part (b) shows the inner pattern-forming biconical horn in green and orange; and part (c) is a bottom view of the antenna and the waveguide connector.

The transmit gain pattern of the TLGA is shown in Figure 2-11. The receive gain pattern is shown in Figure 2-12. The directivity patterns of the Juno LGAs and MGA are expressed in dBic, dB relative to an isotropic circularly polarized antenna. As previously described, the Juno HGA directivity patterns are expressed in dBiL.

**Table 2-4: TLGA parameters**

| Parameter | Value |
|---|---|
| Design | Biconical horn |
| Receive frequency, MHz | 7153.065586 channel 6 |
| Transmit frequency, MHz | 8404.135802 channel 6 |
| Required gain, boresight, dBic | 5.5 ± 0.5 receive<br>6.5 ± 0.5 transmit |
| Polarization | RHCP |
| Beamwidth, deg | ± 10.0 receive<br>± 10.0 transmit |
| Axial ratio, on boresight, dB | <2.0 for ± 10 deg |

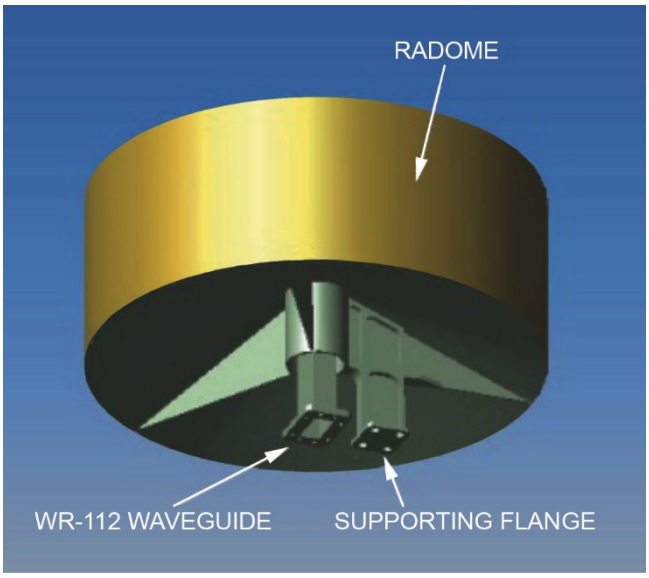


(a)

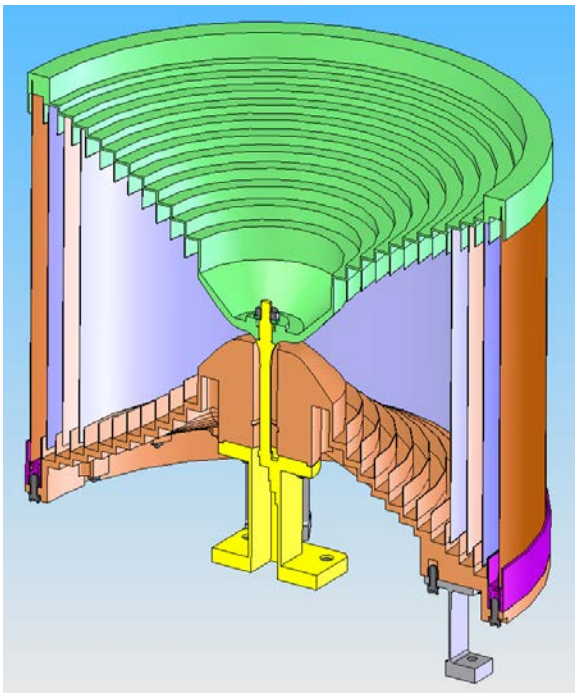

(b)

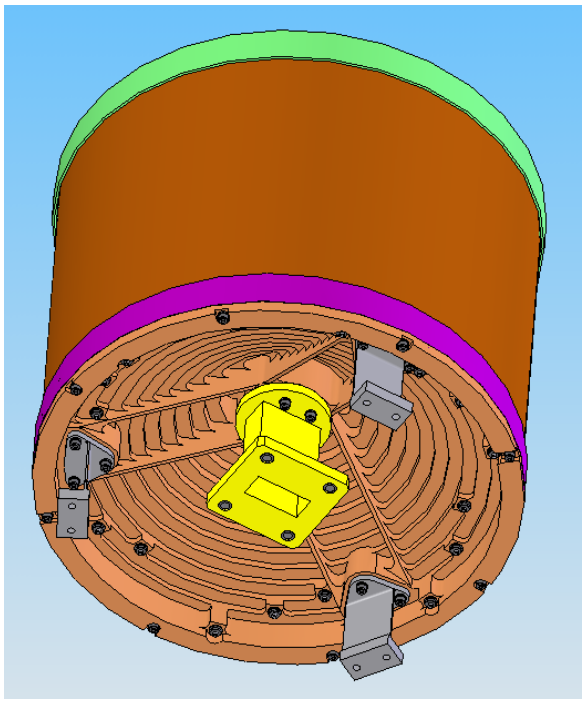

(c)

**Figure 2-10: External and internal views of TLGA: (a) side view under dome; (b) biconical horn; (c) bottom and waveguide connector.**

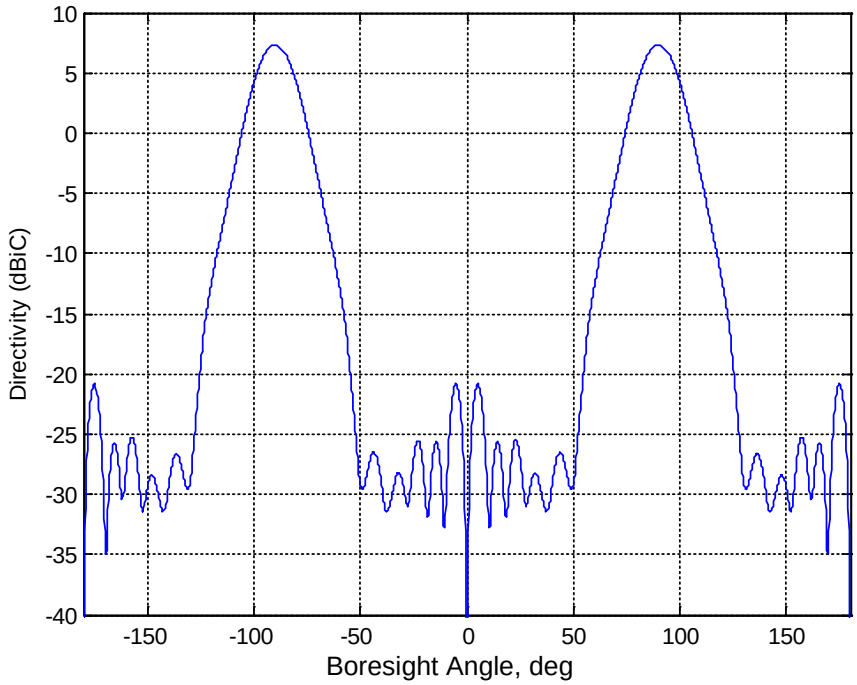


**Figure 2-11: TLGA transmit gain pattern.**

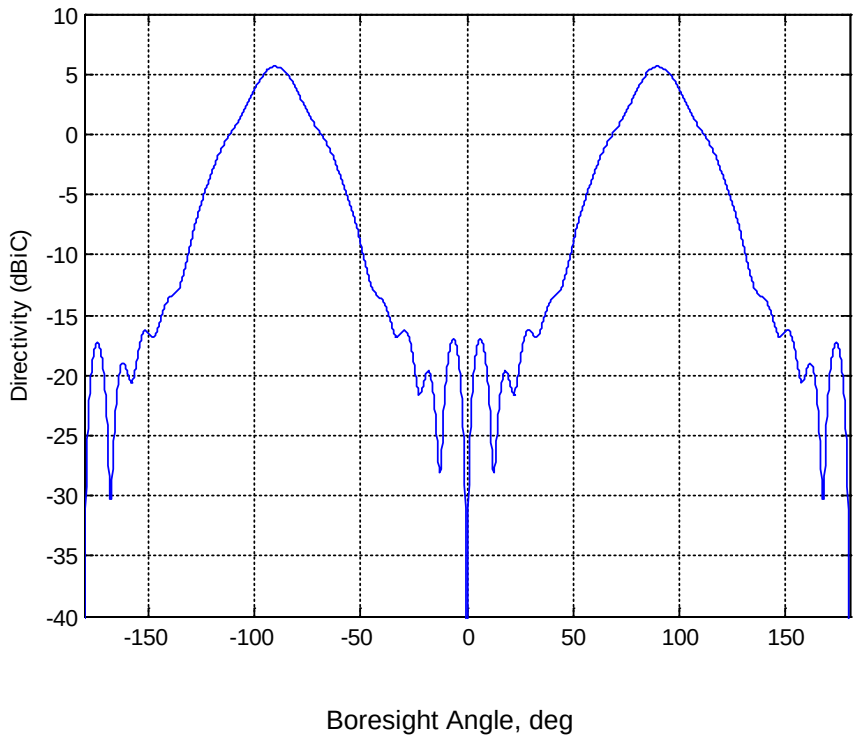


**Figure 2-12: TLGA receive gain pattern.**

### *2.1.4.3 Medium-Gain Antenna (MGA)*

The medium-gain antenna (MGA) was used for communications during Cruise and is being used for safe mode on orbit. It may also be used for the post-orbital trim maneuver (OTM) navigation passes. The Juno MGA is the same design as the Mars Exploration Rover (MER) MGA.

The MGA is attached adjacent to the HGA, aligned to the spacecraft spin axis (+Z). See Figure 2-5 for the MGA placement and size relative to the 2.5-m diameter HGA.

Figure 2-13 shows a photograph and a drawing to illustrate the MGA. The brick color in the drawing shows the antenna horn, and the pink and red colors show the mechanical support and the waveguide feed up to the horn.

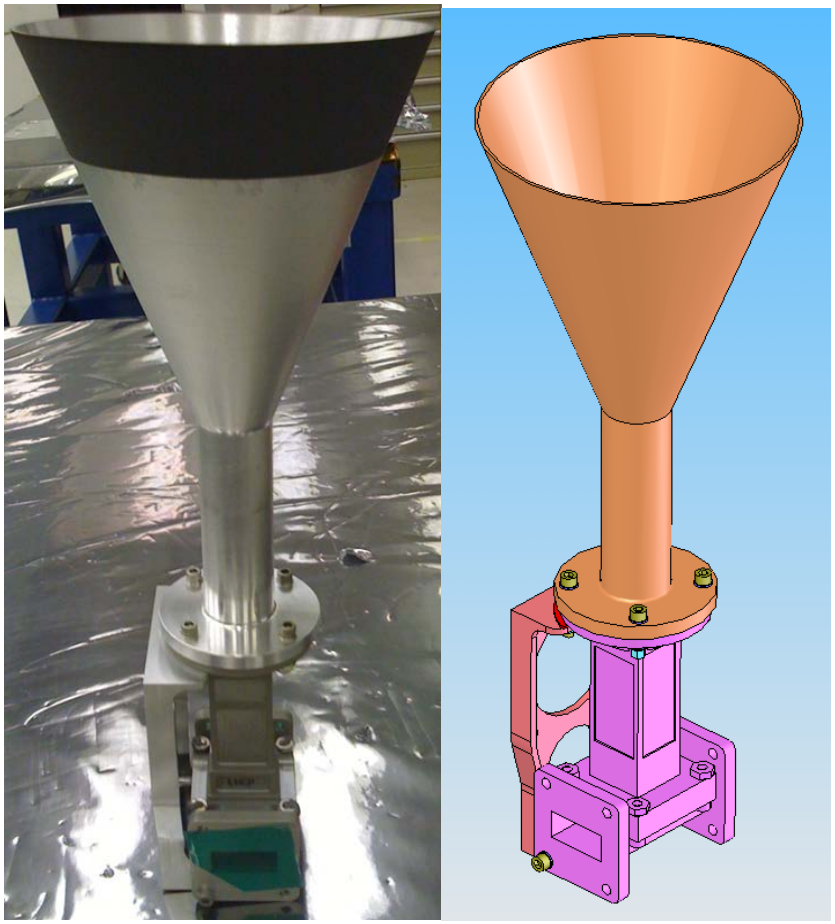

**Figure 2-13: Photograph (left) and drawing (right) of the MGA.**

Table 2-5 summarizes the main parameters. Figures 2-14 and 2-15 provide gain patterns, assuming an ideal polarizer. Each shows the co-polarized pattern in blue and the cross-polarized pattern in red. This results in the blue curve being the RHCP pattern when the RHCP port of the polarizer is in use and being the LHCP pattern when the LHCP port is in use. In these figures, gain is measured in dBic, and the term CP in the title stands for circular polarization.

**Table 2-5: MGA parameters.**

| Parameter | Value |
|---|---|
| Design | RF conical horn |
| Receive frequency, MHz | 7153.065586 channel 6 |
| Transmit frequency, MHz | 8404.135802 channel 6 |
| Required gain, boresight, dBic | 18.1 ± 0.4 receive<br>18.8 ± 0.4 transmit |
| Polarization | RHCP and LHCP |
| 3 dB beamwidth, deg | ± 10.3 receive<br>± 9.3 transmit |
| Axial Ratio, on boresight, dB | 1.01 receive; 0.27 transmit |
| Axial Ratio, 20 deg off boresight, dB | 6.29 receive; 7.53 transmit |

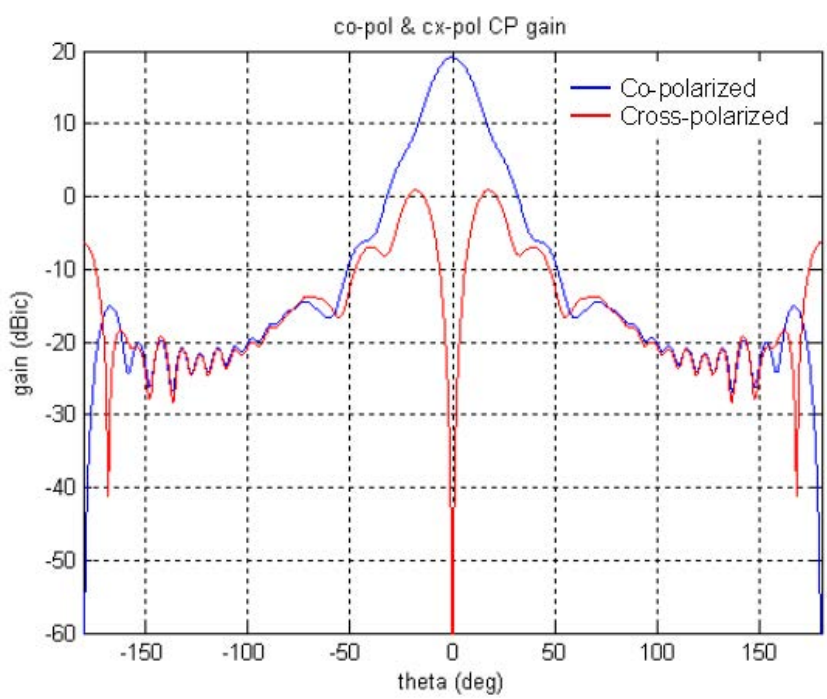


**Figure 2-14: MGA downlink gain pattern.**

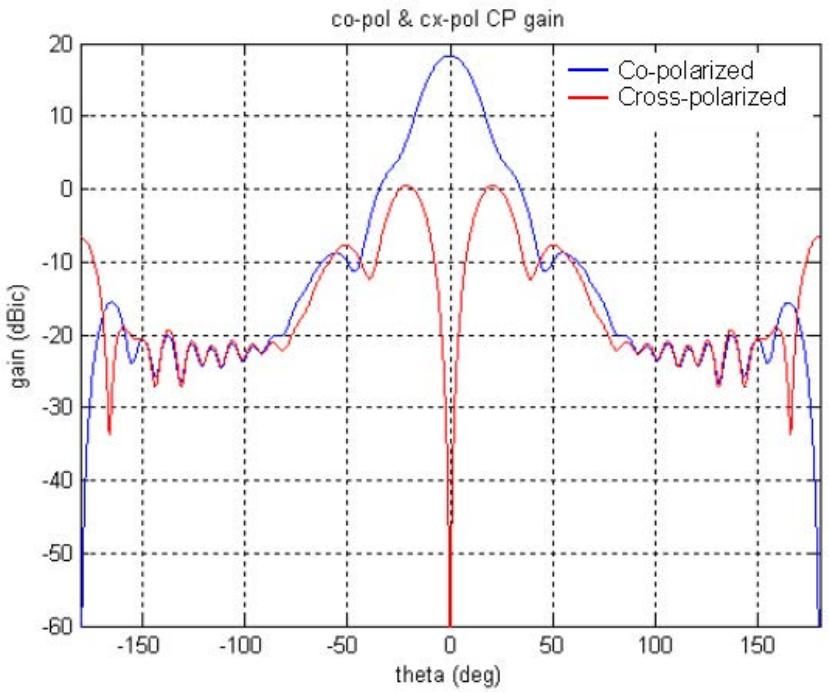


**Figure 2-15: MGA uplink gain pattern.**

### *2.1.4.4 Forward Low-Gain Antenna and Aft Low-Gain Antenna*

The forward low-gain antenna and the aft low-gain antenna (FLGA and ALGA) were used during early Cruise, and they were also used for near-Earth communications (around Earth Flyby) and after fault responses. With a gain about 10 dB lower than that of the MGA (compare Table 2-5 and Table 2-6), the LGAs are not used during Jupiter orbit operations.

The FLGA boresight is aligned along the S/C +Z axis as shown in Figure 2-5.

The design for the antennas is the same as the MRO LGA. Figure 2-16 includes a color-coded drawing of the LGA, as well as photographs of the FLGA and ALGA. In the drawing, similar to the MGA, the red and pink show the mechanical support and the waveguide transition, respectively, while the yellow shows the antenna radiating element.

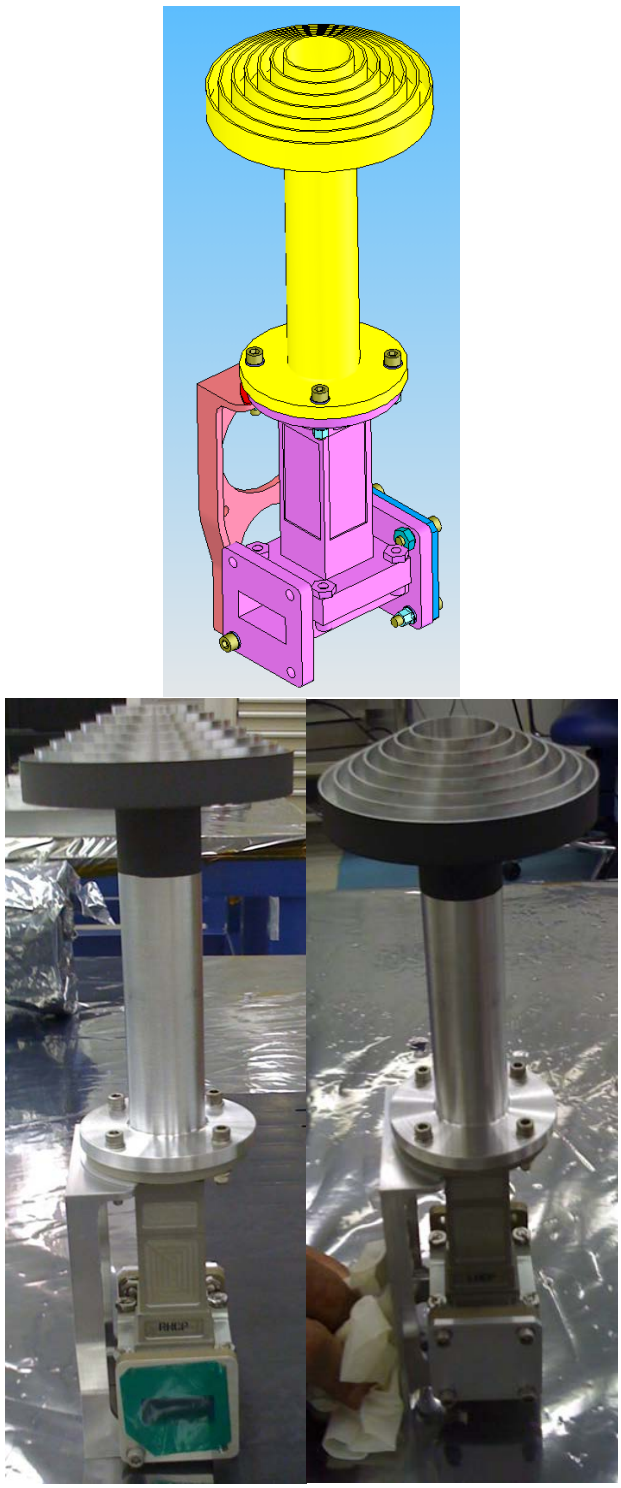

**Figure 2-16: Forward (left) and Aft (right) LGAs with concept above.**

Table 2-6 summarizes the main parameters, while Figures 2-17 and 2-18 present the antenna downlink and uplink patterns. Parameter values and patterns are considered identical for FLGA and ALGA for link modeling.

**Table 2-6: LGA parameters.**

| Parameter | Value |
|---|---|
| Design | Choked horn |
| Receive frequency, MHz | 7153.065586 channel 6 |
| Transmit frequency, MHz | 8404.135802 channel 6 |
| Required gain, boresight, dBic | 8.7 ± 0.4 dB receive<br>7.7 ± 0.4 dB transmit |
| Polarization | RHCP |
| 3-dB beamwidth | ± 40 deg receive<br>± 42 deg transmit |
| Axial ratio, on boresight | 2.0 dB receive<br>2.0 dB transmit |

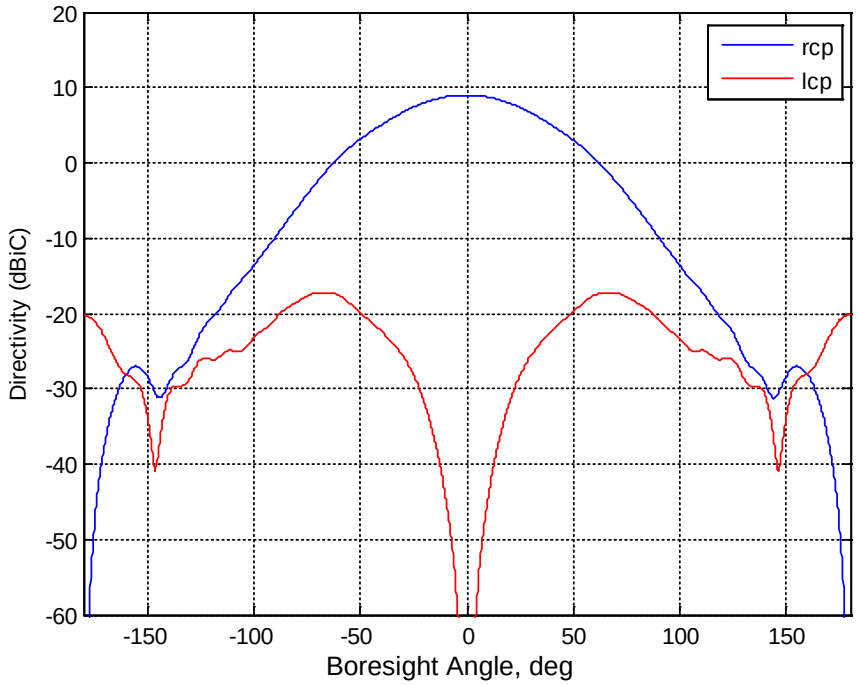


**Figure 2-17: LGA downlink gain.**

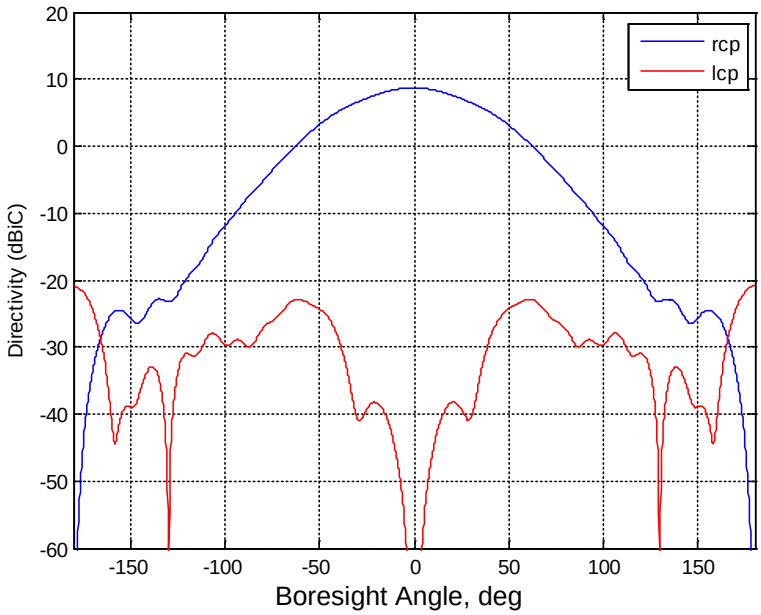


**Figure 2-18: LGA uplink gain.**

### 2.1.5 Waveguide Transfer Switch

The Waveguide Transfer Switches (WTSes) are MER heritage. Switches for both Juno and MSL are provided by Sector Microwave, with slight modifications based on MRO flight experience. Table 2-7 defines the top-level parameters for the switch, and Figure 2-19 shows a picture of a WTS.

**Table 2-7: WTS parameters.**

| Parameter | Value |
|---|---|
| Insertion Loss | < 0.05 dB at 7.1 GHz and 8.4 GHz |
| Isolation between unconnected RF ports | > 55 dB |

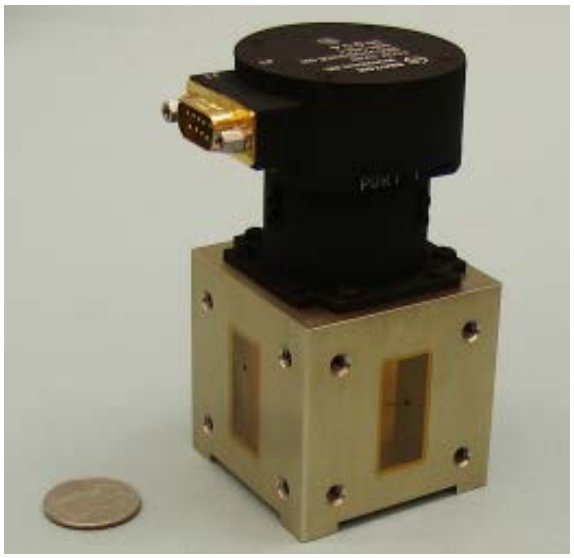

**Figure 2-19: Picture of a WTS (quarter provided for scale).**

### 2.1.6 X-Band Diplexer

The diplexer is a passive device connecting a receiver, a transmitter, and an antenna. The purpose of a diplexer's filters is to allow signals to be radiated by the antenna at one frequency while much weaker signals are received from the antenna at another frequency. On Juno, the diplexer reduces the TWTA output at the input of the SDST receiver to a safe and non-interfering level.

The Juno baseline design is MER residual hardware built by MCCI.

Table 2-8 defines the top-level parameters for the diplexer and Figure 2-20 is a photograph of several MER diplexers.

**Table 2-8: X-band diplexer parameters.**

| Parameter | Condition | Value |
|---|---|---|
| Passband: | Transmit (TX) | 8.29–8.545 GHz |
| | Receive (RX) | 7.1–7.23 GHz |
| Insertion loss | TX | 0.3 dB max |
| | RX | 0.3 dB max |
| Passband voltage standing wave ratio (VSWR) | TX port, RX port, or Antenna Port | 1.15:1 max (representative) |
| Isolation | TX/RX | > 120 dB (7.1 to 7.2 GHz)<br>> 50 dB (8.4 to 8.5 GHz<br>> 35 dB (2nd harmonic)<br>> 35 dB (3rd harmonic)<br>> 35 dB (4th harmonic) |
| Group delay variation | | < 300 picoseconds (ps) in any 1-MHz range in the receive and transmit |

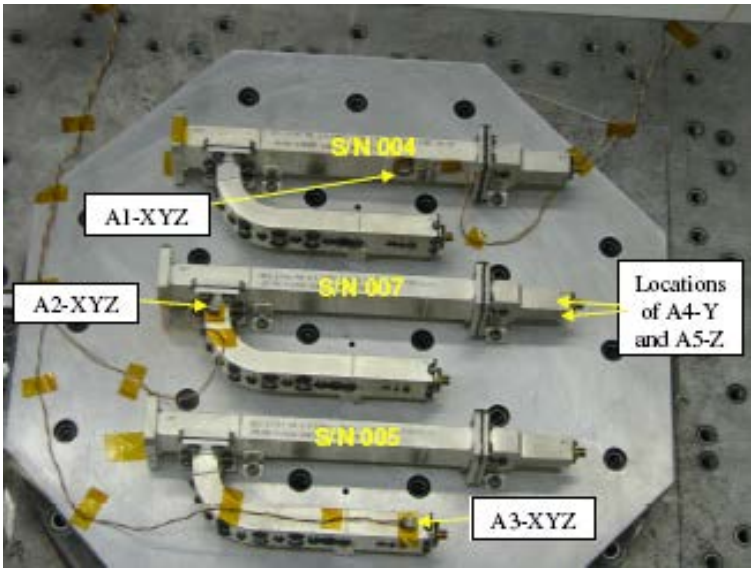


**Figure 2-20: Photograph of several MER diplexers.**

## 2.2 Ka-Band Radio Science

### 2.2.1 Ka-Band Translator – KaTS

The KaTS is a Ka/Ka translator (also sometimes called a transponder, analogous to the SDST) that is used for Gravity Science Doppler tracking at Jupiter. It is a science instrument provided to the Juno project by the Italian Space agency (ASI) and is built by Thales Alenia Space-Italy (TAS-I) It receives a Ka-band uplink carrier from DSS 25 at 34 GHz and returns a frequency-translated downlink carrier at 32 GHz, amplified to an output power of 2.5 W (34 dBm). The turn-around ratio is 3360/3599.

Figure 2-21 shows an illustration of the KaTS unit. Table 2-9 lists some of the KaTS parameters, and Figure 2-22 shows the KaTS software architecture. For more detail, see Ref. [13].

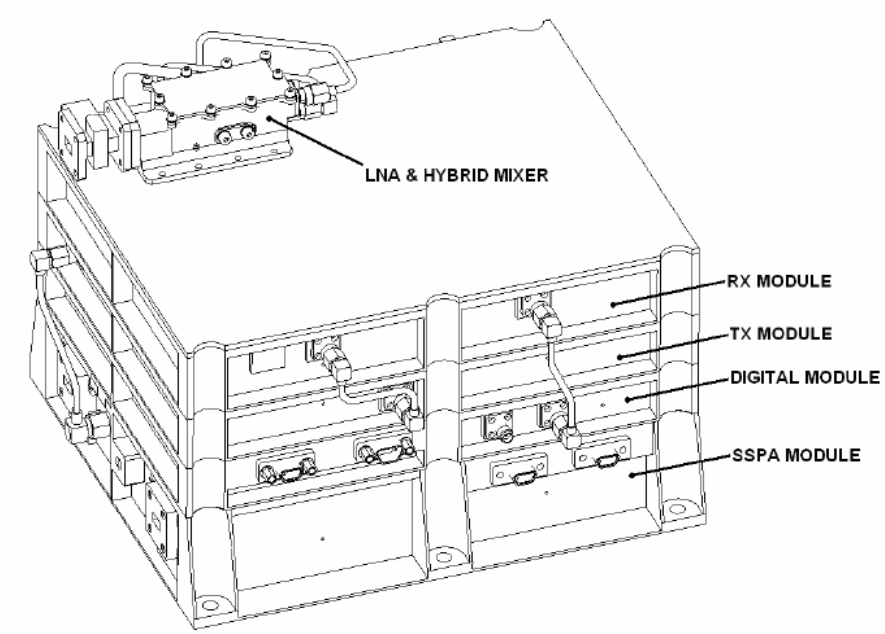


**Figure 2-21: KaTS external view with labeled modules.**

The Ka-band uplink and downlink are exclusively via the HGA.

**Table 2-9: KaTS parameters [3].**

| Parameter | Value | Comments |
|---|---|---|
| Receiver input frequency | 34365.5 ± 3 MHz | DSN channel 5 |
| Frequency output to SSPA | 32088.5 ± 3 MHz | DSN channel 6 |
| Downlink frequency | 32083.3 MHz | Coherent or noncoherent |
| Downlink/uplink turnaround ratio | 3360/3599 | |
| Receiver input power range | –130 dBm to –90 dBm | |
| Receiver acquisition threshold | –130 dBm | With 4 kHz/s frequency rate |
| Receiver tracking threshold | –135 dBm | With 1.2 kHz/s frequency rate |
| SSPA RF input power | +2 dBm | |
| SSPA RF output power | +34 dBm | |
| Operating temperature | –31.5 C to +60 C | |
| Warmup time | 15 minutes | |

The JUNO KaTS design is based on a combination of advanced signal processing algorithms and modern technological implementation [3]. The KaTS core, based on a digital architecture, led to the following advantages relative to an analog design:

1. Optimization of carrier acquisition and tracking performances.
2. Receiver tuning based on programmable constants.
3. Frequency plan based on direct digital frequency synthesis.

Names and acronyms in Figure 2-22 not defined elsewhere include IFOC = IF-on-chip, OCXO = oven controlled quartz oscillator, μC = micro controller, NCO = numerically controlled oscillator, PFD = phase frequency detector, and SPD = sampling phase detector.

The KaTS is housed in a relatively small box composed of four stacked modules in aluminum alloy (AA6082 T6) with gold-over-nickel plating. The KaTS box has six type M4 fixing screws, allowing the contact surface to dissipate about 45 watts (W) through the S/C mounting panel, while the lateral wall thickness helps to protect the electronics against radiation. Also, as shown in Figure 2-1, the KaTS is inside the radiation-shielding vault.

The housing has 24 venting holes to reduce differential pressure between the interior and the exterior during the launch phase. The box is painted with Aeroglaze Z307 (black) to meet emissivity requirements.

Figure 2-23 is a top view photograph of the exterior of the KaTS. Figure 2-24 is a three-dimensional view of the KaTS with its modules.

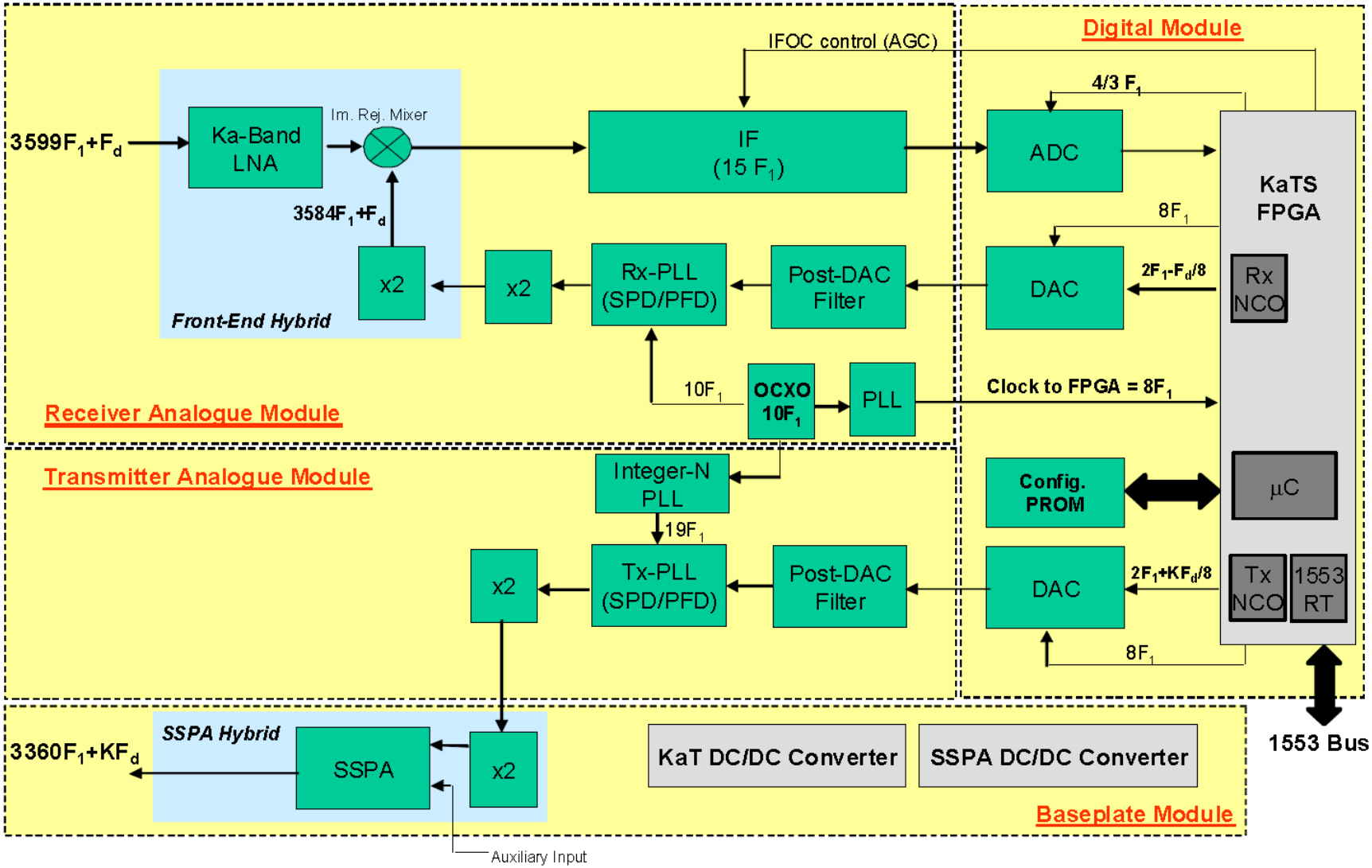


**Figure 2-22: KaTS architecture block diagram [13].**

**Figure 2-23: The KaTS manufacturer's photo.**

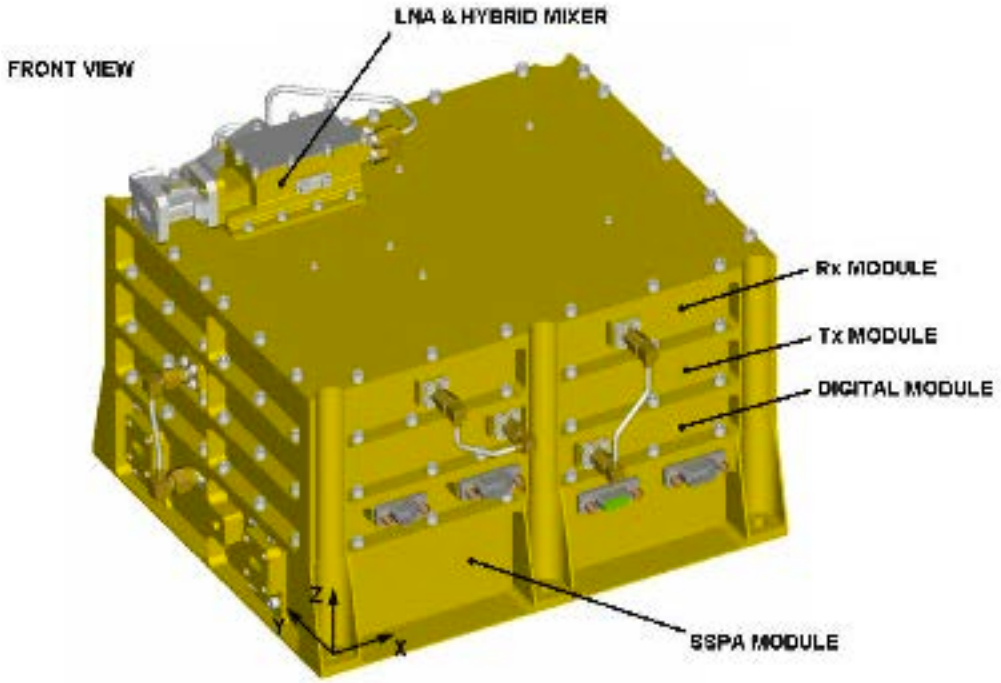


**Figure 2-24: KaTS illustration with modules [3].**

## 2.3 Subsystem Power and Mass Estimates

Table 2-10 shows the Juno Telecom Power and Mass Equipment List.

Note that the KaTS is powered off except during checkout and during gravity science operations.

**Table 2-10: Juno telecommunications power and mass equipment list.**

| Component | Units | Input Power, W | Mass/Unit, kg | Component Masses, kg |
|---|---|---|---|---|
| SDST (X/X/Ka) | 1 | 16.4 | | 3.2 |
| SDST (X/S) | 1 | 15.7 | | 3.0 |
| TWTA | 2 | 54.0 | 2.4 | 4.8 |
| KaTS | | 46.2 | | 3.1 |
| HGA | 1 | | | 21.3 |
| MGA | 1 | | | 0.5 |
| TLGA | 1 | | | 1.9 |
| FLGA | 1 | | | 0.5 |
| ALGA | 1 | | | 0.6 |
| Diplexer | 2 | | 0.4 | 0.8 |
| Isolator | 2 | | 0.55 | 1.1 |
| WTS | 5 | | 0.44 | 2.2 |
| X-band waveguide | 1 | | | 6.3 |
| X-band coax cable | 1 | | | 0.9 |
| Ka-band waveguide | 1 | | | 0.2 |
| Telecom panel | 1 | | | 26.7 |
| Miscellaneous microwave | | | | 1.0 |
| Harness, fasteners, etc. | | | | 5.1 |
| | | | | |
| **Total power** (X-band) | | 70.4 | | |
| **Total power** (X/Ka) | | 116.6 | | |
| **Total Mass** | | | | 83.2 |

**Blank**

# 3 Link Performance

## 3.1 Summary of Link Performance

Below is a summary of the link performance for the different phases of the mission.

- Initial Acquisition
  - Juno performed initial acquisition over Canberra through the coupled LGAs. Because of the very strong downlink signal at initial acquisition, Juno planned the links the same as other recent deep space missions: (1) defining a prime and a backup station for downlink and for uplink, (2) scheduling 34-m stations, and (3) setting station downlink polarization to LHCP to reduce the received power from the RHCP downlink to prevent equipment damage. The data rate was 1745 bps with Reed–Solomon coding and an interleave depth of 5.
- Cruise
  - Cruise communications generally exceed requirements of 100 bps TLM rate and 7.8125 bps CMD rate.
  - Mission planning assumed ranging on for most passes during Cruise.
  - There was one brief period before Earth Flyby, when a switch from the toroidal antenna to the ALGA was made. The performance from either antenna had minimal margin due to large off-boresight angles.
  - The S/C transitioned from use of the ALGA to use of the FLGA during Earth Flyby—Note: no switching was required because the two antennas are coupled together.
- Orbital Operations
  - Juno is nominally on the HGA throughout orbital operations except for brief tracking periods after orbit trim maneuvers (OTMs). The MGA is available for Doppler tracking during these periods.
  - The Telecom Subsystem design supports a minimum telemetry rate of 18 kbps into a DSN 34-m ground station for a nominal pass.
- Critical Event Coverage
  - Telecom coverage during the main engine burns is through the TLGA, downlink only.
  - At these times, there is no telemetry capability, but the link will support tones to a 70-m ground station.
- Safe Mode
  - In safe mode, a 70-m ground station is assumed for all support.
  - Minimum data rates are 7.8125 bps for command and 10 bps for telemetry.
  - The spacecraft maintains its attitude with respect to the Sun. Antenna switching is used to maintain communications (for example, HGA to MGA in orbit operations.)

Table 3-1 summarizes X-band uplink conditions (optimum modulation index and threshold signal level (uplink $P_t/N_o$)) as a function of command rate.

**Table 3-1: Uplink thresholds and modulation indices.**

| | | No Ranging | Ranging on (3 dB U/L suppr.) |
|---|---|---|---|
| **CMD Rate** | **Mod Index (radians)** | **Req'd $P_t/N_o$** | **Req'd $P_t/N_o$** |
| 7.8125 | 0.94 | 25.44 | 28.44 |
| 15.625 | 1.2 | 26.95 | 29.95 |
| 31.25 | 1.3 | 29.72 | 32.72 |
| 62.5 | 1.5 | 32.35 | 35.35 |
| 125 | 1.5 | 33.97 | 36.97 |
| 250 | 1.5 | 37.11 | 40.11 |
| 500 | 1.5 | 39.93 | 42.93 |
| 1000 | 1.5 | 43.1 | 46.1 |
| 2000 | 1.5 | 46.13 | 49.13 |

Table 3-2 and Table 3-3 summarize X-band downlink conditions (optimum modulation index and threshold signal level (downlink $P_t/N_o$)) as a function of telemetry rate. Table 3-2 is for standard turnaround ranging on the downlink and Table 3-3 for no ranging.

**Table 3-2: Telemetry modes and thresholds with turnaround ranging on.**

| Juno Downlink Telemetry Reference Table (With Ranging) | | | | | | |
|---|---|---|---|---|---|---|
| **Nominal Rate** | **Actual BPS** | **Symbol Rate** | **Coding** | **Mod Index (deg)** | **Subcarrier** | **Req'd $P_t/N_o$** |
| 10 | 12 | 23 | RS+(7,1/2) short | 46 | 25 kHz | 19.15 |
| 40 | 47 | 93 | RS+(7,1/2) short | 60 | 25 kHz | 22.08 |
| 100 | 100 | 602 | Turbo-1/6 | 63.25 | 25 kHz | 22.87 |
| 250 | 250 | 1,505 | Turbo-1/6 | 70 | 25 kHz | 26.21 |
| 1,000 | 1,000 | 6,018 | Turbo-1/6 | 72 | 25 kHz | 31.77 |
| 1,745 | 2,000 | 4,000 | RS+(7,1/2) long | 72 | 25 kHz | 36.10 |
| 2,000 | 2,000 | 12,036 | Turbo-1/6 | 72 | 281.25 kHz | 34.69 |
| 4,000 | 4,002 | 24,088 | Turbo-1/6 | 72 | 281.25 kHz | 37.49 |
| 12,000 | 12,011 | 72,289 | Turbo-1/6 | 72 | 281.25 kHz | 42.04 |
| 18,000 | 18,036 | 108,553 | Turbo-1/6 | 72 | 281.25 kHz | 43.74 |
| 22,000 | 21,931 | 132,000 | Turbo-1/6 | 72 | 281.25 kHz | 44.59 |
| 26,000 | 25,893 | 155,844 | Turbo-1/6 | 72 | 281.25 kHz | 45.29 |
| 30,000 | 30,125 | 181,319 | Turbo-1/6 | 72 | 281.25 kHz | 45.90 |
| 35,000 | 34,978 | 210,526 | Turbo-1/6 | 72 | Direct BPSK | 46.55 |
| 40,000 | 39,875 | 240,000 | Turbo-1/6 | 72 | Direct BPSK | 47.12 |
| 50,000 | 49,844 | 300,000 | Turbo-1/6 | 72 | Direct BPSK | 48.06 |
| 100,000 | 99,687 | 600,000 | Turbo-1/6 | 72 | Direct BPSK | 51.00 |
| 120,000 | 119,191 | 717,391 | Turbo-1/6 | 72 | Direct BPSK | 51.78 |
| 150,000 | 152,300 | 916,667 | Turbo-1/6 | 72 | Direct BPSK | 52.73 |
| 200,000 | 199,375 | 1,200,000 | Turbo-1/6 | 72 | Direct BPSK | 53.95 |

**Table 3-3: Telemetry modes and thresholds with turnaround ranging off.**

| Juno Downlink Telemetry Reference Table (No Ranging) | | | | | | |
|---|---|---|---|---|---|---|
| **Nominal Rate** | **Actual BPS** | **Symbol Rate** | **Coding** | **Mod Index (deg)** | **Subcarrier** | **Req'd $P_t/N_o$** |
| 10 | 12 | 23 | RS+(7,1/2) short | 46 | 25 kHz | 18.86 |
| 40 | 47 | 93 | RS+(7,1/2) short | 60 | 25 kHz | 21.78 |
| 100 | 100 | 602 | Turbo-1/6 | 63.25 | 25 kHz | 22.57 |
| 250 | 250 | 1,505 | Turbo-1/6 | 70 | 25 kHz | 25.91 |
| 1,000 | 1,000 | 6,018 | Turbo-1/6 | 72 | 25 kHz | 31.47 |
| 1,745 | 2,000 | 4,000 | RS+(7,1/2) long | 72 | 25 kHz | 35.80 |
| 2,000 | 2,000 | 12,036 | Turbo-1/6 | 72 | 281.25 kHz | 34.39 |
| 4,000 | 4,002 | 24,088 | Turbo-1/6 | 74 | 281.25 kHz | 37.19 |
| 12,000 | 12,011 | 72,289 | Turbo-1/6 | 76 | 281.25 kHz | 41.74 |
| 18,000 | 18,036 | 108,553 | Turbo-1/6 | 76 | 281.25 kHz | 43.44 |
| 22,000 | 21,931 | 132,000 | Turbo-1/6 | 76 | 281.25 kHz | 44.29 |
| 26,000 | 25,893 | 155,844 | Turbo-1/6 | 77 | 281.25 kHz | 44.99 |
| 30,000 | 30,125 | 181,319 | Turbo-1/6 | 77 | 281.25 kHz | 45.60 |
| 35,000 | 34,978 | 210,526 | Turbo-1/6 | 77 | Direct BPSK | 46.25 |
| 40,000 | 39,875 | 240,000 | Turbo-1/6 | 78 | Direct BPSK | 46.82 |
| 50,000 | 49,844 | 300,000 | Turbo-1/6 | 78 | Direct BPSK | 47.76 |
| 100,000 | 99,687 | 600,000 | Turbo-1/6 | 80 | Direct BPSK | 50.70 |
| 120,000 | 119,191 | 717,391 | Turbo-1/6 | 80 | Direct BPSK | 51.48 |
| 150,000 | 152,300 | 916,667 | Turbo-1/6 | 80 | Direct BPSK | 52.43 |
| 200,000 | 199,375 | 1,200,000 | Turbo-1/6 | 80 | Direct BPSK | 53.65 |

In these tables, the first three columns indicate the nominal bit rate in bps, the actual information rate in bps, and the symbol rate in symbols/second on the RF channel between Juno and the ground station. The symbol rate is a function of the information rate and the coding. Note in the second column from the right that the telemetry modulation index values in the two tables differ for rates of 40 kbps and higher, depending on whether ranging is present on the downlink carrier. The rightmost column indicates the required $Pt/N_o$ for the combination of data rate, coding, modulation index, and absence or presence of simultaneous ranging modulation.

## *3.2 Detailed Link Performance*

### 3.2.1 Link Performance Assumptions

Juno will primarily use the DSN 34-m subnet. For nominal communications with any 34-m station, the performance of DSS-34 is used to make long-range predictions. For Gravity Science planning, predictions are made specifically for DSS-25, the only station having Ka-band uplink. For Safe Mode, when a 70-m antenna is used, DSS-63 (Madrid, Spain) is assumed. For certain unique events (e.g., JOI), a specific DSN antenna is specified by the project.

A 90-percent weather model is used for all links. X-band links assume a 15-deg elevation angle while Ka-band links use a 20-deg elevation angle. The link capability plots assume free space antenna patterns. A 2-sigma statistical margin is kept for all link budgets. The required uplink bit error rate (BER) is $1 \times 10^{-5}$. The required downlink BER is $1 \times 10^{-6}$. In terms of downlink threshold signal level (specifically $E_b/N_o$), this downlink BER requirement is nearly identical to the frame error rate (FER) of $1 \times 10^{-4}$, that is shown in the design control tables (sometimes called link budgets) starting with Table 3-4.

## Table 3-4 Juno Cruise HGA X-band downlink DCT.

Produced by JUNO V2.1 XML 5/5/2011

---

| | |
|---|---|
| Predict | 2012-187T19:12:00000 UTC |
| Up/down-link | Two-Way |
| RF band | X:X |
| Diplex mode | N/A |
| LNA selection | LNA-1 |
| Telecom link | DSS26-HighGain-DSS26 |

---

TELEMETRY DOWN-LINK PARAMETER INPUTS

| | |
|---|---|
| Encoding | Turbo (8920,1/6) |
| Carrier tracking | Residual |
| Oscillator | 2 Way VCO |
| Subcarrier mode | Squarewave |
| PLL Bandwidth | 3.00 Hz |
| Tlm usage | Engineering |
| Tlm data rate/mod index | 120000 bps/ 72.00 deg |
| Tlm rng/DOR Mod Index | 0.31 rad/ 0.00 deg |

---

| | |
|---|---|
| Operations mode | Nominal |
| Mission phase | Cruise |
| DSN site | Gold-Gold |
| DSN elevation | In view |
| Weather/CD | 90 |
| Attitude pointing | Earth pointed |

---

EXTERNAL DATA
SPICE Kernels (in load order)
(omitted from this article)

| | | |
|---|---|---|
| Range | (km) | 4.7456e+08 |
| Range | (AU) | 3.1722e+00 |
| DL one-way light time (hh:mm:ss) | | 00:26:22 |
| Station elevation (deg) | | 59.65 |
| DL DOFF: Hga (deg) | | 0.25 |
| DL Clk: Hga (deg) | | 0.36 |
| Added S/C Pnt Offset (deg) | | 0.25 |

---

DSN site considered: DSS-26/DSS-26
At time: 2012-187T19:12:00.000 UTC

---

| Link Parameter | Unit | Design Value | Fav Tol | Adv | Mean Value | Var |
|---|---|---|---|---|---|---|
| TRANSMITTER PARAMETERS | | | | | | |
| 1. S/C transmitter power | dBm | 44.40 | 0.30 | 0.00 | 44.50 | 0.0050 |
| 2. S/C Xmit circuit loss | dB | -0.90 | 0.10 | -0.10 | -0.90 | 0.0033 |
| 3. S/C Antenna Gain | dBi | 44.70 | 0.50 | -0.50 | 44.70 | 0.0417 |
| 4. Degrees-off-boresight (DOFF) loss | dB | 0.93 | -0.00 | -0.00 | 0.93 | 0.0000 |
| 5. S/C transmit pointing loss | dB | 0.00 | 0.00 | 0.00 | 0.00 | 0.0000 |
| 6. EIRP (1+2+3-4+5) | dBm | 87.37 | 0.67 | -0.67 | 87.37 | 0.0500 |
| PATH PARAMETERS | | | | | | |
| 7. Space loss | dB | -284.46 | 0.00 | 0.00 | -284.46 | 0.0000 |
| 8. Atmospheric attenuation | dB | -0.06 | 0.00 | 0.00 | -0.06 | 0.0000 |

Continues on next page

Continued from previous page

| Link Parameter | Unit | Design Value | Fav Tol | Adv Tol | Mean Value | Var |
|---|---|---|---|---|---|---|
| RECEIVER PARAMETERS | | | | | | |
| 9. DSN antenna gain | dBi | 68.26 | 0.10 | -0.20 | 68.22 | 0.0039 |
| 10. DSN antenna pointing loss | dB | -0.10 | 0.10 | -0.10 | -0.10 | 0.0033 |
| 11. Polarization loss | dB | -0.05 | 0.10 | -0.10 | -0.05 | 0.0033 |
| TOTAL POWER SUMMARY | | | | | | |
| 12. Tot Rcvd Pwr (6+7+8+9+10+11) | dBm | -129.08 | -0.74 | 0.74 | -129.08 | 0.0606 |
| 13. SNT due to Antenna-MW | K | 16.33 | -1.00 | 2.00 | 16.67 | 0.3889 |
| 14. SNT due to Atmosphere | K | 3.68 | 0.00 | 0.00 | 3.68 | 0.0000 |
| 15. SNT due to Cosmic Backgnd | K | 2.69 | 0.00 | 0.00 | 2.69 | 0.0000 |
| 16. SNT due to the Sun | K | 0.00 | 0.00 | 0.00 | 0.00 | 0.0000 |
| 17. SNT due to other Hot Bodies | K | 0.00 | 0.00 | 0.00 | 0.00 | 0.0000 |
| 18. SNT (13+14+15+16+17) | K | 22.70 | -1.00 | 2.00 | 23.03 | 0.3889 |
| 19. Noise Spectral Density | dBm/Hz | -185.04 | -0.20 | 0.37 | -184.98 | 0.0136 |
| 20. Received Pt/No (12-19) | dB-Hz | 55.90 | 0.82 | -0.82 | 55.90 | 0.0741 |
| 21. Received Pt/No, mean-2 Sigma | dB-Hz | 55.36 | 0.00 | 0.00 | 55.36 | 0.0000 |
| 22. Required Pt/No | dB-Hz | 51.80 | 0.00 | 0.00 | 51.80 | 0.0000 |
| 23. Pt/No Margin (20–22) | dB | 4.10 | 0.82 | -0.82 | 4.10 | 0.0741 |
| 24. Pt/No Margin, mean-2 Sigma (21–22) | dB | 3.55 | 0.00 | -0.00 | 3.55 | 0.0000 |
| CARRIER PERFORMANCE | | | | | | |
| 25. Recovered Pt/No (20+[AGC+BPF]) | dB-Hz | 55.90 | 0.82 | -0.82 | 55.90 | 0.0741 |
| 26. Telemetry Carrier Suppression | dB | -10.20 | 1.52 | -1.89 | -10.32 | 0.4854 |
| 27. Ranging Carrier Suppression | dB | -0.30 | 0.06 | -0.06 | -0.30 | 0.0006 |
| 28. DOR Carrier Suppression | dB | 0.00 | -0.00 | -0.00 | -0.00 | 0.0000 |
| 29. Carrier Power (AGC) (12+26+27+28) | dBm | -139.70 | -2.22 | 2.22 | -139.70 | 0.5466 |
| 30. Received Pc/No (25+26+27+28) | dB-Hz | 45.28 | 2.25 | -2.25 | 45.28 | 0.5602 |
| 31. Carrier Loop Noise BW | dB-Hz | 4.77 | 0.00 | 0.00 | 4.77 | 0.0000 |
| 32. Carrier Phase Error Var (from 30,31,xpond,solar) | rad^2 | 4.8e-03 | 0.00 | 0.00 | 4.8e-03 | 0.0000 |
| 33. Carrier Loop SNR (CNR) (from 32) | dB | 23.19 | 2.25 | -2.25 | 23.19 | 0.5602 |
| 34. CNR, mean-2 Sigma | dB | 21.69 | 0.00 | 0.00 | 21.69 | 0.0000 |
| 35. Recommended CNR | dB | 10.00 | 0.00 | 0.00 | 10.00 | 0.0000 |
| 36. CNR Margin (33–35) | dB | 13.19 | 2.25 | -2.25 | 13.19 | 0.5602 |
| 37. CNR Margin, mean-2 Sigma (34–35) | dB | 11.69 | 0.00 | -0.00 | 11.69 | 0.0000 |
| TELEMETRY PERFORMANCE | | | | | | |
| 38. Telemetry Data Suppression | dB | -0.44 | -0.20 | 0.16 | -0.45 | 0.0053 |
| 39. Ranging Data Suppression | dB | -0.30 | 0.06 | -0.06 | -0.30 | 0.0006 |
| 40. DOR Data Suppression | dB | 0.00 | -0.00 | -0.00 | -0.00 | 0.0000 |
| 41. Received Pd/No (25+38+39+40) | dB-Hz | 55.15 | 0.85 | -0.85 | 55.15 | 0.0800 |
| 42. Received Pd/No, mean-2 Sigma | dB-Hz | 54.59 | 0.00 | 0.00 | 54.59 | 0.0000 |
| 43. Data Rate, Symbols (dB-Hz) | dB-Hz | 50.79 | 0.00 | 0.00 | 50.79 | 0.0000 |
| 44. Available Eb/No (41-43) | dB | 4.36 | 0.85 | -0.85 | 4.36 | 0.0800 |
| 45. Radio Loss | dB | 0.30 | 0.00 | 0.00 | 0.30 | 0.0000 |
| 46. Subcarrier Demod Loss | dB | 0.00 | 0.00 | 0.00 | 0.00 | 0.0000 |
| 47. Symbol Sync Loss | dB | 0.00 | 0.00 | 0.00 | 0.00 | 0.0000 |
| 48. Decoder Loss | dB | -0.00 | -0.00 | -0.00 | -0.00 | 0.0000 |
| 49. Waveform Distortion Loss | dB | 0.10 | -0.10 | 0.10 | 0.10 | 0.0017 |
| 50. SDST Filtering Loss | dB | -0.08 | -0.00 | -0.00 | -0.08 | 0.0000 |
| 51. High Rate Ranging Loss | dB | -0.00 | -0.00 | -0.00 | -0.00 | 0.0000 |
| 52. Output Eb/No (44–51) | dB | 4.04 | 0.86 | -0.86 | 4.04 | 0.0817 |
| 53. Output Eb/No, mean-2 Sigma | dB | 3.46 | 0.00 | 0.00 | 3.46 | 0.0000 |
| 54. Required Eb/No | dB | -0.10 | 0.00 | 0.00 | -0.10 | 0.0000 |
| 55. Eb/No Margin (52–54) | dB | 4.14 | 0.86 | -0.86 | 4.14 | 0.0817 |
| 56. Eb/No Margin, mean-2 Sigma | dB | 3.56 | 0.00 | -0.00 | 3.56 | 0.0000 |
| 57. Down Data Rate Cap (21,22) | bps | 2e+05 | | | | |

The design control tables, Table 3-4 through Table 3-9, were generated by the Telecom Forecaster Predictor (TFP), a standard link analysis tool. While they have been lightly reformatted for this article, generally the computer outputs are left untouched. Acronyms, for example, may differ slightly from the style in the article.

The tables include the following acronyms not used elsewhere in the article.

| | |
|---|---|
| Adv | adverse |
| CD | cumulative distribution (also called "percent weather") |
| Fav | favorable |
| MW | microwave |
| Pnt | pointing offset of spacecraft antenna (also called "DOFF") |
| Tol | tolerance |
| Var | variance |

#### *3.2.1.1 Pointing Errors Assumptions*

For Cruise, we assume an antenna pointing error given by the Flight System based on thermal and power predicts for the spacecraft.

When the HGA is used, it is assumed that the antenna pointing is 4.4 milliradians (mrad) (0.25 deg).

#### *3.2.1.2 Downlink Performance Assumptions*

The current baseline is 20 downlink rates, between 10 and 200,000 bps.

Turbo encoding (rate 1/6, 8920 frame length) is the baseline for all downlink rates except 10, 40, and 1745 bps, and it is performed by the C&DH Subsystem. For 10, 40, and 1745 bps, a concatenated convolutional (7, 1/2) + Reed–Solomon (interleave depth 1 for 10 and 40 bps and interleave depth 5 for 1745 bps) outer code are used.

The X-band downlink performance estimates assume a TWTA output power of 25 W.

#### *3.2.1.3 Uplink Performance Assumptions*

The uplink threshold estimates (*see* Table 3-1) are based on test results.

For uplink performance estimates, we make the same assumptions as in the downlink analyses section regarding the antenna patterns and path losses. For SDST noise, we use the average (2.1 dB) of all SDST flight units for capabilities assessment, and the end of life estimate (2.8 dB) for requirements verification.

#### *3.2.1.4 Ranging Performance Assumptions*

The following formula gives the 1-sigma ranging uncertainty in meters due to thermal noise only (810-005 [4], Module 203) for sinewave operations:

$$\sigma(r) = \sqrt{\frac{285}{F_c^2(MHz)T_1 \frac{P_r}{N_o}}}$$

Where Fc is the clock frequency (approximately 1 MHz), Pr/No is the downlink power to noise ratio in the ranging channel, and T1 is the integration time for the clock component.

In order to resolve range ambiguity, lower-frequency components are used. The probability of acquisition, $P_{\text{acq}}$, is:

$$P_{acq} = \left\{ \frac{1}{2} + \frac{1}{2} erf\left[ \sqrt{T_2 \times P_r / N_0} \right] \right\}^n$$

where $n$ is the number of components and $T_2$ the integration time of each of them.

The values for $T_1$ and $T_2$ can then be used in the formula for the cycle time:

$$T_{cyc} = T_1 + 3 + n + nT_2$$

For a specified sigma and $P_{\text{acq}}$, the cycle time is a function of $P_r/N_o$ and $n$.

For a sigma of 5 m and a total cycle time of 1000 seconds, the received $P_r/N_o$ must be between –10 and –7 dB-Hz depending on the number of lower-frequency components the Juno navigation team determines are required to resolve the range ambiguity. Since telecom does not control how many components are needed, we assume a value of –9.0 dB-Hz as the threshold.

#### *3.2.1.5 Differential One-way Ranging*

Delta-DOR is a type of data complementary to turnaround ranging and Doppler. While ranging provides an estimate of the location of the spacecraft (in a radial sense, i.e., how far away the S/C is), delta-DOR gives very good angular location (relative to a known quasar; this is also referred to as “plane of sky location,” or “tangential” motion). It requires the spacecraft to modulate the downlink carrier with a pair of DOR tones at approximately ±19 MHz. The telecom configuration for delta-DOR includes a telemetry subcarrier frequency of 281.25 kHz (with nothing modulating the subcarrier) that is also modulated onto the carrier during DOR measurements.

The DOR tone modulation index is selected to be 70 deg for the Juno SDST. This increases power in the DOR channel with respect to the value of 28 deg used on the MER SDSTs by about 6.5 dB.

### 3.2.2 Ka-Band Assumptions

The Ka-band part of the Radio Frequency Instrument Subsystem (RFIS), another name for the Telecom Subsystem) is to support dual-frequency Gravity Science. Ka-band is used only with the HGA and the DSS-25 ground station at Goldstone, California. The Ka-band signal is carrier only, no telemetry. During Ka-band operation, the HGA pointing accuracy is 4.4 mrad (0.25 deg). There is only one path for the uplink and downlink as the Ka-band equipment is single string.

### 3.2.3 Link Analysis

The link analyses below cover nominal Cruise phase, Jovian orbits, and safe mode. Link performance varies with station elevation angle. For Juno link planning, an elevation angle of 15 deg is assumed.

#### *3.2.3.1 Cruise Phase*

One basic requirement covering all of the antennas is that a minimum downlink bit rate of 100 bps must be supported throughout Cruise. It is assumed that ranging is on.

Another basic requirement covering all of the antennas is that a minimum uplink command rate of 7.8125 bps must be supported through Cruise. It is assumed that ranging is on.

Figure 3-1 shows the expected downlink performance throughout the mission. Note that the chosen antenna changes throughout the mission. As seen in Figure 3-1, most of the time the spacecraft is on the HGA. The also shows that throughout Cruise, the Telecom Subsystem can support a minimum of 100 bps. Figure 3-2 shows a similar curve for the uplink. This shows ample margin to support the 7.8125 bps command rate.

X-band performance on the HGA is illustrated by an example taken from the July 5, 2012 (day of year, DOY 187) X-band pass over DSS-26 (34-m beam waveguide antenna at Goldstone, California). Table 3-4 and Table 3-5 are design control tables to illustrate X-band predicted performance at 19:12 UTC on that day. The predictions are for DSS-26 (a 34-m station at Goldstone) which was actually performing this pass. The station elevation angle was nearly 60 deg. A comparison of predicted performance and actual performance follows in Figures 3-3 through 3-6.

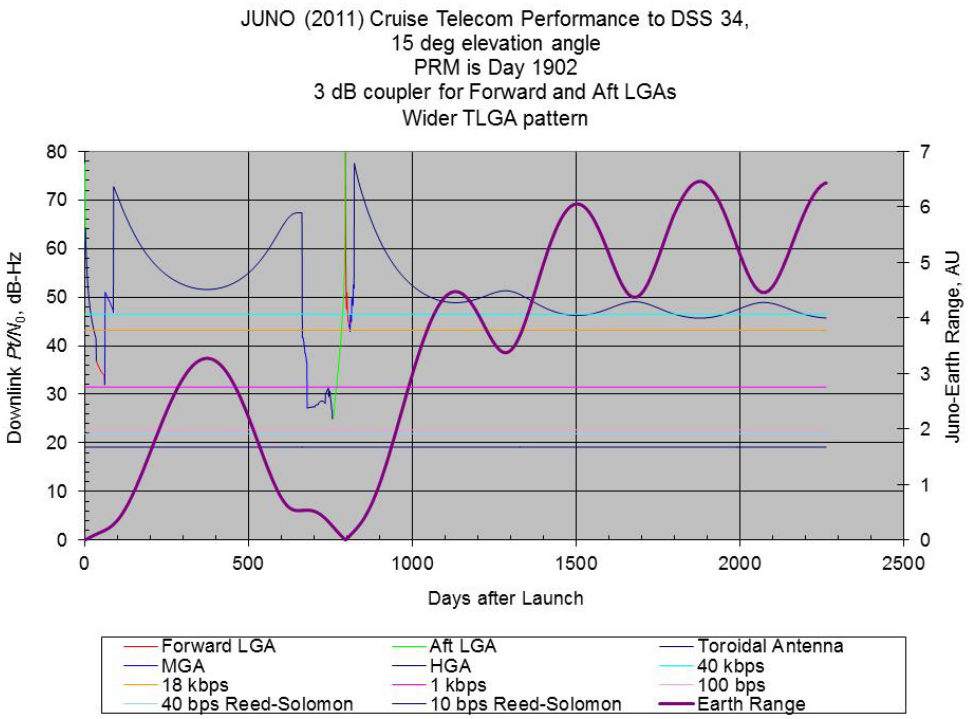


**Figure 3-1: Juno predicted downlink performance.**

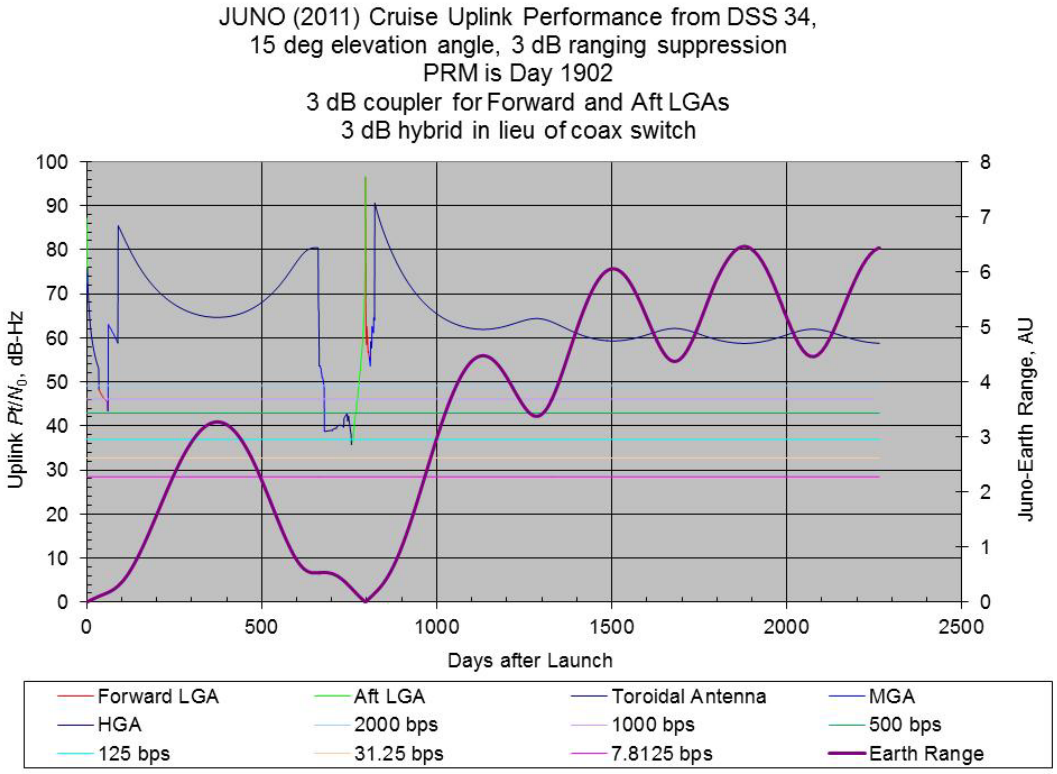


**Figure 3-2: Juno predicted uplink performance.**

## Table 3-5: Juno Cruise HGA X-band uplink DCT.

Produced by JUNO V2.1 XML 5/5/2011

---

Predict 2012-187T19:12:00.000 UTC
Up/Down-Link Two-Way
RF Band X:X
Telecom Link DSS26-HighGain-DSS26

---

COMMAND UP-LINK PARAMETER INPUTS
Cmd Data Rate 2000.0000 bps
Cmd Mod Index 1.50 radians
Cmd RngMod Index 44.9 degrees

---

Operations Mode Nominal
Mission Phase Cruise
DSN Site Gold-Gold
DSN Elevation In View
Weather/CD 90
Attitude Pointing Earth Pointed

---

EXTERNAL DATA
SPICE Kernels (in load order)
(omitted from this article)

Range (km) 4.7459e+08
Range (AU) 3.1724e+00
One-Way Light Time (OWLT) (hh:mm:ss) 00:26:23
Station Elevation (deg) 59.65
UL DOFF: Hga (deg) 0.25
UL Clk: Hga (deg) 0.51
Added S/C Pnt Offset (deg) 0.25

---

DSN Site Considered: DSS-26/DSS-26
At Time: 2012-187T19:12:00.000 UTC

---

| Link Parameter | Unit | Design Value | Fav Tol | Adv Tol | Mean Value | Var |
|---|---|---|---|---|---|---|
| TRANSMITTER PARAMETERS | | | | | | |
| 1. Total Transmitter Power | dBm | 73.01 | 0.50 | -0.50 | 73.01 | 0.0417 |
| 2. Xmitter Waveguide Loss | dB | -0.60 | 0.10 | -0.10 | -0.60 | 0.0017 |
| 3. DSN Antenna Gain | dBi | 66.92 | 0.20 | -0.30 | 66.89 | 0.0106 |
| 4. Antenna Pointing Loss | dB | -0.10 | 0.10 | -0.10 | -0.10 | 0.0017 |
| 5. EIRP (1+2+3+4) | dBm | 139.20 | 0.71 | -0.71 | 139.20 | 0.0556 |
| PATH PARAMETERS | | | | | | |
| 6. Space Loss | dB | -283.06 | 0.00 | 0.00 | -283.06 | 0.0000 |
| 7. Atmospheric Attenuation | dB | -0.06 | 0.00 | 0.00 | -0.06 | 0.0000 |
| RECEIVER PARAMETERS | | | | | | |
| 8. Polarization Loss | dB | -0.07 | 0.10 | -0.10 | -0.07 | 0.0033 |
| 9. Degrees-off-boresight (DOFF) Loss | dB | 0.71 | -0.00 | -0.00 | 0.71 | 0.0000 |
| 10. S/C Antenna Gain (at boresight) | dBi | 42.84 | 0.50 | -0.50 | 42.84 | 0.0417 |
| 11. S/C Receive Pointing Loss | dB | 0.00 | 0.00 | 0.00 | 0.00 | 0.0000 |
| 12. Lumped Circuit Loss | dB | -4.00 | 0.50 | -0.50 | -4.00 | 0.0833 |

---

Continues on next page

Continued from previous page

| Link Parameter | Unit | Design Value | Fav Tol | Adv Tol | Mean Value | Var |
|---|---|---|---|---|---|---|
| TOTAL POWER SUMMARY | | | | | | |
| 13. Tot Rcvd Pwr (5+6+7+8-9+10+11+12) | dBm | -105.87 | -1.29 | 1.29 | -105.87 | 0.1839 |
| 14. Noise Spectral Density | dBm/Hz | -172.57 | -1.40 | 0.75 | -172.78 | 0.1979 |
| 15. System Noise Temperature | K | 401.25 | -110.49 | 75.37 | 389.54 | 1456.4778 |
| 16. Received Pt/No (13–14) | dB-Hz | 66.92 | 1.85 | -1.85 | 66.92 | 0.3817 |
| 17. Received Pt/No, mean-3 Sigma | dB-Hz | 65.06 | 0.00 | 0.00 | 65.06 | 0.0000 |
| 18. Required Pt/No | dB-Hz | 49.13 | 0.00 | 0.00 | 49.13 | 0.0000 |
| 19. Pt/No Margin (16-18) | dB | 17.79 | 1.85 | -1.85 | 17.79 | 0.3817 |
| 20. Pt/No Margin, mean-3 Sigma (17–18) | dB | 15.93 | 0.00 | -0.00 | 15.93 | 0.0000 |
| CARRIER PERFORMANCE | | | | | | |
| 21. Recovered Pt/No (16+[AGC+BPF]) | dB-Hz | 66.92 | 1.85 | -1.85 | 66.92 | 0.3817 |
| 22. Command Carrier Suppression | dB | -5.82 | 0.58 | -0.58 | -5.82 | 0.0564 |
| 23. Ranging Carrier Suppression | dB | -3.00 | 0.20 | -0.21 | -3.00 | 0.0069 |
| 24. Carrier Power (AGC) | dBm | -114.68 | -1.49 | 1.49 | -114.68 | 0.2472 |
| 25. Received Pc/No (21+22+23) | dB-Hz | 58.10 | 2.00 | -2.00 | 58.10 | 0.4451 |
| 26. Carrier Loop Noise BW | dB-Hz | 20.47 | -0.20 | 0.15 | 20.45 | 0.0102 |
| 27. Carrier Loop SNR (CNR) (25–26) | dB | 37.65 | 2.02 | -2.02 | 37.65 | 0.4553 |
| 28. CNR, mean-3 Sigma | dB | 35.63 | 0.00 | 0.00 | 35.63 | 0.0000 |
| 29. Recommended CNR | dB | 12.00 | 0.00 | 0.00 | 12.00 | 0.0000 |
| 30. CNR Margin (27–29) | dB | 25.65 | 2.02 | -2.02 | 25.65 | 0.4553 |
| 31. CNR Margin, mean-3 Sigma (28–29) | dB | 23.63 | 0.00 | -0.00 | 23.63 | 0.0000 |
| CHANNEL PERFORMANCE | | | | | | |
| 32. Command Data Suppression | dB | -2.06 | -0.14 | 0.12 | -2.07 | 0.0029 |
| 33. Ranging Data Suppression | dB | -3.00 | 0.20 | -0.21 | -3.00 | 0.0069 |
| 34. Received Pd/No (21+32+33) | dB-Hz | 61.85 | 1.88 | -1.88 | 61.85 | 0.3915 |
| 35. Received Pd/No, mean-3 Sigma | dB-Hz | 59.97 | 0.00 | 0.00 | 59.97 | 0.0000 |
| 36. Data Rate (dB-Hz) | dB-Hz | 33.01 | 0.00 | 0.00 | 33.01 | 0.0000 |
| 37. Available Eb/No (34–36) | dB | 28.84 | 1.88 | -1.88 | 28.84 | 0.3915 |
| 38. Implementation Loss | dB | 1.48 | -0.84 | 0.75 | 1.45 | 0.1054 |
| 39. Radio Loss | dB | 0.00 | 0.00 | 0.00 | 0.00 | 0.0000 |
| 40. Output Eb/No (37–39) | dB | 27.39 | 2.11 | -2.11 | 27.39 | 0.4970 |
| 41. Output Eb/No, mean-3 Sigma | dB | 25.28 | 0.00 | 0.00 | 25.28 | 0.0000 |
| 42. Required Eb/No | dB | 9.60 | 0.00 | 0.00 | 9.60 | 0.0000 |
| 43. Eb/No Margin (40–42) | dB | 17.79 | 2.11 | -2.11 | 17.79 | 0.4970 |
| 44. Eb/No Margin, mean-3 Sigma (41–42) | dB | 15.68 | 0.00 | -0.00 | 15.68 | 0.0000 |
| 45. BER (from 40) | | none | 7.8657e-241 | | | |

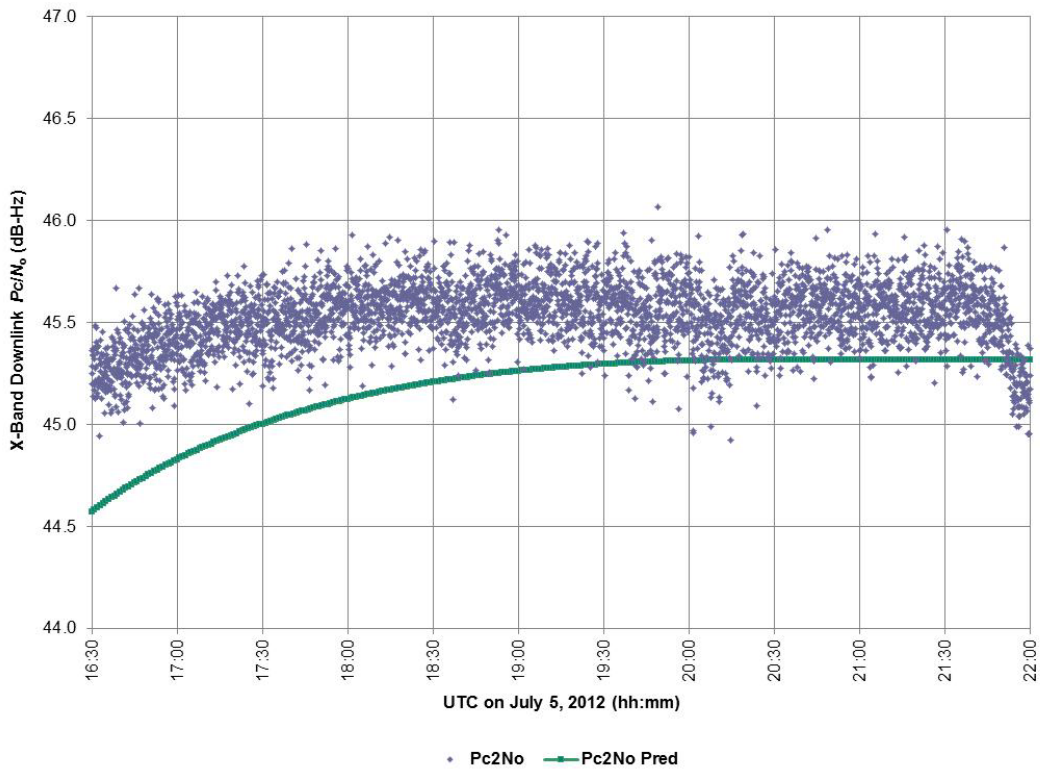


**Figure 3-3: Predicted and actual carrier power to noise spectral density ($P_c/N_o$) on July 5, 2012.**

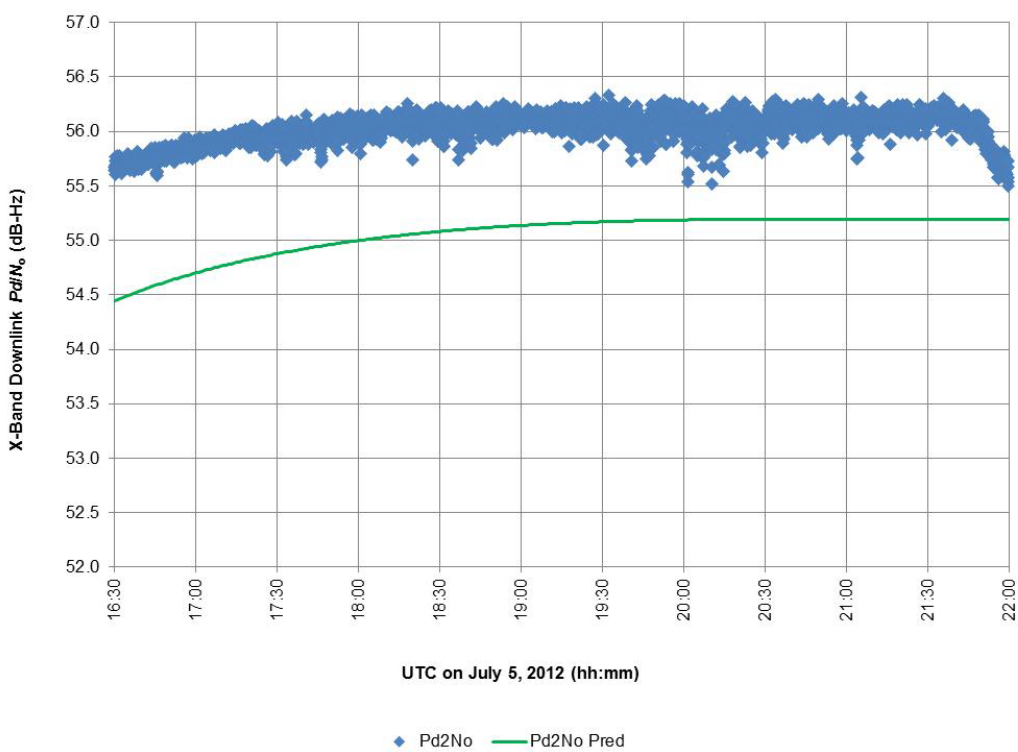


**Figure 3-4: Predicted and actual data power to noise spectral density ($P_d/N_o$) on July 5, 2012.**

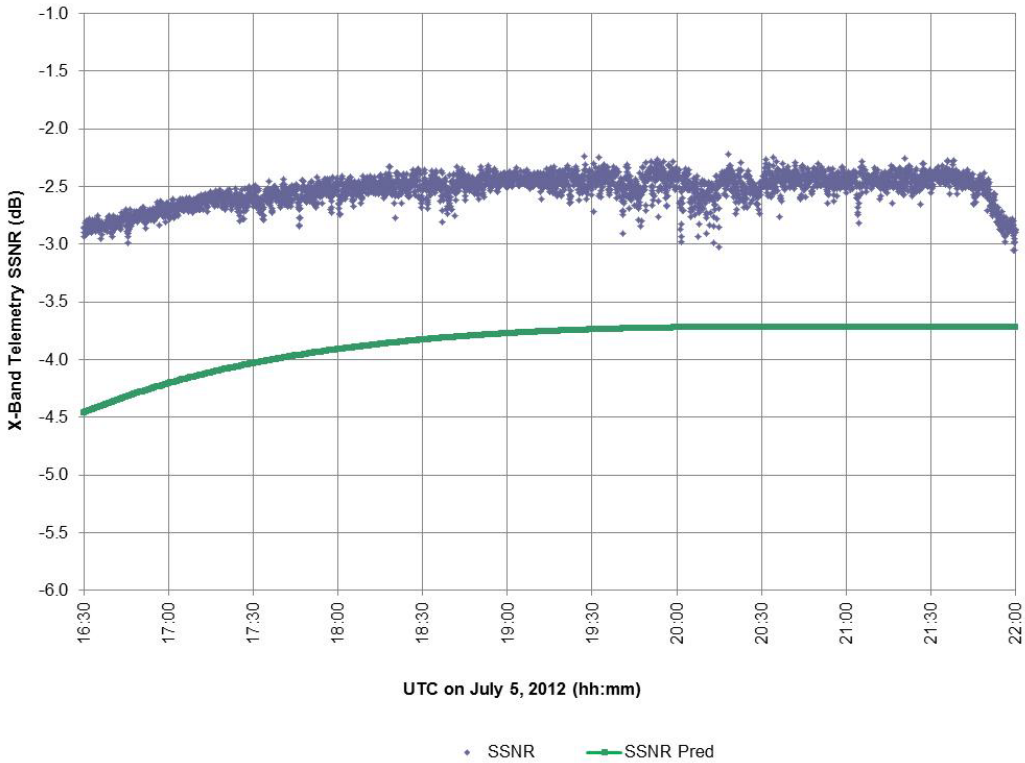


**Figure 3-5: Predicted and actual symbol SNR on July 5, 2012.**

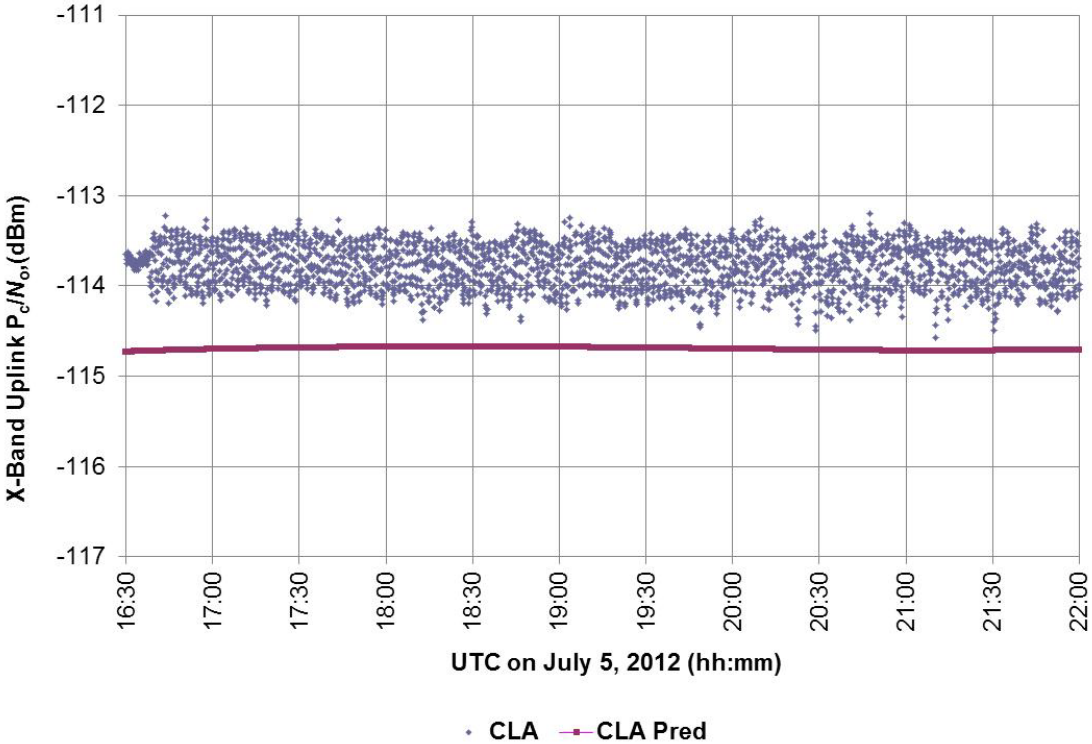


**Figure 3-6: Predicted and actual uplink carrier power to noise spectral density ($P_c/N_o$) on July 5, 2012.**

#### *3.2.3.2 Orbital Phase*

During the orbital phase, the flight system must be capable of receiving commands transmitted on X-band at 2000 bps via the HGA and of downlinking X-band telemetry to a 34-m beam waveguide antenna at no less than 18 kbps.

Table 3-6 and Table 3-7 are downlink and uplink design control tables (DCT) that illustrate predicted X-band telemetry and command performance, respectively, in orbit. Note that these DCTs are generated for DSS-34 (as representative of any 34-m station), at a fixed station elevation angle of 15 deg, and for doy 2016-270 (September 26, 2016).

Table 3-7 and Table 3-8 are design control tables for the Ka-band downlink and Ka-band uplink, respectively. They are carrier-only, and are generated for DSS-25 at a fixed 15-deg elevation angle.

These DCTs were done at the maximum orbital range. Most of the gravity science passes are actually at significantly shorter ranges, which leads to larger margins.

Figure 3-7 shows the predicted Ka-band downlink $P_t/N_o$ during the orbital phase. The prediction is shown in three curves, assuming station elevation angle fixed at 25 deg (top curve), 20 deg, and 15 deg.

The typical uplink and downlink performance shown in Fig 3-3 through Fig 3-6 in July 2012 has continued through orbit operations (2016-2017).

The actual uplink and downlink performance at X-band has averaged within one or two dB of predictions [14]. The actual performance ($P_t/N_o$ and telemetry SSNR) follows the predicted performance since launch, thus showing no trends during orbit operations that would suggest degradation from Jupiter radiation effects of the onboard receiving and transmitting equipment.

The expected difference in capability observed between 70-m and 34-m stations has also been maintained, as well as small differences among the 34-m stations and among the 70-m stations. These differences are comparable to what is observed with other deep space missions.

**Table 3-6: Juno X-band downlink DCT at maximum range in 2016.**

| | |
|---|---|
| Predict | 2016-270T07:00:00000 UTC |
| Up/Down-Link | Two-Way |
| RF Band | X:X |
| Diplex Mode | N/A |
| LNA Selection | LNA-1 |
| Telecom Link | DSS34-HighGain-DSS34 |

TELEMETRY DOWN-LINK PARAMETER INPUTS

| | |
|---|---|
| Encoding | Turbo (8920,1/6) |
| Carrier Tracking | Residual |
| Oscillator | 2 Way VCO |
| Sub-Carrier Mode | Squarewave |
| PLL Bandwidth | 3.00 Hz |
| Tlm Usage | Engineering |
| Tlm Data Rate/Mod Index | 18000 bps/ 72.00 degrees |
| Tlm Rng/DOR Mod Index | 0.31 Rad/ 0.00 degrees |

| | |
|---|---|
| Operations Mode | Nominal |
| Mission Phase | Cruise |
| DSN Site | Canb-Canb |
| DSN Elevation | Fixed Val Deg |
| Weather/CD | 90 |
| Attitude Pointing | Earth Pointed |

EXTERNAL DATA
SPICE Kernels (in load order)
(omitted from this article)

| | | |
|---|---|---|
| Range | (km) | 9.6625e+08 |
| Range | (AU) | 6.4590e+00 |
| DL One-Way Light Time (hh:mm:ss) | | 00:53:43 |
| Station Elevation (deg) | | 15.00 |
| DL DOFF: Hga (deg) | | 0.25 |
| DL Clk: Hga (deg) | | 4.45 |
| Added S/C Pnt Offset (deg) | | 0.25 |

DSN Site Considered: DSS-34/DSS-34
At Time: 2016-270T07:00:00.000 UTC

| Link Parameter | Unit | Design Value | Fav Tol | Adv Tol | Mean Value | Var |
|---|---|---|---|---|---|---|
| TRANSMITTER PARAMETERS | | | | | | |
| 1. S/C Transmitter Power | dBm | 44.40 | 0.30 | 0.00 | 44.50 | 0.0050 |
| 2. S/C Xmit Circuit Loss | dB | -0.90 | 0.10 | -0.10 | -0.90 | 0.0033 |
| 3. S/C Antenna Gain | dBi | 44.70 | 0.50 | -0.50 | 44.70 | 0.0417 |
| 4. Degrees-off-boresight (DOFF) Loss | dB | 0.93 | -0.00 | -0.00 | 0.93 | 0.0000 |
| 5. S/C Transmit Pointing Loss | dB | 0.00 | 0.00 | 0.00 | 0.00 | 0.0000 |
| 6. EIRP (1+2+3-4+5) | dBm | 87.37 | 0.67 | -0.67 | 87.37 | 0.0500 |
| PATH PARAMETERS | | | | | | |
| 7. Space Loss | dB | -290.64 | 0.00 | 0.00 | -290.64 | 0.0000 |
| 8. Atmospheric Attenuation | dB | -0.20 | 0.00 | 0.00 | -0.20 | 0.0000 |
| RECEIVER PARAMETERS | | | | | | |
| 9. DSN Antenna Gain | dBi | 68.26 | 0.10 | -0.20 | 68.23 | 0.0039 |
| 10. DSN Antenna Pnt Loss | dB | -0.10 | 0.10 | -0.10 | -0.10 | 0.0033 |
| 11. Polarization Loss | dB | -0.05 | 0.10 | -0.10 | -0.05 | 0.0033 |

Continued from previous page

| Link Parameter | Unit | Design Value | Fav Tol | Adv | Mean Value | Var |
|---|---|---|---|---|---|---|
| TOTAL POWER SUMMARY | | | | | | |
| 12. Tot Rcvd Pwr (6+7+8+9+10+11) | dBm | -135.40 | -0.74 | 0.74 | -135.40 | 0.0606 |
| 13. SNT due to Antenna-MW | K | 16.81 | -1.00 | 2.00 | 17.14 | 0.3889 |
| 14. SNT due to Atmosphere | K | 12.78 | 0.00 | 0.00 | 12.78 | 0.0000 |
| 15. SNT due to Cosmic Backgnd | K | 2.60 | 0.00 | 0.00 | 2.60 | 0.0000 |
| 16. SNT due to the Sun | K | 17.54 | 0.00 | 0.00 | 17.54 | 0.0000 |
| 17. SNT due to other Hot Bodies | K | 0.00 | 0.00 | 0.00 | 0.00 | 0.0000 |
| 18. SNT (13+14+15+16+17) | K | 49.72 | -1.00 | 2.00 | 50.06 | 0.3889 |
| 19. Noise Spectral Density | dBm/Hz | -181.63 | -0.09 | 0.17 | -181.61 | 0.0029 |
| 20. Received Pt/No (12-19) | dB-Hz | 46.21 | 0.76 | -0.76 | 46.21 | 0.0635 |
| 21. Received Pt/No, mean-2 Sigma | dB-Hz | 45.71 | 0.00 | 0.00 | 45.71 | 0.0000 |
| 22. Required Pt/No | dB-Hz | 43.64 | 0.00 | 0.00 | 43.64 | 0.0000 |
| 23. Pt/No Margin (20-22) | dB | 2.57 | 0.76 | -0.76 | 2.57 | 0.0635 |
| 24. Pt/No Margin, mean-2 Sigma (21-22) | dB | 2.06 | 0.00 | -0.00 | 2.06 | 0.0000 |
| CARRIER PERFORMANCE | | | | | | |
| 25. Recovered Pt/No (20+[AGC+BPF]) | dB-Hz | 46.21 | 0.76 | -0.76 | 46.21 | 0.0635 |
| 26. Telemetry Carrier Suppression | dB | -10.20 | 1.52 | -1.89 | -10.32 | 0.4854 |
| 27. Ranging Carrier Suppression | dB | -0.30 | 0.06 | -0.06 | -0.30 | 0.0006 |
| 28. DOR Carrier Suppression | dB | 0.00 | -0.00 | -0.00 | -0.00 | 0.0000 |
| 29. Carrier Power (AGC) (12+26+27+28) | dBm | -146.02 | -2.22 | 2.22 | -146.02 | 0.5466 |
| 30. Received Pc/No (25+26+27+28) | dB-Hz | 35.58 | 2.22 | -2.22 | 35.58 | 0.5495 |
| 31. Carrier Loop Noise BW | dB-Hz | 4.77 | 0.00 | 0.00 | 4.77 | 0.0000 |
| 32. Carrier Phase Error Var (from 30,31,xpond,solar) | rad^2 | 5.9e-03 | 0.00 | 0.00 | 5.9e-03 | 0.0000 |
| 33. Carrier Loop SNR (CNR) (from 32) | dB | 22.31 | 2.22 | -2.22 | 22.31 | 0.5495 |
| 34. CNR, mean-2 Sigma | dB | 20.83 | 0.00 | 0.00 | 20.83 | 0.0000 |
| 35. Recommended CNR | dB | 10.00 | 0.00 | 0.00 | 10.00 | 0.0000 |
| 36. CNR Margin (33-35) | dB | 12.31 | 2.22 | -2.22 | 12.31 | 0.5495 |
| 37. CNR Margin, mean-2 Sigma (34-35) | dB | 10.83 | 0.00 | -0.00 | 10.83 | 0.0000 |
| TELEMETRY PERFORMANCE | | | | | | |
| 38. Telemetry Data Suppression | dB | -0.44 | -0.20 | 0.16 | -0.45 | 0.0053 |
| 39. Ranging Data Suppression | dB | -0.30 | 0.06 | -0.06 | -0.30 | 0.0006 |
| 40. DOR Data Suppression | dB | 0.00 | -0.00 | -0.00 | -0.00 | 0.0000 |
| 41. Received Pd/No (25+38+39+40) | dB-Hz | 45.46 | 0.79 | -0.79 | 45.46 | 0.0693 |
| 42. Received Pd/No, mean-2 Sigma | dB-Hz | 44.93 | 0.00 | 0.00 | 44.93 | 0.0000 |
| 43. Data Rate, Symbols (dB-Hz) | dB-Hz | 42.55 | 0.00 | 0.00 | 42.55 | 0.0000 |
| 44. Available Eb/No (41-43) | dB | 2.91 | 0.79 | -0.79 | 2.91 | 0.0693 |
| 45. Radio Loss | dB | 0.30 | 0.00 | 0.00 | 0.30 | 0.0000 |
| 46. Subcarrier Demod Loss | dB | 0.00 | 0.00 | 0.00 | 0.00 | 0.0000 |
| 47. Symbol Sync Loss | dB | 0.00 | 0.00 | 0.00 | 0.00 | 0.0000 |
| 48. Decoder Loss | dB | -0.00 | -0.00 | -0.00 | -0.00 | 0.0000 |
| 49. Waveform Distortion Loss | dB | 0.10 | -0.10 | 0.10 | 0.10 | 0.0017 |
| 50. SDST Filtering Loss | dB | -0.10 | -0.00 | -0.00 | -0.10 | 0.0000 |
| 51. High Rate Ranging Loss | dB | -0.00 | -0.00 | -0.00 | -0.00 | 0.0000 |
| 52. Output Eb/No (44-45-46-47-48-49-50-51) | dB | 2.60 | 0.80 | -0.80 | 2.60 | 0.0710 |
| 53. Output Eb/No, mean-2 Sigma | dB | 2.07 | 0.00 | 0.00 | 2.07 | 0.0000 |
| 54. Required Eb/No | dB | -0.10 | 0.00 | 0.00 | -0.10 | 0.0000 |
| 55. Eb/No Margin (52-54) | dB | 2.70 | 0.80 | -0.80 | 2.70 | 0.0710 |
| 56. Eb/No Margin, mean-2 Sigma | dB | 2.17 | 0.00 | -0.00 | 2.17 | 0.0000 |
| 57. Down Data Rate Cap (21,22) | bps | 30000 | | | | |

**Table 3-7: Juno X-band uplink DCT at maximum range in 2016.**

| | |
|---|---|
| Predict | 2016-270T07:00:00.000 UTC |
| Up/Down-Link | Two-Way |
| RF Band | X:X |
| Telecom Link | DSS34-HighGain-DSS34 |

COMMAND UP-LINK PARAMETER INPUTS

| | |
|---|---|
| Cmd Data Rate | 2000.0000 bps |
| Cmd Mod Index | 1.50 radians |
| Cmd RngMod Index | 44.9 degrees |

| | |
|---|---|
| Operations Mode | Nominal |
| Mission Phase | Cruise |
| DSN Site | Canb-Canb |
| DSN Elevation | Fixed Val Deg |
| Weather/CD | 90 |
| Attitude Pointing | Earth Pointed |

EXTERNAL DATA
SPICE Kernels (in load order)
(omitted from this article)

| | | |
|---|---|---|
| Range | (km) | 9.6625e+08 |
| Range | (AU) | 6.4590e+00 |
| One-Way Light Time (OWLT) (hh:mm:ss) | | 00:53:43 |
| Station Elevation (deg) | | 15.00 |
| UL DOFF: Hga (deg) | | 0.25 |
| UL Clk: Hga, (deg) | | 4.43 |
| Added S/C Pnt Offset (deg) | | 0.25 |

| | |
|---|---|
| DSN Site Considered: | DSS-34/DSS-34 |
| At Time: | 2016-270T07:00:00.000 UTC |

| Link Parameter | Unit | Design Value | Fav Tol | Adv Tol | Mean Value | Var |
|---|---|---|---|---|---|---|
| TRANSMITTER PARAMETERS | | | | | | |
| 1. Total Transmitter Power | dBm | 73.01 | 0.50 | -0.50 | 73.01 | 0.0417 |
| 2. Xmitter Waveguide Loss | dB | -0.60 | 0.10 | -0.10 | -0.60 | 0.0017 |
| 3. DSN Antenna Gain | dBi | 66.93 | 0.20 | -0.30 | 66.90 | 0.0106 |
| 4. Antenna Pointing Loss | dB | -0.10 | 0.10 | -0.10 | -0.10 | 0.0017 |
| 5. EIRP (1+2+3+4) | dBm | 139.21 | 0.71 | -0.71 | 139.21 | 0.0556 |
| PATH PARAMETERS | | | | | | |
| 6. Space Loss | dB | -289.24 | 0.00 | 0.00 | -289.24 | 0.0000 |
| 7. Atmospheric Attenuation | dB | -0.20 | 0.00 | 0.00 | -0.20 | 0.0000 |
| RECEIVER PARAMETERS | | | | | | |
| 8. Polarization Loss | dB | -0.07 | 0.10 | -0.10 | -0.07 | 0.0033 |
| 9. Degrees-off-boresight (DOFF) Loss | dB | 0.71 | -0.00 | -0.00 | 0.71 | 0.0000 |
| 10. S/C Antenna Gain (at boresight) | dBi | 42.84 | 0.50 | -0.50 | 42.84 | 0.0417 |
| 11. S/C Receive Pointing Loss | dB | 0.00 | 0.00 | 0.00 | 0.00 | 0.0000 |
| 12. Lumped Circuit Loss | dB | -4.00 | 0.50 | -0.50 | -4.00 | 0.0833 |

Continues on next page

Continued from previous page
-

| Link Parameter | Unit | Design Value | Fav Tol | Adv Tol | Mean Value | Var |
|---|---|---|---|---|---|---|
| TOTAL POWER SUMMARY | | | | | | |
| 13. Tot Rcvd Pwr (5+6+7+8-9+10+11+12) | dBm | -112.18 | -1.29 | 1.29 | -112.18 | 0.1839 |
| 14. Noise Spectral Density | dBm/Hz | -172.57 | -1.40 | 0.75 | -172.78 | 0.1979 |
| 15. System Noise Temperature | K | 401.25 | -110.49 | 75.37 | 389.54 | 1456.4778 |
| 16. Received Pt/No (13–14) | dB-Hz | 60.60 | 1.85 | -1.85 | 60.60 | 0.3817 |
| 17. Received Pt/No, mean-3 Sigma | dB-Hz | 58.75 | 0.00 | 0.00 | 58.75 | 0.0000 |
| 18. Required Pt/No | dB-Hz | 49.13 | 0.00 | 0.00 | 49.13 | 0.0000 |
| 19. Pt/No Margin (16–18) | dB | 11.47 | 1.85 | -1.85 | 11.47 | 0.3817 |
| 20. Pt/No Margin, mean-3 Sigma (17–18) | dB | 9.62 | 0.00 | -0.00 | 9.62 | 0.0000 |
| CARRIER PERFORMANCE | | | | | | |
| 21. Recovered Pt/No (16+[AGC+BPF]) | dB-Hz | 60.60 | 1.85 | -1.85 | 60.60 | 0.3817 |
| 22. Command Carrier Suppression | dB | -5.82 | 0.58 | -0.58 | -5.82 | 0.0564 |
| 23. Ranging Carrier Suppression | dB | -3.00 | 0.20 | -0.21 | -3.00 | 0.0069 |
| 24. Carrier Power (AGC) | dBm | -121.00 | -1.49 | 1.49 | -121.00 | 0.2472 |
| 25. Received Pc/No (21+22+23) | dB-Hz | 51.79 | 2.00 | -2.00 | 51.79 | 0.4451 |
| 26. Carrier Loop Noise BW | dB-Hz | 20.31 | -0.20 | 0.15 | 20.28 | 0.0102 |
| 27. Carrier Loop SNR (CNR) (25–26) | dB | 31.50 | 2.02 | -2.02 | 31.50 | 0.4553 |
| 28. CNR, mean-3 Sigma | dB | 29.48 | 0.00 | 0.00 | 29.48 | 0.0000 |
| 29. Recommended CNR | dB | 12.00 | 0.00 | 0.00 | 12.00 | 0.0000 |
| 30. CNR Margin (27–29) | dB | 19.50 | 2.02 | -2.02 | 19.50 | 0.4553 |
| 31. CNR Margin, mean-3 Sigma (28-29) | dB | 17.48 | 0.00 | -0.00 | 17.48 | 0.0000 |
| CHANNEL PERFORMANCE | | | | | | |
| 32. Command Data Suppression | dB | -2.06 | -0.14 | 0.12 | -2.07 | 0.0029 |
| 33. Ranging Data Suppression | dB | -3.00 | 0.20 | -0.21 | -3.00 | 0.0069 |
| 34. Received Pd/No (21+32+33) | dB-Hz | 55.54 | 1.88 | -1.88 | 55.54 | 0.3915 |
| 35. Received Pd/No, mean-3 Sigma | dB-Hz | 53.66 | 0.00 | 0.00 | 53.66 | 0.0000 |
| 36. Data Rate (dB-Hz) | dB-Hz | 33.01 | 0.00 | 0.00 | 33.01 | 0.0000 |
| 37. Available Eb/No (34–36) | dB | 22.53 | 1.88 | -1.88 | 22.53 | 0.3915 |
| 38. Implementation Loss | dB | 1.48 | -0.84 | 0.75 | 1.45 | 0.1054 |
| 39. Radio Loss | dB | 0.00 | 0.00 | 0.00 | 0.00 | 0.0000 |
| 40. Output Eb/No (37-38-39) | dB | 21.08 | 2.11 | -2.11 | 21.08 | 0.4970 |
| 41. Output Eb/No, mean-3 Sigma | dB | 18.96 | 0.00 | 0.00 | 18.96 | 0.0000 |
| 42. Required Eb/No | dB | 9.60 | 0.00 | 0.00 | 9.60 | 0.0000 |
| 43. Eb/No Margin (40–42) | dB | 11.48 | 2.11 | -2.11 | 11.48 | 0.4970 |
| 44. Eb/No Margin, mean-3 Sigma (41–42) | dB | 9.36 | 0.00 | -0.00 | 9.36 | 0.0000 |
| 45. BER (from 40) | none | 5.5332e-58 | | | | |

## Table 3-8: Juno HGA Ka-band carrier downlink at maximum range.

Produced by JUNO V2.1 XML 5/5/2011

---

Predict 2016-270T07:00:00000 UTC
Up/Down-Link Two-Way
RF Band Ka:Ka/X
LNA Selection LNA-1
Telecom Link DSS25-HighGain-DSS25

---

TELEMETRY DOWN-LINK PARAMETER INPUTS
Encoding Turbo (8920,1/6)
Carrier Tracking Residual
Oscillator 2 Way VCO
Sub-Carrier Mode Squarewave
PLL Bandwidth 3.00 Hz
Tlm Usage Engineering
Tlm Data Rate/Mod Index 0 bps/ 0.00 Degrees
Tlm Rng/DOR Mod Index 0.00 Rad/ 0.00 Degrees

---

Operations Mode Nominal
Mission Phase Cruise
DSN Site Gold-Gold
DSN Elevation Fixed Val Deg
Weather/CD 90
Attitude Pointing EarthPointed

---

Range (km) 9.6626e+08
Range (AU) 6.4590e+00
DL One-Way Light Time (hh:mm:ss) 00:53:43
Station Elevation (deg) 15.00
DL DOFF: Hga (deg) 0.25
DL Clk: Hga (deg) 2.74
Added S/C Pnt Offset (deg) 0.25

---

DSN Site Considered: DSS-25/DSS-25
At Time: 2016-270T07:00:00.000 UTC

---

| Link Parameter | Unit | Design Value | Fav Tol | Adv Tol | Mean Value | Var |
|---|---|---|---|---|---|---|
| TRANSMITTER PARAMETERS | | | | | | |
| 1. S/C Transmitter Power | dBm | 34.31 | 0.50 | -0.50 | 34.31 | 0.0417 |
| 2. S/C Xmit Circuit Loss | dB | -2.20 | 0.20 | -0.20 | -2.20 | 0.0133 |
| 3. S/C Antenna Gain | dBi | 48.72 | 0.60 | -0.60 | 48.72 | 0.0600 |
| 4. Degrees-off-boresight (DOFF) Loss | dB | 3.65 | -0.00 | -0.00 | 3.65 | 0.0000 |
| 5. S/C Transmit Pointing Loss | dB | 0.00 | 0.00 | 0.00 | 0.00 | 0.0000 |
| 6. EIRP (1+2+3-4+5) | dBm | 77.18 | 1.02 | -1.02 | 77.18 | 0.1150 |
| PATH PARAMETERS | | | | | | |
| 7. Space Loss | dB | -302.28 | 0.00 | 0.00 | -302.28 | 0.0000 |
| 8. Atmospheric Attenuation | dB | -1.09 | 0.00 | 0.00 | -1.09 | 0.0000 |
| RECEIVER PARAMETERS | | | | | | |
| 9. DSN Antenna Gain | dBi | 78.41 | 0.30 | -0.30 | 78.41 | 0.0150 |
| 10. DSN Antenna Pnt Loss | dB | -0.11 | 0.10 | -0.10 | -0.11 | 0.0033 |
| 11. Polarization Loss | dB | -0.07 | 0.10 | -0.10 | -0.07 | 0.0033 |

---

Continues on next page

Continued from previous page

| Link Parameter | Unit | Design Value | Fav Tol | Adv Tol | Mean Value | Var |
|---|---|---|---|---|---|---|
| TOTAL POWER SUMMARY | | | | | | |
| 12. Tot Rcvd Pwr (6+7+8+9+10+11) | dBm | -147.96 | -1.11 | 1.11 | -147.96 | 0.1367 |
| 13. SNT due to Antenna-MW | K | 33.35 | -1.00 | 2.00 | 33.68 | 0.3889 |
| 14. SNT due to Atmosphere | K | 61.38 | 0.00 | 0.00 | 61.38 | 0.0000 |
| 15. SNT due to Cosmic Backgnd | K | 2.12 | 0.00 | 0.00 | 2.12 | 0.0000 |
| 16. SNT due to the Sun | K | 17.58 | 0.00 | 0.00 | 17.58 | 0.0000 |
| 17. SNT due to other Hot Bodies | K | 0.00 | 0.00 | 0.00 | 0.00 | 0.0000 |
| 18. SNT (13+14+15+16+17) | K | 114.43 | -1.00 | 2.00 | 114.76 | 0.3889 |
| 19. Noise Spectral Density | dBm/Hz | -178.01 | -0.04 | 0.08 | -178.00 | 0.0006 |
| 20. Received Pt/No (12-19) | dB-Hz | 30.04 | 1.11 | -1.11 | 30.04 | 0.1372 |
| 21. Received Pt/No, mean-2 Sigma | dB-Hz | 29.30 | 0.00 | 0.00 | 29.30 | 0.0000 |
| CARRIER PERFORMANCE | | | | | | |
| 25. Recovered Pt/No (20+[AGC+BPF]) | dB-Hz | 30.04 | 1.11 | -1.11 | 30.04 | 0.1372 |
| 26. Telemetry Carrier Suppression | dB | 0.00 | 0.00 | 0.00 | 0.00 | 0.0000 |
| 27. Ranging Carrier Suppression | dB | 0.00 | 0.00 | 0.00 | 0.00 | 0.0000 |
| 28. DOR Carrier Suppression | dB | 0.00 | -0.00 | -0.00 | -0.00 | 0.0000 |
| 29. Carrier Power (AGC) (12+26+27+28) | dBm | -147.96 | -1.11 | 1.11 | -147.96 | 0.1367 |
| 30. Received Pc/No (25+26+27+28) | dB-Hz | 30.04 | 1.11 | -1.11 | 30.04 | 0.1372 |
| 31. Carrier Loop Noise BW | dB-Hz | 4.77 | 0.00 | 0.00 | 4.77 | 0.0000 |
| 32. Carrier Phase Error Var (from 30,31,xpond,solar) | rad^2 | 7.5e-03 | 0.00 | 0.00 | 7.5e-03 | 0.0000 |
| 33. Carrier Loop SNR (CNR) (from 32) | dB | 21.26 | 1.11 | -1.11 | 21.26 | 0.1372 |
| 34. CNR, mean-2 Sigma | dB | 20.52 | 0.00 | 0.00 | 20.52 | 0.0000 |
| 35. Recommended CNR | dB | 10.00 | 0.00 | 0.00 | 10.00 | 0.0000 |
| 36. CNR Margin (33-35) | dB | 11.26 | 1.11 | -1.11 | 11.26 | 0.1372 |
| 37. CNR Margin, mean-2 Sigma (34-35) | dB | 10.52 | 0.00 | -0.00 | 10.52 | 0.0000 |

**Table 3-9: Juno HGA Ka-band carrier uplink at maximum range.**

Produced by JUNO V2.1 XML 5/5/2011

| | |
|---|---|
| Predict | 2016-270T07:00:00.000 UTC |
| Up/Down-Link | Two-Way |
| RF Band | Ka:Ka/X |
| Telecom Link | DSS25-HighGain-DSS25 |

COMMAND UP-LINK PARAMETER INPUTS

| | | |
|---|---|---|
| Cmd Mod Index | 0.00 | Radians |
| Cmd RngMod Index | 0.0 | Degrees |

| | |
|---|---|
| Operations Mode | Nominal |
| Mission Phase | Cruise |
| DSN Site | Gold-Gold |
| DSN Elevation | Fixed Val Deg |
| Weather/CD | 90 |
| Attitude Pointing | EarthPointed |

| | | |
|---|---|---|
| Range | (km) | 9.6626e+08 |
| Range | (AU) | 6.4590e+00 |
| One-Way Light Time (OWLT) (hh:mm:ss) | | 00:53:43 |
| Station Elevation (deg) | | 15.00 |
| UL DOFF: Hga (deg) | | 0.25 |
| UL Clk: Hga (deg) | | 2.17 |
| Added S/C Pnt Offset (deg) | | 0.25 |

Continued from previous page

DSN Site Considered: DSS-25/DSS-25
At Time: 2016-270T07:00:00.000 UTC

| Link Parameter | Unit | Design Value | Fav Tol | Adv Tol | Mean Value | Var |
|---|---|---|---|---|---|---|
| TRANSMITTER PARAMETERS | | | | | | |
| 1. Total Transmitter Power | dBm | 59.00 | 0.50 | -0.50 | 59.00 | 0.0417 |
| 2. Xmitter Waveguide Loss | dB | -0.25 | 0.10 | -0.10 | -0.25 | 0.0017 |
| 3. DSN Antenna Gain | dBi | 79.52 | 0.20 | -0.30 | 79.49 | 0.0106 |
| 4. Antenna Pointing Loss | dB | -0.12 | 0.00 | 0.00 | -0.12 | 0.0000 |
| 5. EIRP (1+2+3+4) | dBm | 138.12 | 0.70 | -0.70 | 138.12 | 0.0539 |
| PATH PARAMETERS | | | | | | |
| 6. Space Loss | dB | -302.87 | 0.00 | 0.00 | -302.87 | 0.0000 |
| 7. Atmospheric Attenuation | dB | -1.09 | 0.00 | 0.00 | -1.09 | 0.0000 |
| RECEIVER PARAMETERS | | | | | | |
| 8. Polarization Loss | dB | -0.07 | 0.10 | -0.10 | -0.07 | 0.0033 |
| 9. Degrees-off-boresight (DOFF) Loss | dB | 8.77 | -0.00 | -0.00 | 8.77 | 0.0000 |
| 10. S/C Antenna Gain (at boresight) | dBi | 49.36 | 0.60 | -0.60 | 49.36 | 0.0600 |
| 11. S/C Receive Pointing Loss | dB | 0.00 | 0.00 | 0.00 | 0.00 | 0.0000 |
| 12. Lumped Circuit Loss | dB | -2.93 | 0.30 | -0.30 | -2.93 | 0.0300 |
| TOTAL POWER SUMMARY | | | | | | |
| 13. Tot Rcvd Pwr (5+6+7+8-9+10+11+12) | dBm | -128.25 | -1.15 | 1.15 | -128.25 | 0.1472 |
| 14. Noise Spectral Density | dBm/Hz | -169.73 | -1.17 | 0.64 | -169.91 | 0.1401 |
| 15. System Noise Temperature | K | 770.63 | -182.12 | 121.67 | 750.48 | 3896.1095 |
| 16. Received Pt/No (13-14) | dB-Hz | 41.66 | 1.61 | -1.61 | 41.66 | 0.2873 |
| CARRIER PERFORMANCE | | | | | | |
| 21. Recovered Pt/No (16+[AGC+BPF]) | dB-Hz | 41.66 | 1.61 | -1.61 | 41.66 | 0.2873 |
| 22. Command Carrier Suppression | dB | 0.00 | -0.00 | 0.00 | 0.00 | 0.0000 |
| 23. Ranging Carrier Suppression | dB | 0.00 | 0.00 | 0.00 | 0.00 | 0.0000 |
| 24. Carrier Power (AGC) | dBm | -128.25 | -1.15 | 1.15 | -128.25 | 0.1472 |
| 25. Received Pc/No (21+22+23) | dB-Hz | 41.66 | 1.61 | -1.61 | 41.66 | 0.2873 |
| 26. Carrier Loop Noise BW | dB-Hz | 19.18 | -0.20 | 0.15 | 19.16 | 0.0102 |
| 27. Carrier Loop SNR (CNR) (25-26) | dB | 22.50 | 1.64 | -1.64 | 22.50 | 0.2975 |
| 28. CNR, mean-3 Sigma | dB | 20.86 | 0.00 | 0.00 | 20.86 | 0.0000 |
| 29. Recommended CNR | dB | 12.00 | 0.00 | 0.00 | 12.00 | 0.0000 |
| 30. CNR Margin (27-29) | dB | 10.50 | 1.64 | -1.64 | 10.50 | 0.2975 |
| 31. CNR Margin, mean-3 Sigma (28-29) | dB | 8.86 | 0.00 | -0.00 | 8.86 | 0.0000 |

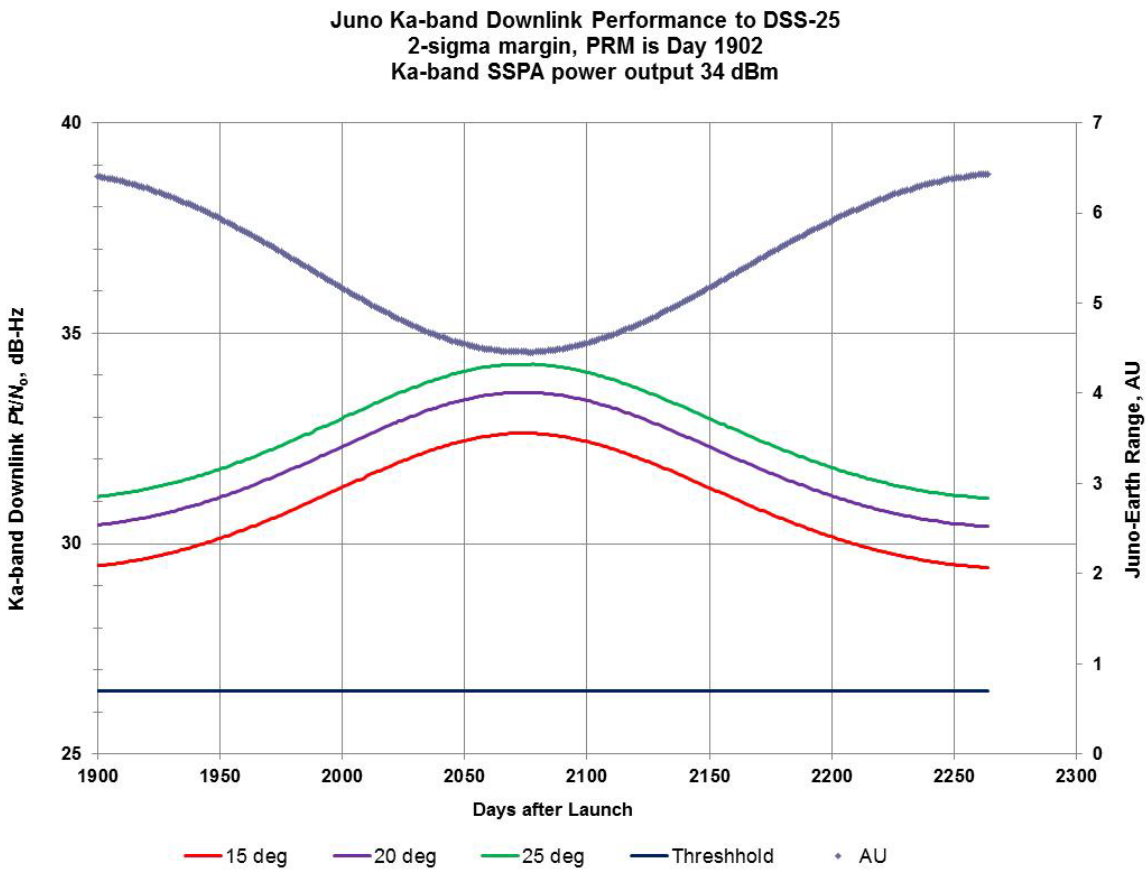


**Figure 3-7: Predicted Juno Ka-band downlink $P_t/N_o$ during orbit phase.**

### *3.2.3.3 Telecom during Main Engine Burns*

There were four main engine burns planned during the mission. The first two were the Deep Space Maneuver (DSM) Parts 1 and 2 in 2012. The third was the Jupiter Orbit Insertion (JOI) burn and the fourth (cancelled) was the Period Reduction Maneuver (PRM) in 2016. Following the Orbit phase, there is also a deorbit burn[12] planned to end the mission for planetary quarantine purposes.

The JOI burn placed the spacecraft into a 107-day orbit around Jupiter. The PRM puts the spacecraft into a roughly 11-day orbit around Jupiter. This 11-day final orbit was designed to place perijove over DSS-25 for the Gravity Science passes. During the main engine burns, the spacecraft puts the velocity vector close to normal to the Earth line.

The toroidal LGA (TLGA) supports communications during the burns. Because of the limited capability of an LGA and the distance to the Earth, the downlink would not support telemetry. Instead, the spacecraft transmitted tones, similar to MER Entry, Descent, and Landing (EDL) telecom, to a 70-m ground station. The two DSM burns were performed with dual 70-m coverage for redundancy, as was the JOI burn. The (cancelled) PRM burn would have been over Goldstone to allow for orbit alignment with DSS-25. For JOI the off-Earth antenna angle was 2 deg

[12] The thrusters in the REM towers are capable of providing medium delta-V and are sufficient for the Deorbit Burn of 75m/s [11].

maximum, and for PRM it would have been 4-deg maximum. Though both JOI and PRM were at Jupiter range, PRM would have been at a slightly longer range and wider angle so in the original plan it was a tougher communications requirement to meet than JOI.

During each burn sequence, the S/C starts on the HGA, switches to the MGA and then to the TLGA as the spacecraft turns to burn attitude. The station is not required to uplink during the main engine burns. Therefore, the tone downlinks are one-way. The S/C will go back to the MGA for navigation and engineering TLM downlink. After each burn, the S/C attitude will have to be adjusted to align the HGA with the spacecraft spin axis. It will need adjustment because the mass properties of the spacecraft will have changed due to propellant usage. After S/C alignment is complete, the S/C will return to using the HGA.

#### *3.2.3.4 Safe Mode*

In safe mode, the spacecraft goes into a configuration that is power positive, thermally stable, and commandable. Juno has two types of safe mode, depending on whether three-axis attitude knowledge is retained or not. If attitude knowledge is retained, the spacecraft pointing (including that of the antenna toward Earth) is not changed. If attitude knowledge is lost, the spacecraft will "cone" within 2 deg of the Sun. That is, the solar panel pointing to the Sun will describe a cone with 2-deg radius centered on the Sun.

The nominal safe mode data rates are 40 bps for downlink telemetry and 7.8125 bps for the uplink command. The downlink rate may be changed by flight software during phases of the mission when the range is short. Ranging is to be switched off for all safe mode telecom. Nominal and safe mode TWTA and antenna choices are mission phase dependent. In safing, the uplink loss executive (ULLE) and the downlink loss executive (DLLE) have the ability to swap hardware and to use the backup antenna paths if the primary antenna path to the given safe mode antenna were to fail [15].

Attitude knowledge not lost: Figures 3-8 and 3-9 show the safe mode capability (downlink and uplink predicted $P_t/N_o$, respectively) to a 70-m ground station throughout the mission. Both of these figures were plotted with two assumptions: (1) the spacecraft-pointing attitude toward Earth does not change in going to safe mode and (2) the spacecraft ends up on the MGA.

Attitude knowledge is lost: Figures 3-10 and 3-11 show similar safe mode predictions, but they assume that the spacecraft has lost spacecraft attitude knowledge and is coning 2 deg off the Sun line, as a worst-case condition. Note that for these cases, safe mode might have to switch to an LGA to maintain communications.

In either case, the system can meet the safe mode communications requirements.

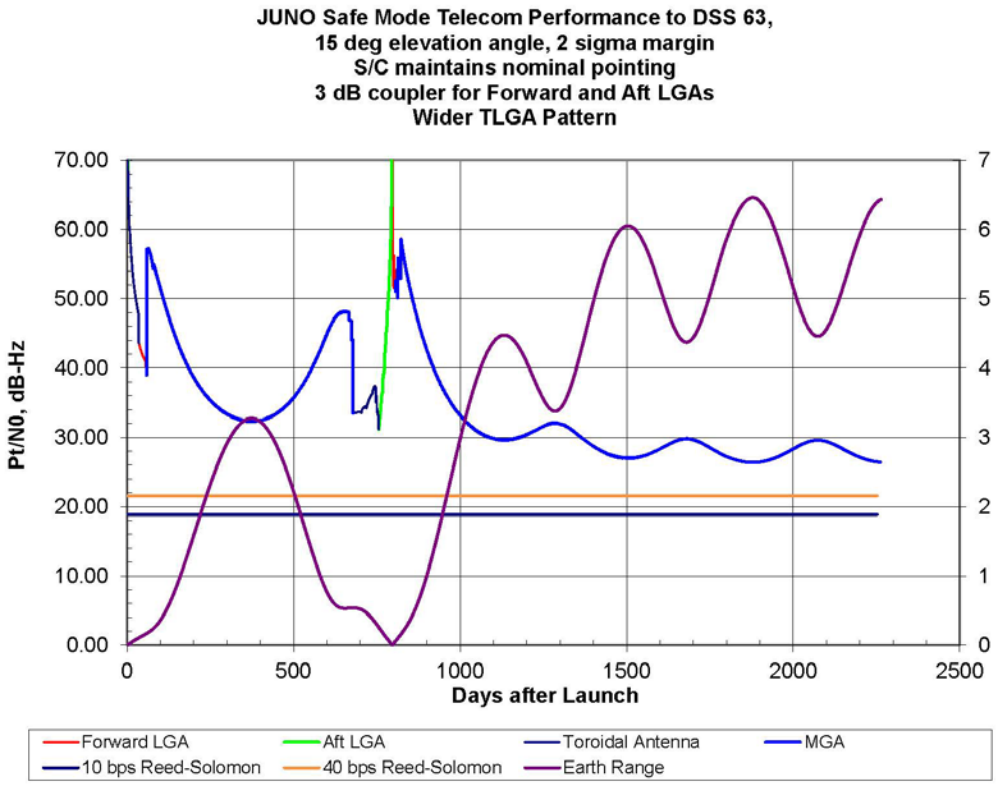


**Figure 3-8: Predicted safe mode downlink $P_t/N_o$ – no attitude change.**

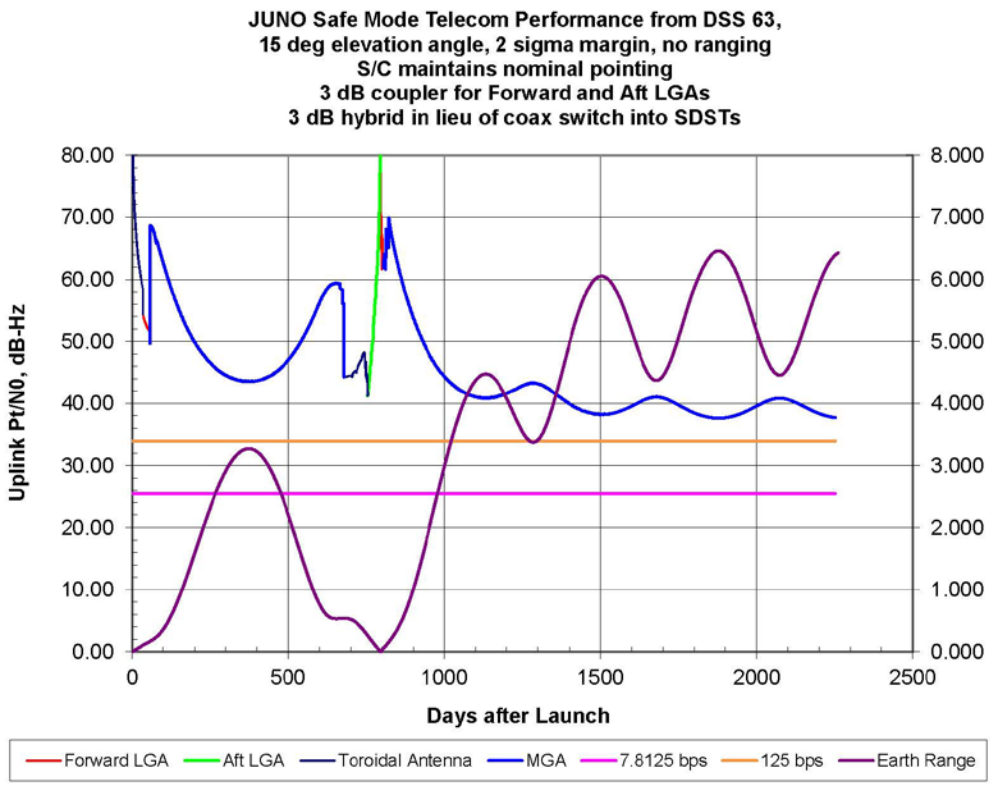


**Figure 3-9: Predicted safe mode uplink $P_t/N_o$ – no attitude change.**

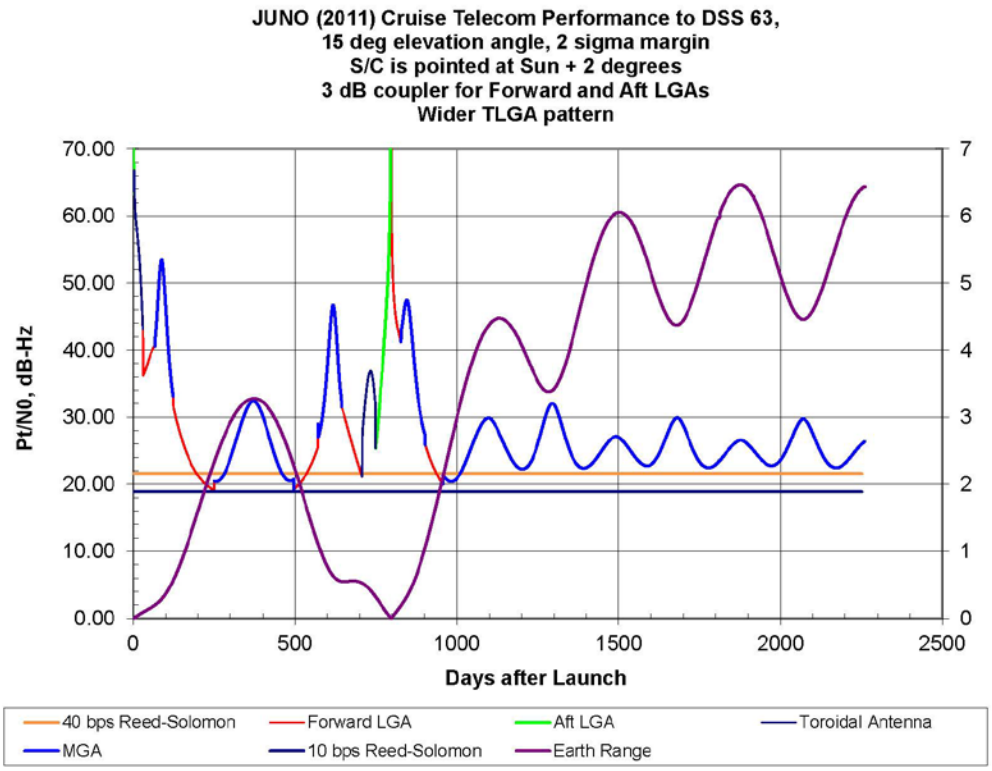


**Figure 3-10: Predicted safe mode downlink $P_t/N_o$ – Sun-pointed.**

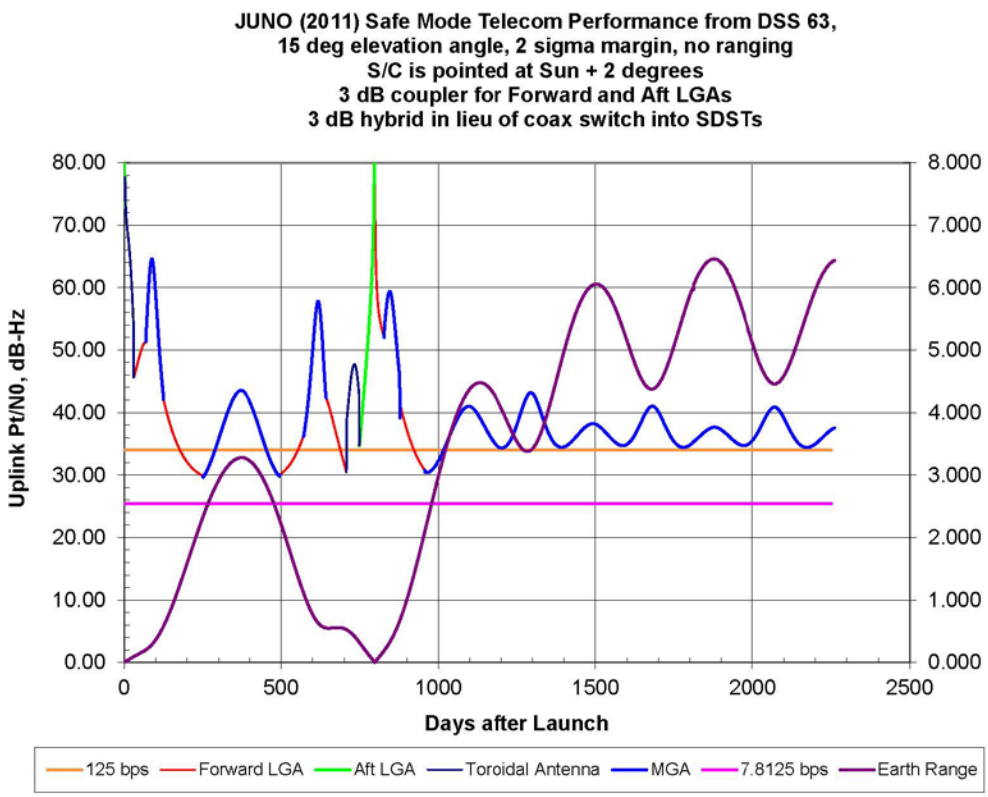


**Figure 3-11: Predicted safe mode uplink $P_t/N_o$ – Sun-pointed.**

**Blank**

# 4 Ground Systems

## *4.1 Deep Space Network*

As described in the Dawn article in this series [6] and in the Deep Space Network (DSN) web site [7], the National Aeronautics and Space Administration (NASA) DSN is a network of antennas at three deep space communications facilities that are located approximately 120 degrees (deg) apart around the world. One site is at Goldstone in the California Mojave Desert, another is near Madrid, Spain (Figure 4-1), and the third is near Canberra, Australia. These locations permit constant observation of spacecraft as the Earth rotates. Each complex contains one 70-meter (m) diameter antenna and a set of 34-m diameter antennas as well.

The Juno mission will often rely on 34-m antennas in nominal operations. However, in orbit around Jupiter, 70-m stations will be used if the spacecraft enters safe mode. Additionally, 70-m stations were used for tone detection during the Deep Space Maneuvers (DSM) and the Jupiter Orbit Insertion (JOI) as well as for increased science data return at Jupiter. DSN antennas include a group at Madrid [7] in Fig 4-1.

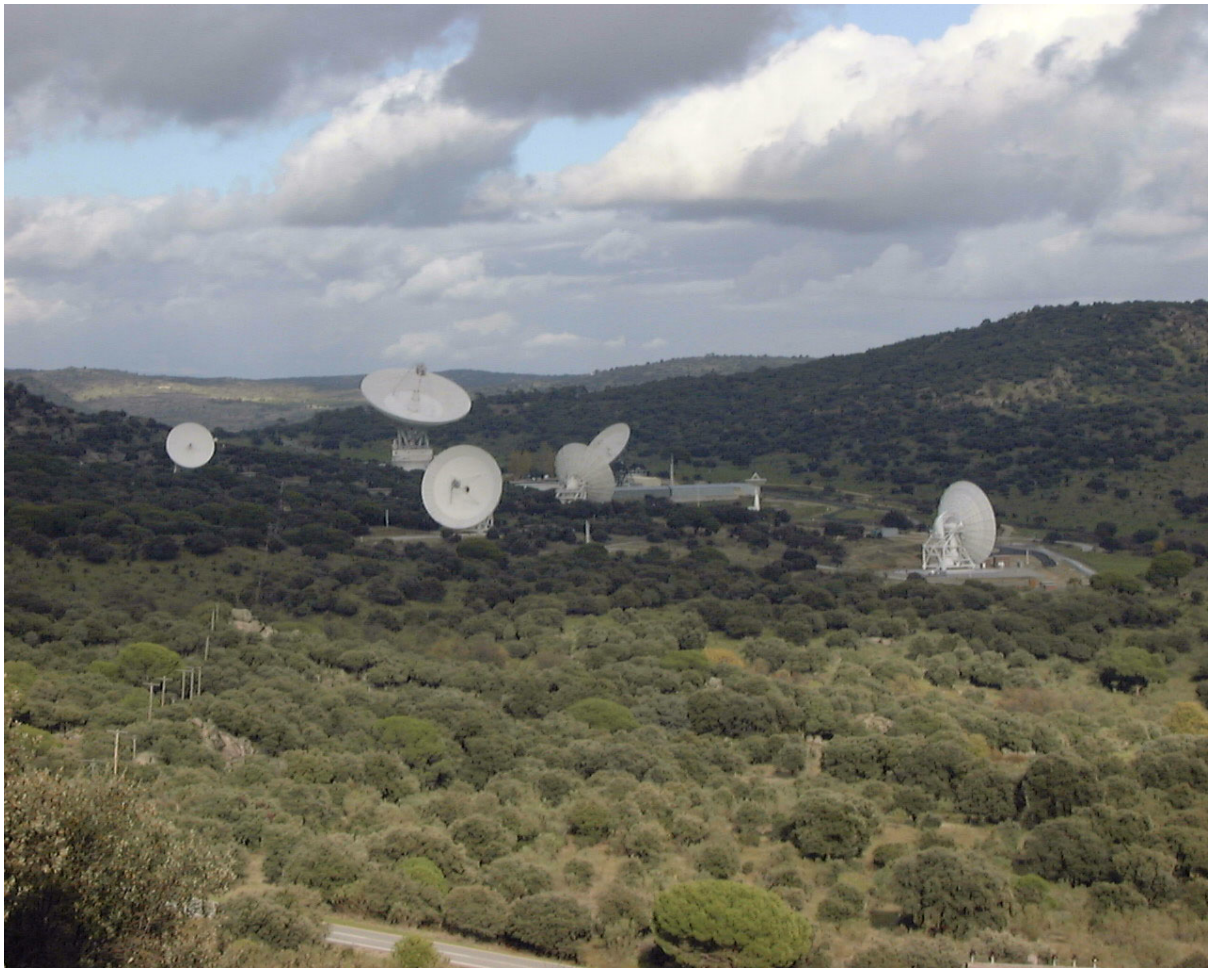

**Figure 4-1: The Madrid DSN complex.**

## 4.2 Initial Acquisition Support from the European Space Agency

Though DSN stations were prime for Juno initial acquisition, the European Space Agency (ESA) stations provided backup for initial capture of telemetry. The objective of the cross-support service from ESA's Perth and New Norcia stations was to mitigate the risk of critical data loss through the entire launch period. Without the ESA stations, the critical data period was subject to a short visibility gap between separation of the spacecraft from the launch vehicle and initial acquisition at the DSN Canberra Complex. Furthermore, because Perth is fitted with an X-band acquisition aid antenna with auto-track capability, acquisition and tracking of the spacecraft downlink signal could have been accomplished even in case of a non-nominal trajectory.

As stated in the *Juno Operations Interface Control Document* (OICD) [8] and chiefly in the Juno LEOP implementing agreement [9], during the latter portions of the launch period, the elevation angle at Canberra would have been low, sometimes close to or below 6 deg. The elevation angle in Northwest Australia is much higher and if launch had occurred later in the launch period, there would have been cases in which Canberra would not have been in view for separation.

For these cases, only ESA's Australia stations at Perth or New Norcia Stations would have been in view. Figures 4-2 and 4-3 show the spacecraft ground track, and site views for the actual August 5 launch date and for a launch-period closing date of August 26. The red line on each plot is the ground track of Juno on launch day. The dotted portion of the red curve (going generally from left to right as time increases) is before the Juno transmitter radiates a downlink, and is therefore before any station could receive a downlink. Starting with transmitter on (at 16:21 UTC on the actual launch date), the curve becomes solid, and has superimposed red markers on one-hour centers. The yellow areas originating at the Perth (or New Norcia), Canberra, Madrid and Goldstone sites depict the views (begin-of-track to end-of-track) from these sites. A station can receive the downlink when the solid red line is within that site's yellow view.

The difference in post-separation station elevation angle profiles for the early and late launch dates is shown in Figure 4-4 (actual August 5 launch) and Figure 4-5 (August 26). Similarly, the post-separation spacecraft-to-station slant range profiles for early and late launch dates are shown in Figures 4-6 and 4-7.

Critical operations, such as the deployment of the solar panels, could possibly have fallen into the period when the spacecraft had not yet been acquired by Canberra, and the data acquired at Perth would have become important for forensic purposes. To further mitigate the risk of having a visibility gap, ESA also acquired the signal at the New Norcia station. In addition to the normal telemetry acquisition at New Norcia, that station was configured to perform open-loop recording of the downlink signal to have a basis for analysis in the event that telemetry acquisition had failed.

As New Norcia has neither an acquisition-aid antenna nor auto-track, the pointing of the New Norcia antenna with respect to the predicts would have been corrected as needed on the basis of the actual pointing determined by the Perth station in auto-track mode. Furthermore, an along-track offset observed at Perth would have been communicated via the voice loop to the Canberra complex to aid initial acquisition there.

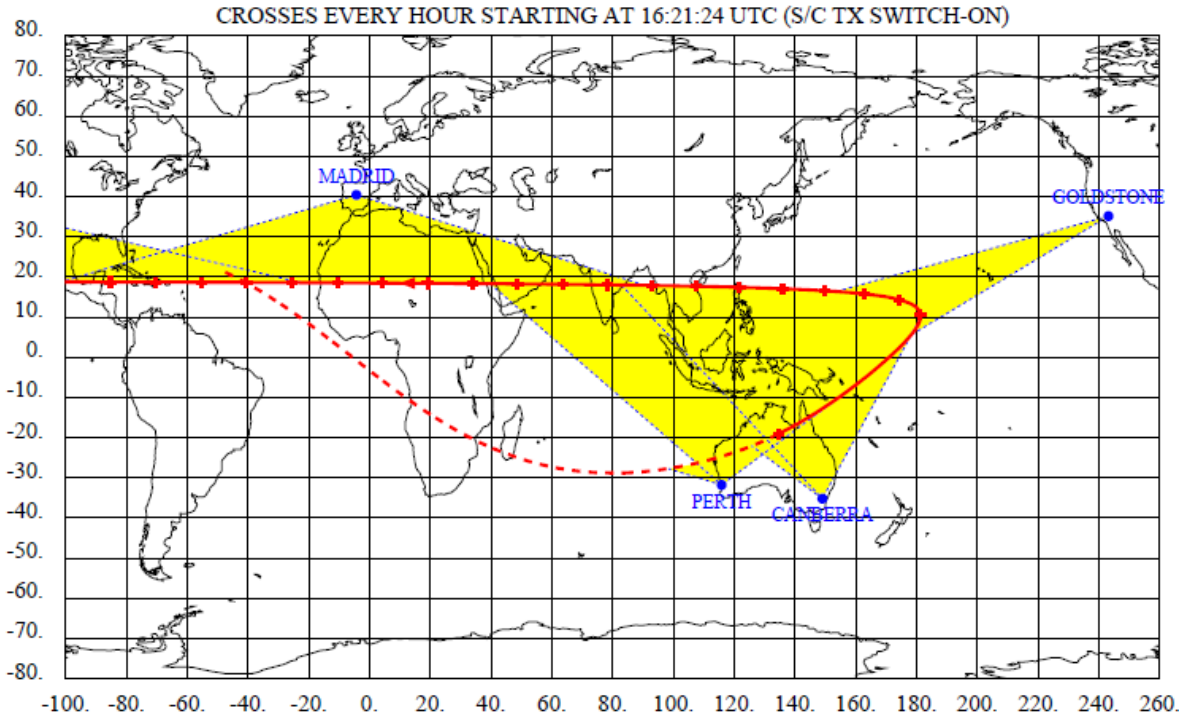


**Figure 4-2: Juno ground track after separation (launch on August 5, 2011).**

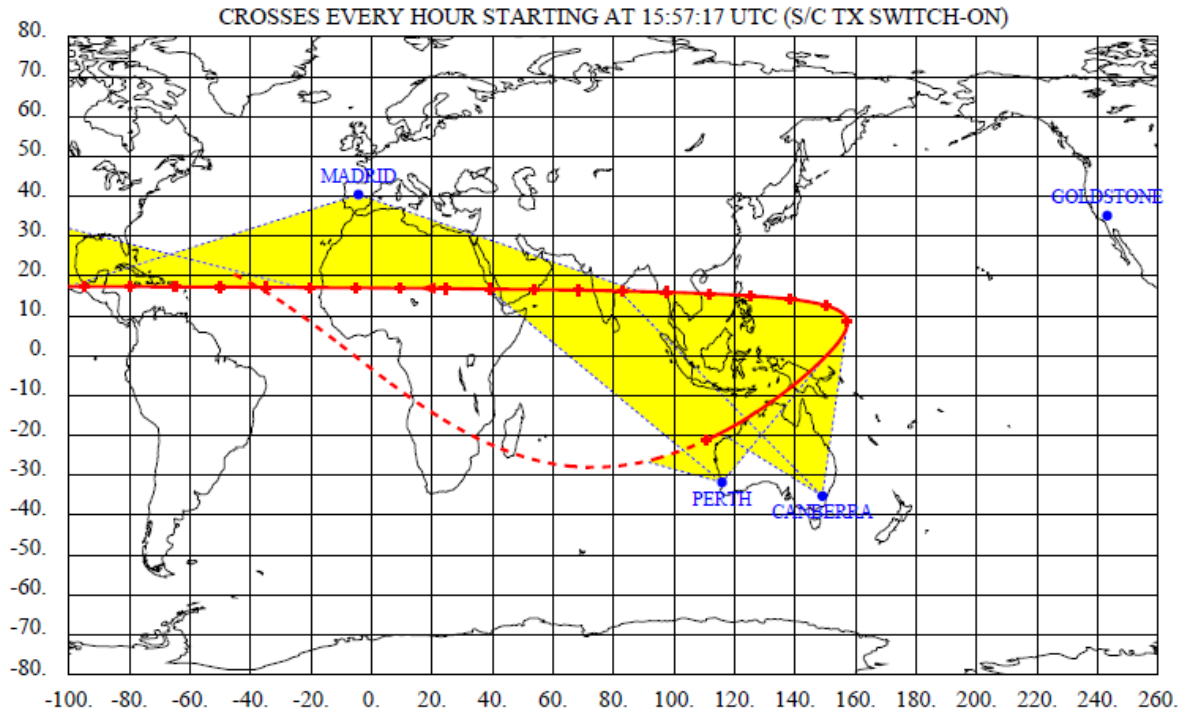


**Figure 4-3: Juno ground track after separation (launch on August 26, 2011).**

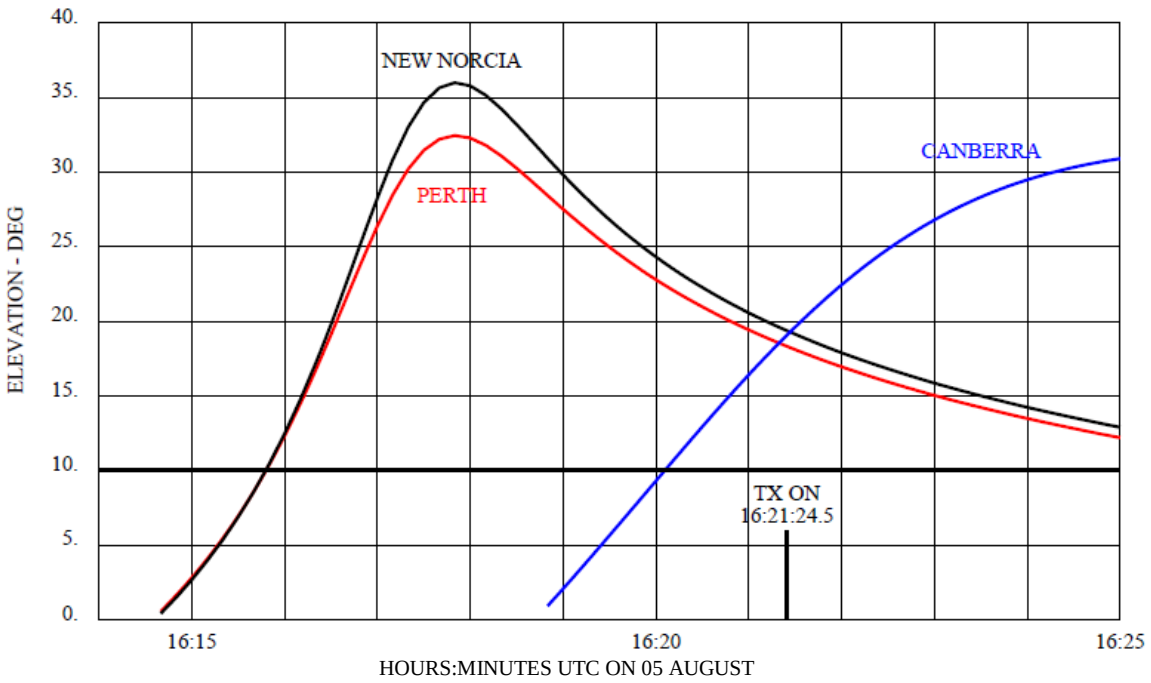


**Figure 4-4: Elevation at the LEOP stations (launch on August 5, 2011).**

A secondary objective for the ESA support was to acquire spacecraft telemetry and route it on a best-efforts basis to the Juno Project so that in case of a serious spacecraft problem as much telemetry as possible would have been available for offline diagnosis of the problem, although launch proved to be nominal on August 5, 2011. The signal from Perth was routed to a spectrum analyzer, and a live view of the spectrum analyzer display was projected to Astrotech[13] where Juno engineering personnel watched for the signal in real time, although the image from the webcam at Perth was delayed to a certain extent by Internet delays before reaching Astrotech.

The signal level emitted by the Juno spacecraft after separation in the direction of the antenna boresight was quite high (47.5 decibels referenced to milliwatts, dBm) while the slant range at acquisition (station transmitter ON, labeled TX ON) could have been as low as 2000 km from Perth and from New Norcia had launch been delayed (*see* Figure 4-7). The low-noise amplifier (LNA) at each station would have received a signal comfortably below its compression point with the Juno LGA pointed at the station at a distance of 2000 km. With standard gain settings, however, the Intermediate Frequency Modem System (IFMS) would have been saturated and in its nonlinear operations range. Therefore, this support required temporary installation of attenuators (20 dB at Perth and 30 dB at New Norcia).

[13] Astrotech Space Operations at Titusville, Florida, readied the Juno spacecraft for launch as the payload aboard the Atlas V launch vehicle. The launch vehicle was the responsibility of the United Launch Alliance, a joint venture between Lockheed Martin Corporation and the Boeing Company.

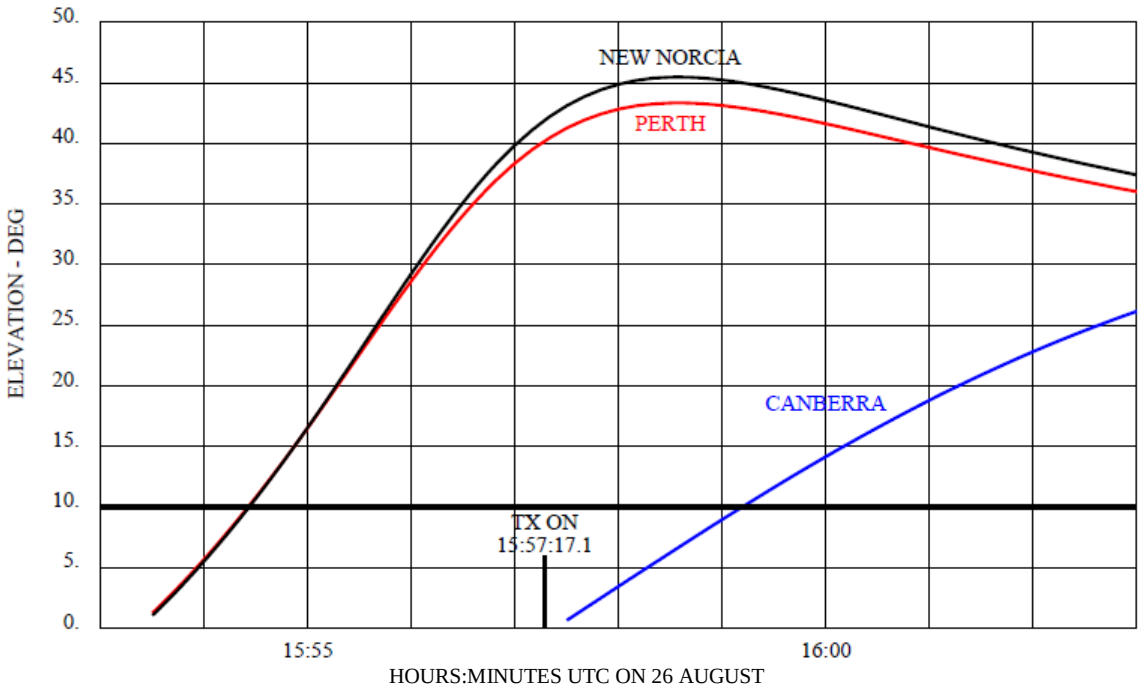


**Figure 4-5: Elevation at the LEOP stations (launch on August 26, 2011).**

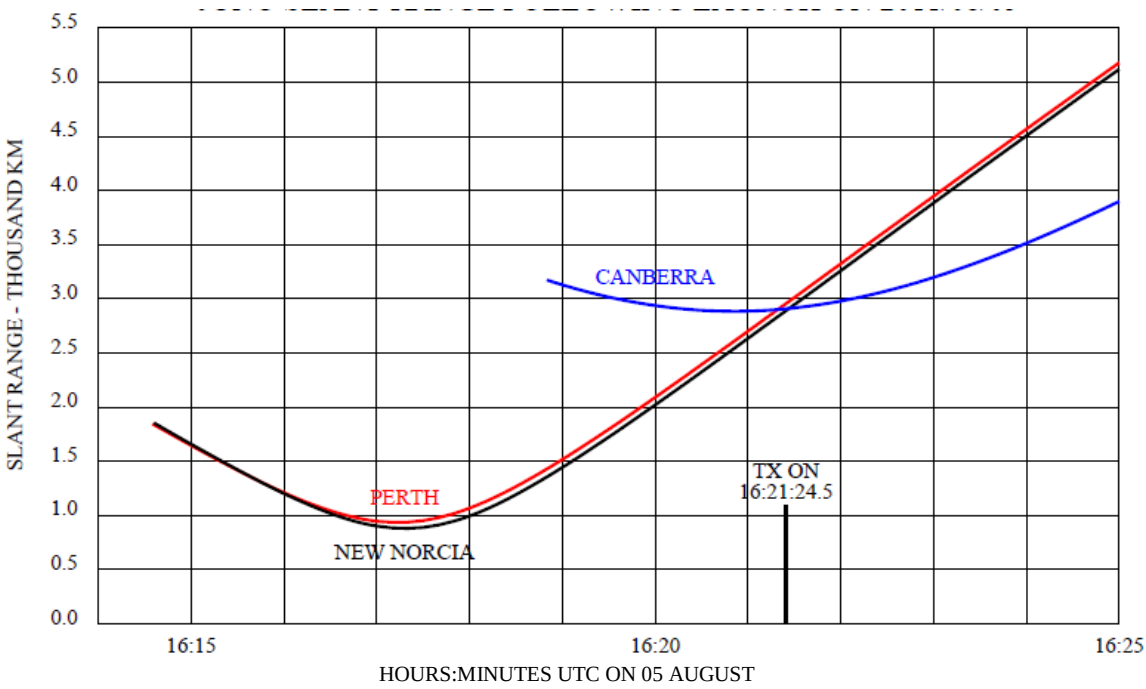


**Figure 4-6: Slant range from the LEOP stations (launch on August 5, 2011).**

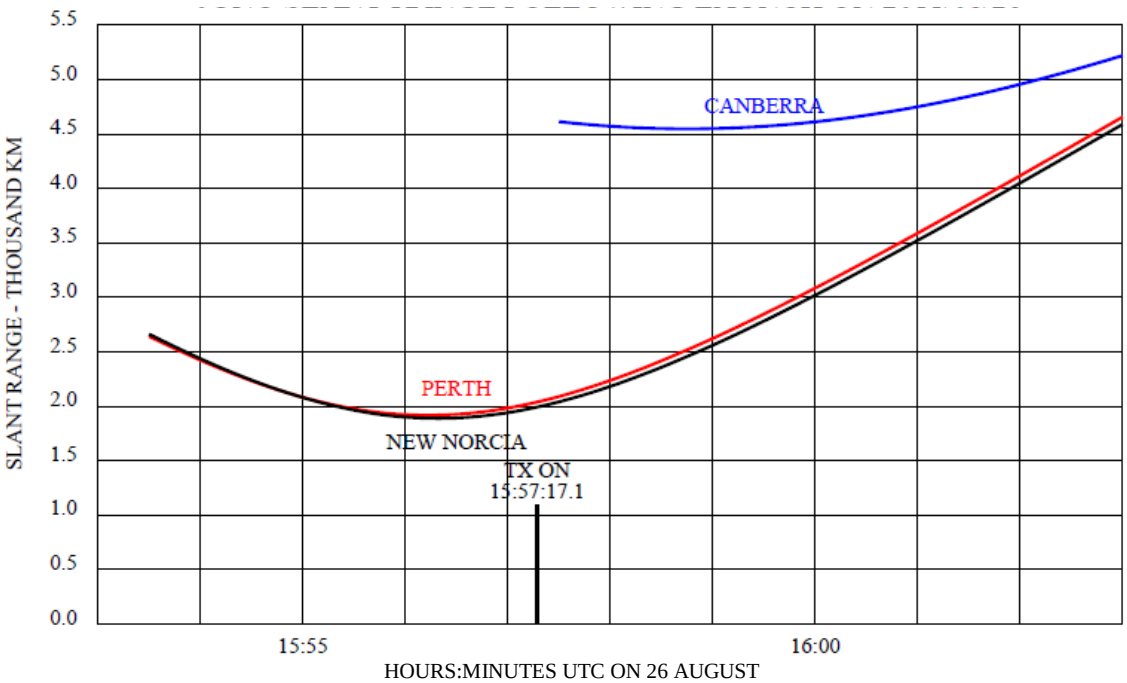


**Figure 4-7: Slant range from the LEOP stations (Launch on August 26).**

The European Space Tracking (ESTRACK) 15-m station at Perth supported Juno LEOP operations. A simplified block diagram of the station is provided in Figure 4-8. The antenna was initially pointed in accordance with the trajectory predicts provided in a file by Juno navigation. ESA's Flight Dynamics operational organization retrieved the file from the DSN Service Preparation System (SPS) and converted the contents to an internal format to forward via the station computer to the Front-End Controller (FEC) and to the IFMS. The FEC used the converted trajectory data to point the antenna, and the IFMS is used them to calculate the Doppler predicts. The above outlined process has been used with other non-ESA projects, e.g., for the SOlar Heliospheric Observatory (SOHO) test tracks at New Norcia.

Acronyms and names that appear in Figure 4-8 that are not previously defined are:

| | |
|---|---|
| HPA | high power amplifier |
| LAN | local area network |
| M&C | monitor and control |
| MCM | monitoring and control module (subsystem controller) |
| TC | telecommand |
| TMTCS | telemetry and telecommand system |

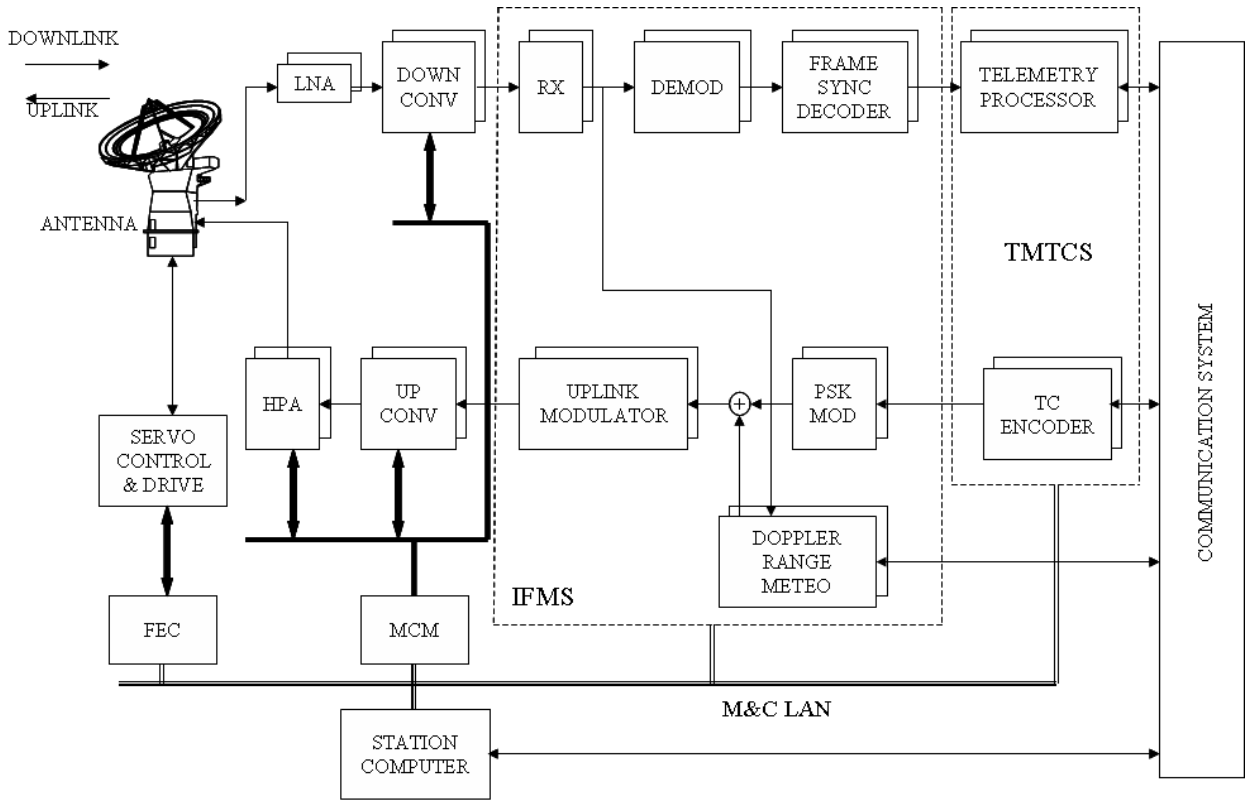


**Figure 4-8: ESA ESTRACK station block diagram.**

The key events that occurred after separation during the Perth and New Norcia view periods are listed below and are illustrated in Figure 4-9, taken from Ref. [9].

- The designated prime traveling wave tube amplifier (TWTA) was sequenced on by the flight software approximately 5 minutes before separation;
- The spacecraft was to start transmitting no earlier than 5 seconds after separation (safety constraint), which was 53:25 after launch;
- The TWTA began to radiate RF 11 seconds after separation when the TWTA transitioned from the warm-up mode to the high-power mode;
- The solar array deployment was planned to be initiated 3.5 minutes after separation and to be complete no later than 15 minutes after separation.

The pre-launch trade referred to in Figure 4-9 was to determine station coverage necessary to insure a downlink could be received before the pyro firing events.

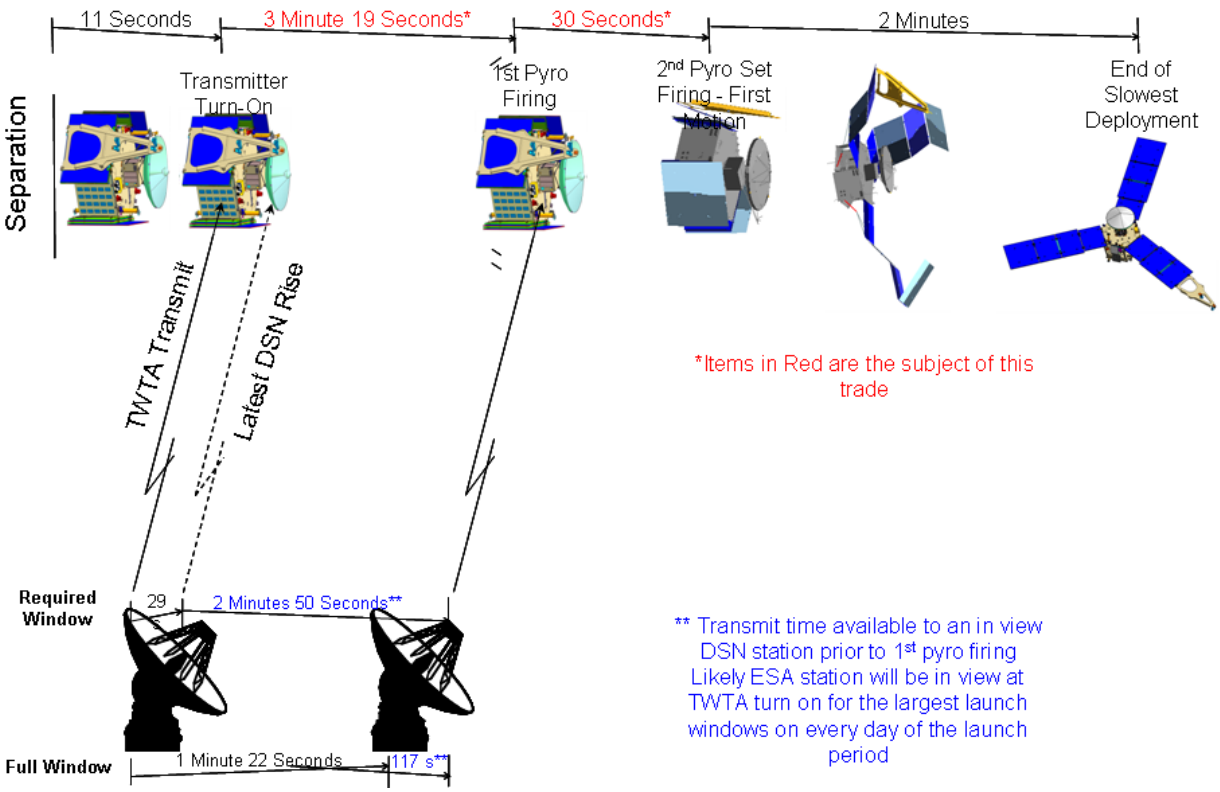


**Figure 4-9: Key events after separation [9].**

# 5 Gravity Science Operations

This section provides a summary of gravity science operations to be carried out during the science orbits phase. It provides an overview of how the Gravity Science orbits are scheduled along with the other basic orbit type, the Microwave Radiometer (MWR) orbits. MWR orbits are conducted earlier in the science orbits phase due to the limited lifetime of the MWR in the presence of radiation. In the original 11-day orbit plan, the last MWR orbit in Table 5-1 is orbit 8. In the 53-day orbit plan, the orbit dates are changed (Table 6-1), and the last MWR orbit is 18.

The bulk of the material in this section comes from the Juno Project Mission Plan, Jet Propulsion Laboratory (JPL) Document D-35556 [1].

## *5.1 Gravity Science Overview*

The Juno Gravity Science (GRAV) investigation is probing into the depths of Jupiter by precisely observing the Doppler Effect on the radio signal during close flybys. The quality of the experiment depends on a number of factors, including the phase stability of the radio links and minimizing the noise due to interplanetary plasma and the Earth's atmosphere. The contribution of dispersive noise sources is inversely proportional to wavelength, making Ka-band (32 GHz or 1 cm) an order of magnitude less susceptible than X-band (8.4 GHz or 3.6 cm). X-band is used for communications and navigation, and X-band and Ka-band are used together for the Gravity Science investigation.

When the X-band and Ka-band signals are received simultaneously on the ground, the dispersive noise contribution is differentially calibrated and removed. To accomplish this, Juno has an instrument called the Ka-band Translator (KaTS), which is separate from the X-band telecom subsystem (the SDST and the X-band TWTA). The KaTS receives a Ka-band uplink unmodulated carrier from the Deep Space Network (DSN) and generates a Ka-band downlink unmodulated carrier that is coherent with the uplink. The coherency maintains the uplink's excellent phase stability derived from hydrogen-maser atomic sources on the ground.

As described in Section 2 of this article, the KaTS includes a Ka-band receiver, digital signal processing, and a Ka-band solid-state power amplifier (SSPA). KaTS operations do not involve extensive commanding, sequencing, or flight software. The only commands affecting the KaTS are when the spacecraft power subsystem turns it on or off.

The Gravity Science investigation uses considerable ground infrastructure as well as the Telecom Subsystem on the spacecraft (Figure 5-1). The major ground operation is to generate a "sweep" uplink transmitter frequency profile to allow the KaTS to lock onto the uplink carrier.

The noise contribution due to the Earth's troposphere is calibrated via ground-based water-vapor radiometers.

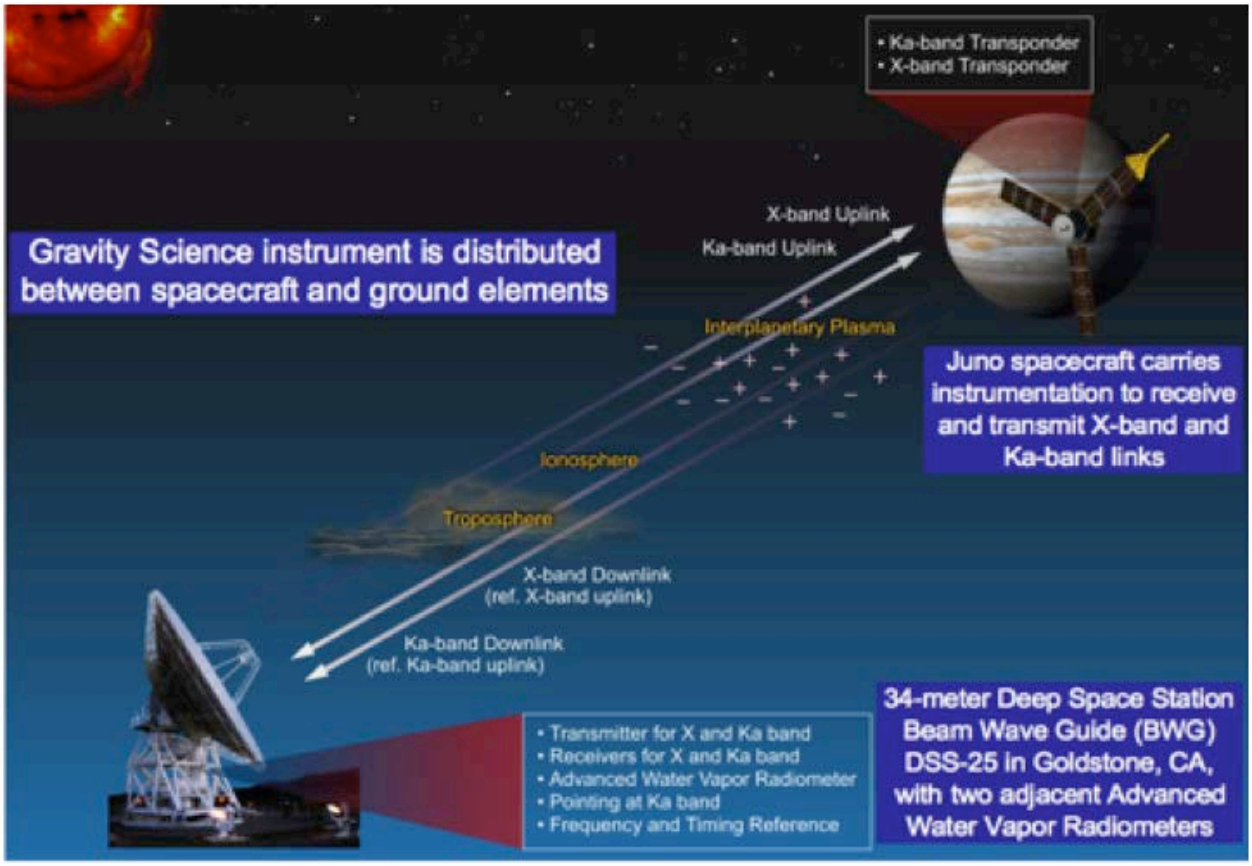


**Figure 5-1: The Gravity Science instrument.**

## *5.2 Science Orbits*

We distinguish activity periods from orbits. Orbits are used to refer to the mission design and navigation strategy (for example, Nav data cutoffs, which occur near apojove (AJ) orbit boundaries, and trajectory events), while activity periods are used to describe science and mission operations such as sequence, generation and data flow from the stations to the scientists.

The Science Orbit phase includes Orbit 3 through Orbit 33 (Figure 5-2). Beginning with Orbit 1, Orbit N is defined from AJ N-1 through AJ N, and includes perijove (PJ) N.

Orbit numbering began with Orbit 0 at JOI. See Table 6-1 for currently planned mission dates. Orbit 0 lasted from Perijove 0 (PJ0) through Apojove 0 (AJ0). This orbit included a JOI cleanup maneuver at JOI + 7.6 d (performed July 13, 2016). Orbit 1 includes PJ1 and ran from AJ0 (July 31) through AJ1 September 23. Orbit 2 included PJ2, ran from AJ1 through AJ2, and included an OTM on October 25. In the early orbits, science was baselined (except for JOI and the cancelled PRM) in Orbit 0 and the first half of Orbit 1 (which together contain the 107-day capture orbit), and in Orbit 2, but not in the last half of Orbit 1 (PJ1 to AJ1).

Orbit 3 was the first science orbit. It included PJ3 and ran from AJ2 through AJ3. The last science orbit is Orbit 33. It will be bookkept as an extra science orbit, since the mission will use Orbits 3 through 32 to obtain 30 perijoves with MAG and other data that meet Level-1 baseline science requirements.

Delta-

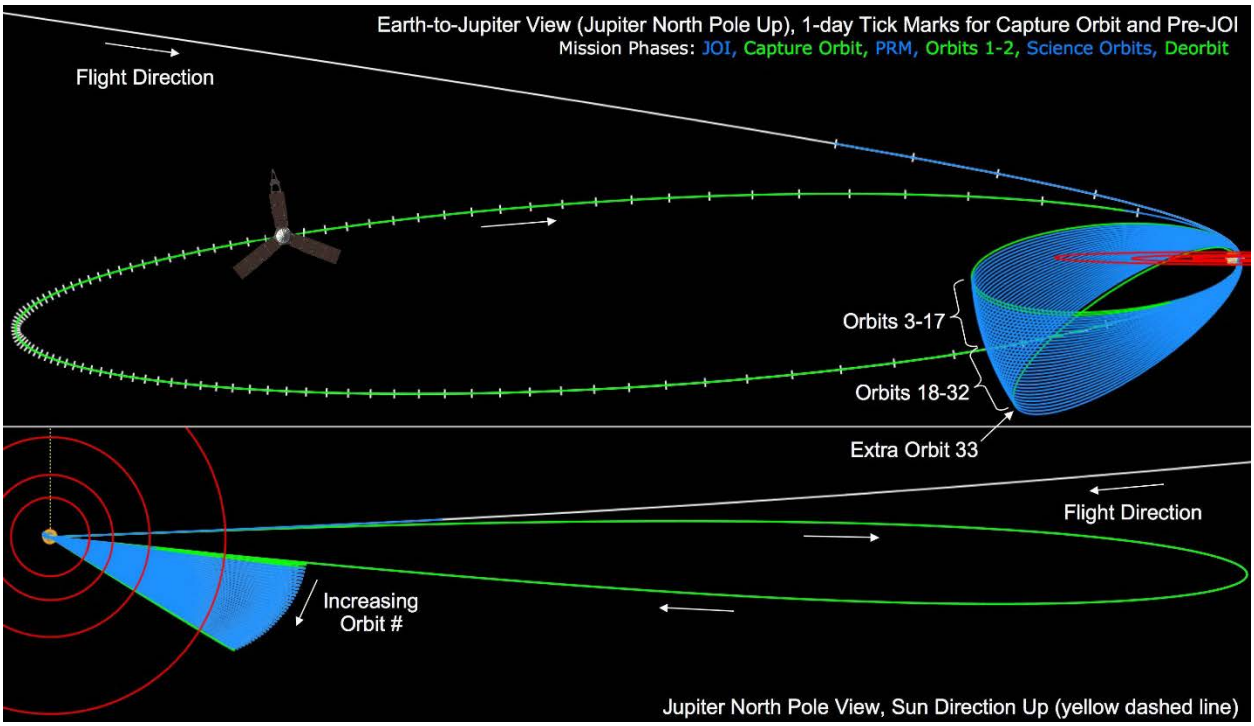


**Figure 5-2 *Superseded: Juno orbital trajectory.**

* See Figures 6-1 and 6-2 for orbit trajectories for the 53-day mission.

Small (0.0–3.0 m/s) orbit trim maneuvers (OTMs) are planned after each set of perijove science observations, at PJ + 4 h in Orbits 3 through 32, to target the perijove longitude required for science observations in the next orbit. There is no need for an OTM at PJ33 + 4 h. The deorbit maneuver (deterministic change in velocity (delta V, DV) = 74 m/s) is planned near AJ33.

An activity period (AP) runs from one PJ – 1 d to the next PJ -1 d. Each AP is defined by the number of the PJ science pass it contains, and the type (MWR or GRAV). Special AP2 was the first activity period in the 11-day-orbit plan and ran from PJ2 – 1 d through PJ3 – 1 d. It was followed by the first standard Science Orbit activity period (an MWR type), from PJ3 – 1 d through PJ4 – 1 d. The Science Orbits phase began at the start of AP3, and continues through AP33. This last AP ends early, at AJ33 – 1 h, before the deorbit burn in the Deorbit phase.

Radiation accumulation will increase substantially as the orbital line of apsides rotates and perijove latitude increases from 3 deg at JOI to 34 deg at PJ33 (Fig. 5-3 for the 11-day orbit plan and Fig. 6-3 for the 53-day orbit plan). Figure 5-4 shows radiation dose vs. orbit number for the 11-day plan; it remains representative for the 53-day plan. Neither plan includes a mission beyond 33 science orbits, though the calendar date for Orbit 33 is later in the 53-day orbit plan. Even without radiation concerns, the delta-V (DV) capability remaining after JOI limits extended mission options. See Section 7 for the 53-day orbit plan.

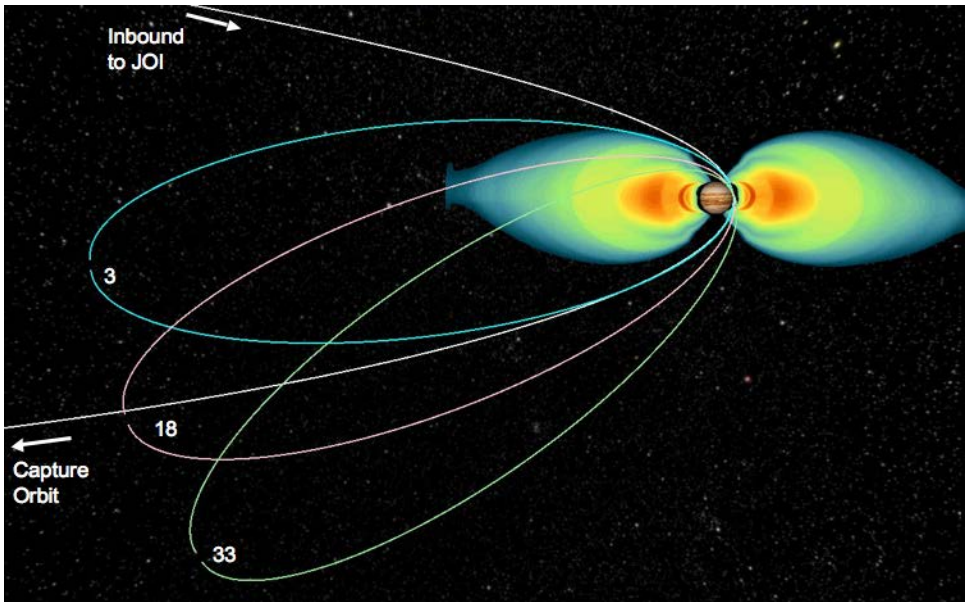


**Figure 5-3 *Superseded : Juno orbital radiation environment.**

* See Figure 6-3 for orbital radiation environment for a mission with 53-day orbits.

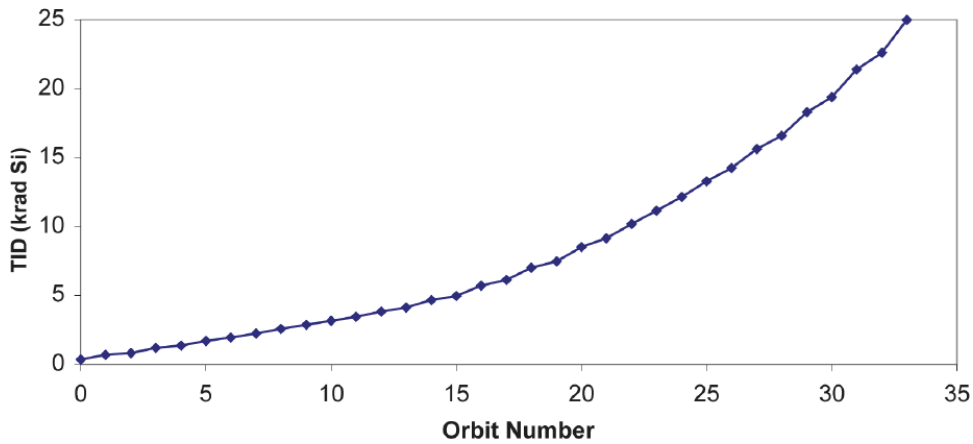


**Figure 5-4 *Representative: Orbital radiation accumulation (vault total dose vs. orbit).**

* This figure for thirty-three 11-day orbits remains representative for the 53-day orbit plan.

In the original mission design with 11-day orbits, each orbit was planned to be ~40 minutes less than ~11 days long (10.9725 days), to allow Juno to be viewable at every perijove from the same ground station (DSS-25 at Goldstone), which is the only DSN antenna capable of Ka-band uplink for Gravity Science. This timing, along with Jupiter's ~9.925-hour rotation period, is designed to shift the System-III longitudes at perijove so that the entire 360-deg longitude range is viewed with 24-deg spacing in the first 15 science orbits.[14]

[14] From Wikipedia, http://en.wikipedia.org/wiki/Jupiter. Definitions of System I, System II, and System III: Because Jupiter is not a solid body, its upper atmosphere undergoes differential rotation. The rotation of Jupiter's polar atmosphere is about 5 minutes longer than that of the equatorial atmosphere; three systems are used as frames of reference, particularly when graphing the motion of atmospheric features. System I applies from the latitudes

In the 11-day-orbit mission plan, the first 15 orbits (3 through 17) represented Juno's minimum mission. The PJ17 + 4 h OTM adjusts the timing so that PJ18 would begin to fill in the intermediate longitudes (with 24-deg spacing). Orbits 3 through 32 together would provide coverage of the entire longitude range with 12-deg spacing (Figure 5-5).

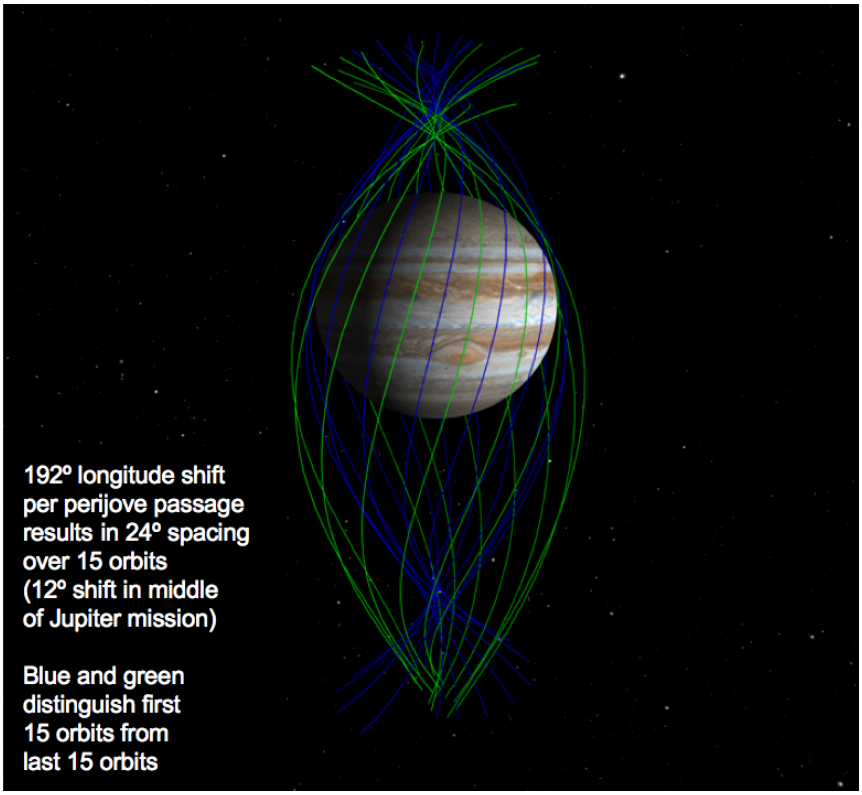


**Figure 5-5 *Superseded: Global coverage resulting from a net of perijove science passes.**

* For the 53-day science orbit, see Fig. 6-1 and Fig. 6-2 that supersede Fig. 5-5 and Fig. 5-6.

MWR was not designed to withstand radiation accumulation past the early orbits. Along with JIRAM and JunoCam, which also observe in the spin plane, MWR in the original mission plan was only to be operated through Orbit 8 (although MWR is designed to survive until Orbit 11). Perijove passes in Orbits 3 and 5–8 were dedicated to MWR, while the other perijove science passes (in Orbits 4 and 9–32, and probably Orbit 33) were dedicated to Gravity Science (GRAV). MWR, JIRAM, and JunoCam are off during GRAV passes, although we do consider using JIRAM and JunoCam as allowed by power, thermal, and other Flight System and mission operations constraints. GRAV (the KaTS) is off for MWR passes. UVS and the fields and particles instruments (JADE, JEDI, MAG, and Waves) are planned to observe during all science passes. To minimize operations costs, activities are planned to be very repetitive from orbit to orbit. We use two principal activity templates, one for MWR activity periods and one for GRAV activity periods.

10 deg N to 10 deg S; its period is the planet's shortest, at 9h 50m 30.0s. System II applies at all latitudes north and south of these; its period is 9h 55m 40.6s. System III was first defined by radio astronomers, and corresponds to the rotation of the planet's magnetosphere; its period is Jupiter's official rotation.

To understand mission requirements, capabilities, and constraints during the Science Orbits phase, for the 11-day-orbit mission we used representative activity periods as Mission Scenarios. Since the early orbits were more constrained by data rate and volume than middle orbits (which were closer to the minimum Earth–spacecraft distance), we used Activity Periods 3 (MWR) and 4 (GRAV) for Mission Scenarios. Later orbits were also constrained by data rate and volume, but we no longer expected to use MWR, JIRAM, and JunoCam. See Section 6 for the plans for the 53-day orbit mission.

The plots at the bottom of Figure 5-6 show how the individual 11-day science orbits vary. Earlier and later orbits occur when Juno is further from the Earth, while middle orbits occur near opposition when the Earth range is near minimum. The green curve shows how the angle between the Earth direction and the negative orbit normal direction varies, starting from its lowest value during Orbit 3. This geometry is important for GRAV, which favors larger negative orbit normal to Earth angles for greater Doppler signal, and which also favors larger SEP angles for simultaneous X- and Ka-band observations (the closer to opposition the better since this means much less noise due to the solar corona at X-band, which is more susceptible than Ka-band). Finally, the negative orbit normal to Sun geometry (yellow curve) affects our ability to use Orbits 9-11 for MWR if needed, since larger angles mean less solar array power.

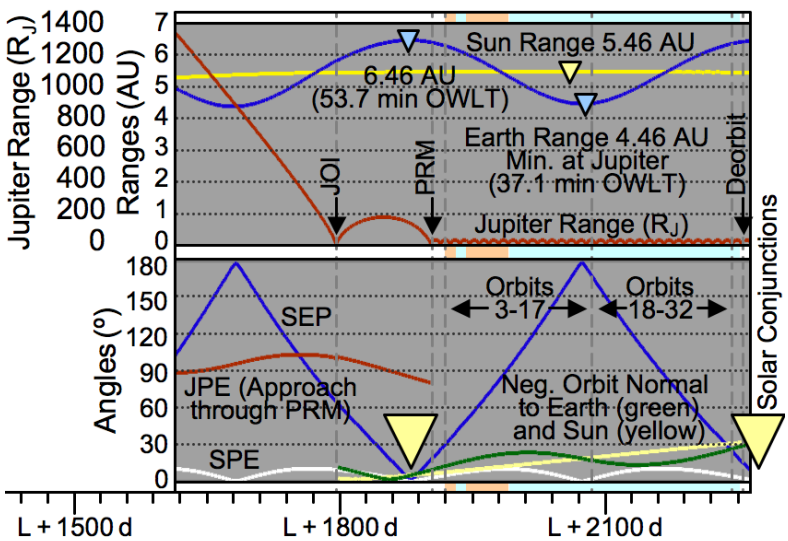


**Figure 5-6 *Representative: Science orbits geometry.**

* This figure is correct to JOI. For the 53-day orbit plan, the time scale from launch is stretched out after JOI (per Table 6-1), and PRM was not done.

Figure 5-7 shows the spacecraft attitude during MWR and GRAV perijove passes.

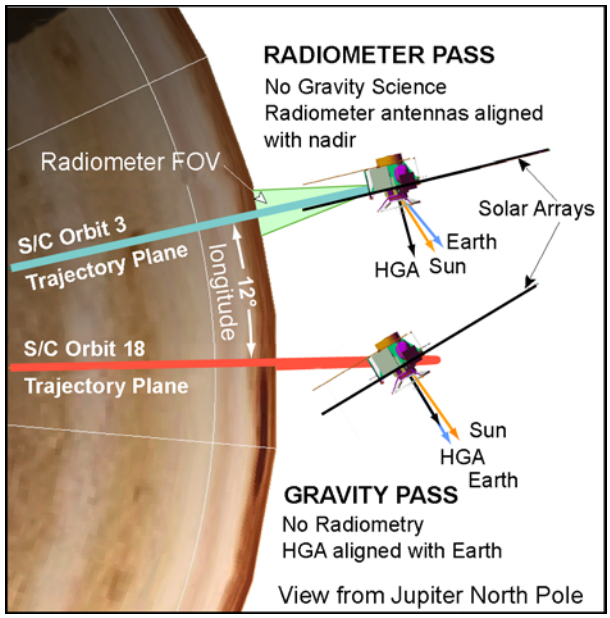


**Figure 5-7: Spacecraft attitude during MWR and GRAV perijove passes.**

During the orbital mission, the spacecraft is Earth-pointed except for turn-burn-turn maneuvers (JOI, PRM (now cancelled), and deorbit), as well as MWR science passes and an MWR calibration. Other maneuvers (JOI and PRM cleanup maneuvers and all other OTMs) are done in vector mode, unless a contingency arises which requires the DV efficiency of a turn-burn-turn maneuver (e.g., if the JOI+7.6d maneuver turns out to be greater than ~20 m/s, which is unlikely). GRAV passes and most other DSN contacts require precise Earth-pointing; we will stay roughly Earth-pointed for most of the rest of the time when we are not in contact. Due to the changing position of the Earth with respect to the spacecraft, we will need to periodically reacquire Earth-point, mainly prior to DSN contacts. We will use the HGA for most DSN contacts. Due to the nutation of the spinning spacecraft following any maneuvers, we will need to allow several hours for nutation damping following Earth-point maneuvers before using the HGA.

For the 11-day orbits, we allow 8 hours before most DSN tracks and 16 hours before the 6-hour MWR or GRAV perijove science passes that start at PJ – 3 h. The one exception to using the HGA for DSN contacts is for the brief pass covering the PJ + 4 h OTM, in which case we currently plan to use the MGA. The reason is that after MWR passes, there is not enough time for nutation damping after a PJ + 3 h Earth-point maneuver, and for both MWR and GRAV passes we do not expect to maintain precise pointing during the OTM to let us use the HGA. (This is being reevaluated for the 53-day orbit mission; it may be possible to remain on the HGA at a rate that is still higher than on the MGA). There are 20 available downlink data rates: 10, 40, 100, 250, 1000, 1745, 2000, 4000, 12000, 18000, 22000, 26000, 30000, 35000, 40000, 50000, 100000, 120000, 150000, and 200000 bps. On the HGA we expect ≥18 kilobits per second (kbps) (≥12 kbps during GRAV passes due to power required for carrier signal), and ≥10 bps on the MGA. We will use the MGA and ≥10 bps for Science Orbits safe mode communication (assuming a 34-m DSN pass).

Note: in Table 5-1 (now superseded by Table 6-1 for 53-day orbits), which is from a computer-generated Juno activity plan, the name “GRAV” used elsewhere in the article is left as GRAV.

**Table 5-1 *Superseded: Trajectory event times (UTC) for reference trajectory.**

| Orbit | Event | Time |
|---|---|---|
| | L [1] | 08/05/2011 16:11 |
| | DSM1 | 09/07/2012 22:29 |
| | DSM2 | 09/14/2012 22:29 |
| | EFB | 10/09/2013 15:29 |
| **0** JOI | PJ0 [2] | 07/05/2016 02:44 |
| | AJ0 | 08/27/2016 10:46 |
| **1** PRM | AJ0 | 08/27/2016 10:46 |
| | PJ1 [2] | 10/19/2016 18:17 |
| | AJ1 | 10/25/2016 05:56 |
| **2** Cleanup | AJ1 | 10/25/2016 05:56 |
| | PJ2 | 10/30/2016 17:36 |
| | AJ2 | 11/05/2016 05:11 |
| **3** MWR | AJ2 | 11/05/2016 05:11 |
| | PJ3 | 11/10/2016 16:46 |
| | AJ3 | 11/16/2016 04:26 |
| **4** GRAV | AJ3 | 11/16/2016 04:26 |
| | PJ4 | 11/21/2016 16:06 |
| | AJ4 | 11/27/2016 03:47 |
| 5 MWR | AJ4 | 11/27/2016 03:47 |
| | PJ5 | 12/02/2016 15:26 |
| | AJ5 | 12/08/2016 03:07 |
| **6** MWR | AJ5 | 12/08/2016 03:07 |
| | PJ6 | 12/13/2016 14:47 |
| | AJ6 | 12/19/2016 02:28 |
| **7** MWR | AJ6 | 12/19/2016 02:28 |
| | PJ7 | 12/24/2016 14:07 |
| | AJ7 | 12/30/2016 01:46 |
| **8** MWR | AJ7 | 12/30/2016 01:46 |
| | PJ8 | 01/04/2017 13:27 |
| | AJ8 | 01/10/2017 01:06 |
| **9** GRAV | AJ8 | 01/10/2017 01:06 |
| | PJ9 | 01/15/2017 12:47 |
| | AJ9 | 01/21/2017 00:28 |
| **10** GRAV | AJ9 | 01/21/2017 00:28 |
| | PJ10 | 01/26/2017 12:07 |
| | AJ10 | 01/31/2017 23:47 |

| Orbit | Event | Time |
|---|---|---|
| **11** GRAV | AJ10 | 01/31/2017 23:47 |
| | PJ11 | 02/06/2017 11:27 |
| | AJ11 | 02/11/2017 23:08 |
| **12** GRAV | AJ11 | 02/11/2017 23:08 |
| | PJ12 | 02/17/2017 10:47 |
| | AJ12 | 02/22/2017 22:26 |
| **13** GRAV | AJ12 | 02/22/2017 22:26 |
| | PJ13 | 02/28/2017 10:07 |
| | AJ13 | 03/05/2017 21:47 |
| **14** GRAV | AJ13 | 03/05/2017 21:47 |
| | PJ14 | 03/11/2017 09:27 |
| | AJ14 | 03/16/2017 21:07 |
| **15** GRAV | AJ14 | 03/16/2017 21:07 |
| | PJ15 | 03/22/2017 08:48 |
| | AJ15 | 03/27/2017 20:30 |
| **16** GRAV | AJ15 | 03/27/2017 20:30 |
| | PJ16 | 04/02/2017 08:08 |
| | AJ16 | 04/07/2017 19:48 |
| **17** GRAV | AJ16 | 04/07/2017 19:48 |
| | PJ17 | 04/13/2017 07:28 |
| | AJ17 | 04/18/2017 18:59 |
| **18** GRAV | AJ17 | 04/18/2017 18:59 |
| | PJ18 | 04/24/2017 06:28 |
| | AJ18 | 04/29/2017 18:08 |
| **19** GRAV | AJ18 | 04/29/2017 18:08 |
| | PJ19 | 05/05/2017 05:48 |
| | AJ19 | 05/10/2017 17:29 |
| **20** GRAV | AJ19 | 05/10/2017 17:29 |
| | PJ20 | 05/16/2017 05:08 |
| | AJ20 | 05/21/2017 16:49 |
| **21** GRAV | AJ20 | 05/21/2017 16:49 |
| | PJ21 | 05/27/2017 04:28 |
| | AJ21 | 06/01/2017 16:09 |
| **22** GRAV | AJ21 | 06/01/2017 16:09 |
| | PJ22 | 06/07/2017 03:49 |
| | AJ22 | 06/12/2017 15:28 |

| Orbit | Event | Time |
|---|---|---|
| **23** GRAV | AJ22 | 06/12/2017 15:28 |
| | PJ23 | 06/18/2017 03:09 |
| | AJ23 | 06/23/2017 14:48 |
| **24** GRAV | AJ23 | 06/23/2017 14:48 |
| | PJ24 | 06/29/2017 02:29 |
| | AJ24 | 07/04/2017 14:09 |
| **25** GRAV | AJ24 | 07/04/2017 14:09 |
| | PJ25 | 07/10/2017 01:49 |
| | AJ25 | 07/15/2017 13:29 |
| **26** GRAV | AJ25 | 07/15/2017 13:29 |
| | PJ26 | 07/21/2017 01:09 |
| | AJ26 | 07/26/2017 12:50 |
| **27** GRAV | AJ26 | 07/26/2017 12:50 |
| | PJ27 | 08/01/2017 00:29 |
| | AJ27 | 08/06/2017 12:08 |
| **28** GRAV | AJ27 | 08/06/2017 12:08 |
| | PJ28 | 08/11/2017 23:49 |
| | AJ28 | 08/17/2017 11:30 |
| **29** GRAV | AJ28 | 08/17/2017 11:30 |
| | PJ29 | 08/22/2017 23:09 |
| | AJ29 | 08/28/2017 10:49 |
| **30** GRAV | AJ29 | 08/28/2017 10:49 |
| | PJ30 | 09/02/2017 22:29 |
| | AJ30 | 09/08/2017 10:11 |
| **31** GRAV | AJ30 | 09/08/2017 10:11 |
| | PJ31 | 09/13/2017 21:49 |
| | AJ31 | 09/19/2017 09:29 |
| **32** GRAV | AJ31 | 09/19/2017 09:29 |
| | PJ32 | 09/24/2017 21:09 |
| | AJ32 | 09/30/2017 08:50 |
| **33** Extra | AJ32 | 09/30/2017 08:50 |
| | PJ33 | 10/05/2017 20:29 |
| | AJ33 | 10/11/2017 08:15 |
| **34** Deorbit | AJ33 | 10/11/2017 08:15 |
| | PJ34 | 10/16/2017 19:33 |

[1] JOI starts 07/05/2016 02:29 (duration = 29:38 min = 1778 s).
[2] PRM starts 10/19/2016 17:59 (duration = 36:53 min = 2213 s).

* See Table 6-1 for an update for the 53-day orbit mission.

Figure 5-8, for 11-day science orbits, shows the timing of PJ and OTM events with respect to the DSS-25 view period, and illustrates how science orbit perijove timing is optimized for Gravity Science, with perijove occurring about the middle of each pass.

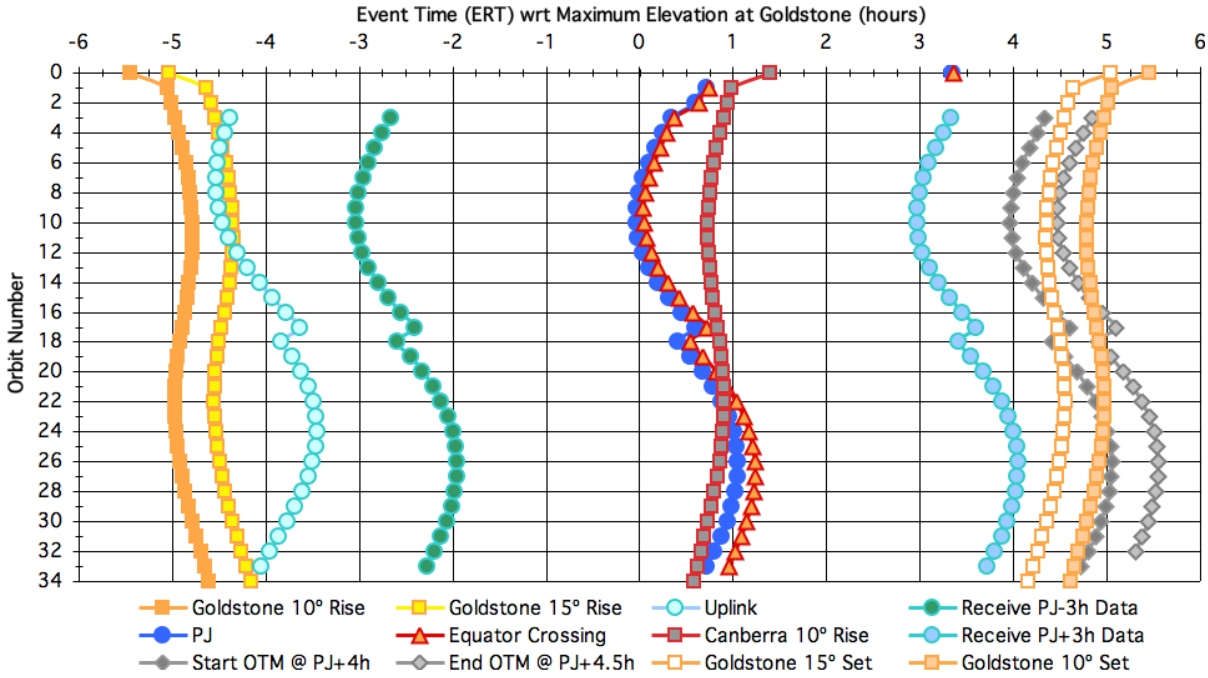


**Figure 5-8 *Superseded: Timing of perijove events over DSS-25.**

* These event times were determined for the pre-JOI 11-day orbits. The article retains this figure for historical purposes.

**Blank**

# 6 Mission and Science Plans for a 53-day Orbit Period

## 6.1 Entry into Safe Mode Just Prior to Second Jupiter Flyby

The Juno spacecraft entered safe mode October 19, 2016. Early indications were that a software performance monitor induced a reboot of the spacecraft's onboard computer. The spacecraft acted as expected during the transition into safe mode, restarted successfully and is healthy. High-rate data was restored, and the team began conducting flight software diagnostics. All instruments were off, and the planned science data collection for the close flyby of Jupiter (perijove 2), did not occur.

“At the time safe mode was entered, the spacecraft was more than 13 hours from its closest approach to Jupiter," said Rick Nybakken, Juno project manager from NASA's Jet Propulsion Laboratory in Pasadena, Calif. “We were still quite a ways from the planet's more intense radiation belts and magnetic fields. The spacecraft is healthy and we are working our standard recovery procedure.”

The spacecraft is designed to enter safe mode if its onboard computer perceives conditions are not as expected. In this case, the safe mode turned off instruments and a few non-critical spacecraft components, and it confirmed the spacecraft was pointed toward the Sun to ensure the solar arrays received power.

Mission managers were continuing to study an unrelated issue with the performance of a pair of valves that are part of the spacecraft's propulsion system. A week prior to the entry into safe mode, they had made the decision to postpone a burn of the spacecraft's main engine that would have reduced Juno's orbital period from 53.4 to 14 days [16].

Mission controllers commanded Juno to exit safe mode on October 24, with confirmation of safe mode exit received on the ground. After safe mode exit, the project turned the instruments back on to get ready for the December flyby.

In preparation for the December flyby of Jupiter, Juno executed an orbital trim maneuver the next day, October 25, using its smaller thrusters. The burn, which lasted just over 31 minutes, changed Juno's orbital velocity by about 5.8 mph (2.6 meters per second, m/s) and consumed about 8 pounds (3.6 kilograms) of propellant [11].

## 6.2 Third Jupiter Flyby: Weighing a Decision to Remain in 53-day Orbit

Juno completed a close flyby of Jupiter on Dec. 1, 2016, beginning its third science orbit. At the time of closest approach (called perijove), Juno was about 2,580 miles (4,150 kilometers) above the Jupiter cloud tops and traveling at a speed of about 129,000 mph (57.8 kilometers per second, km/s) relative to the planet. Seven of Juno's eight science instruments and the JunoCam were on and collecting data during the flyby. The infra-red mapper (JIRAM) was off, as planned, to allow the team to complete an update to the spacecraft software that processes JIRAM's science data.

The spacecraft team continued to weigh its options regarding modifications of Juno's orbital period -- how long it takes the spacecraft to complete one orbit around Jupiter. At present, Juno's orbital period is 53.4 days. There had been plans to perform a period reduction maneuver with the spacecraft's main engine on Oct. 19 to reduce the orbital period to 14 days.

The team made the decision to forgo the maneuver in order to further study the performance of a set of helium valves that are part of the spacecraft's fuel pressurization system [17], [18].

“We have a healthy spacecraft that is performing its mission admirably, and we are able to obtain great science every time we fly by,” said Juno project manager Rick Nybakken. “What we do not want to do is add any unnecessary risk, so we are moving forward carefully.”

## *6.3 “Juno to Remain in Current Orbit at Jupiter”*

NASA's Juno mission to Jupiter, which has been in orbit around the gas giant since July 4, 2016, will remain in its current 53-day orbit for the remainder of the mission [19]. This will allow Juno to accomplish its science goals, while avoiding the risk of a previously planned engine firing that would have reduced the spacecraft's orbital period to 14 days.

“During a thorough review, we looked at multiple scenarios that would place Juno in a shorter-period orbit, but there was concern that another main engine burn could result in a less-than-desirable orbit,” said project manager Rick Nybakken. “The bottom line is a burn represented a risk to completion of Juno's science objectives.”

“Juno is healthy, its science instruments are fully operational, and the data and images we've received are nothing short of amazing,” said Thomas Zurbuchen, associate administrator for NASA's Science Mission Directorate in Washington. He also noted that, “The decision to forego the burn is the right thing to do -- preserving a valuable asset so that Juno can continue its exciting journey of discovery.”

The orbital period does not affect the quality of the science collected by Juno on each flyby, since the altitude over Jupiter is the same at the time of closest approach. In fact, the longer orbit provides new opportunities that allow further exploration of the far reaches of space dominated by Jupiter's magnetic field, increasing the value of Juno's research.

During each orbit, Juno soars low over Jupiter's cloud tops -- as close as about 2,600 miles (4,100 kilometers). During these flybys, Juno probes beneath the obscuring cloud cover and studies Jupiter's auroras to learn more about the planet's origins, structure, atmosphere and magnetosphere.

The original Juno flight plan (Table 1-1) envisioned the spacecraft looping around Jupiter twice in 53-day orbits, then reducing its orbital period to 14 days for the remainder of the mission. However, two helium check valves that are part of the plumbing for the spacecraft's main engine did not operate as expected when the propulsion system was pressurized for the period reduction maneuver (PRM) in October 2016. Telemetry from the spacecraft indicated that it took several minutes for the valves to open during this pressurization, while it took only a few seconds during three previous main engine firings for Deep Space Maneuver (DSM) Part 1 in August 2012, DSM Part 2 in September 2012, and Jupiter Orbit Insertion in July 2016.

Figure 6-1 and Figure 6-2 are updates for a 53-day orbit update to superseded figures in Section 5. Fig. 6-1 shows the view from Jupiter’s North Pole, and Fig. 6-2 shows the view from the Sun.

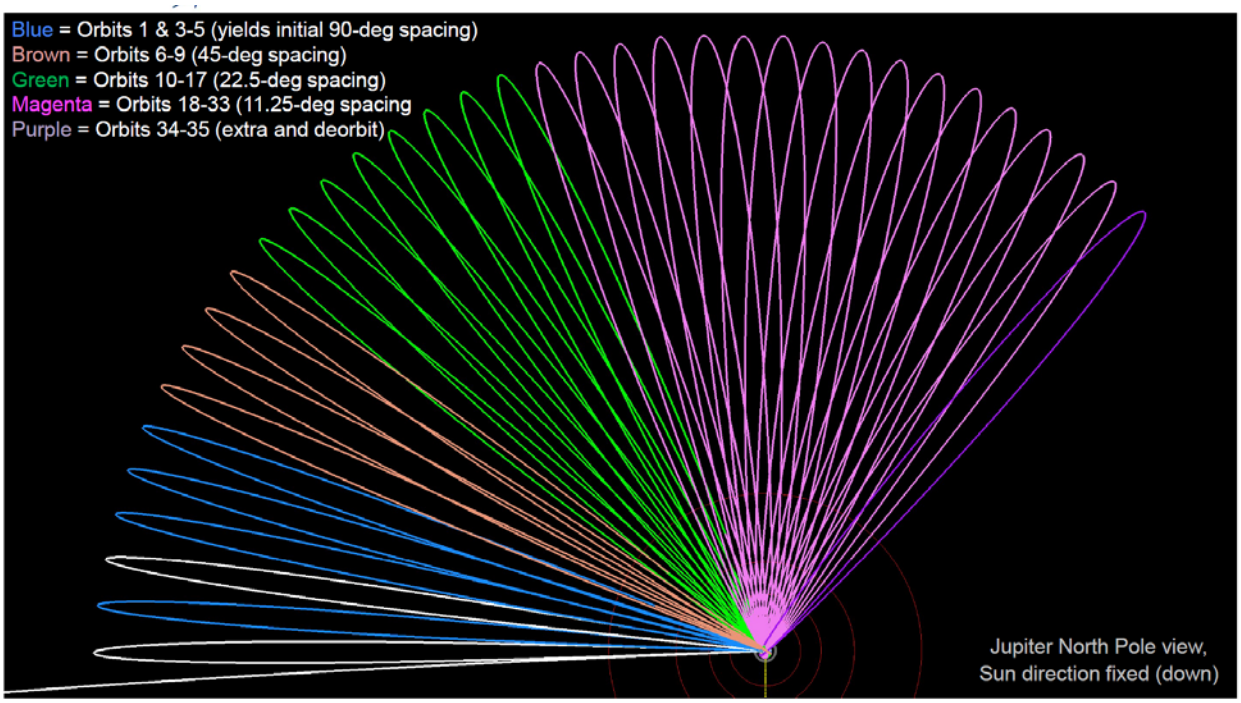


**Figure 6-1: Orbital trajectories for 53-day orbits (view from Jupiter's North Pole).**

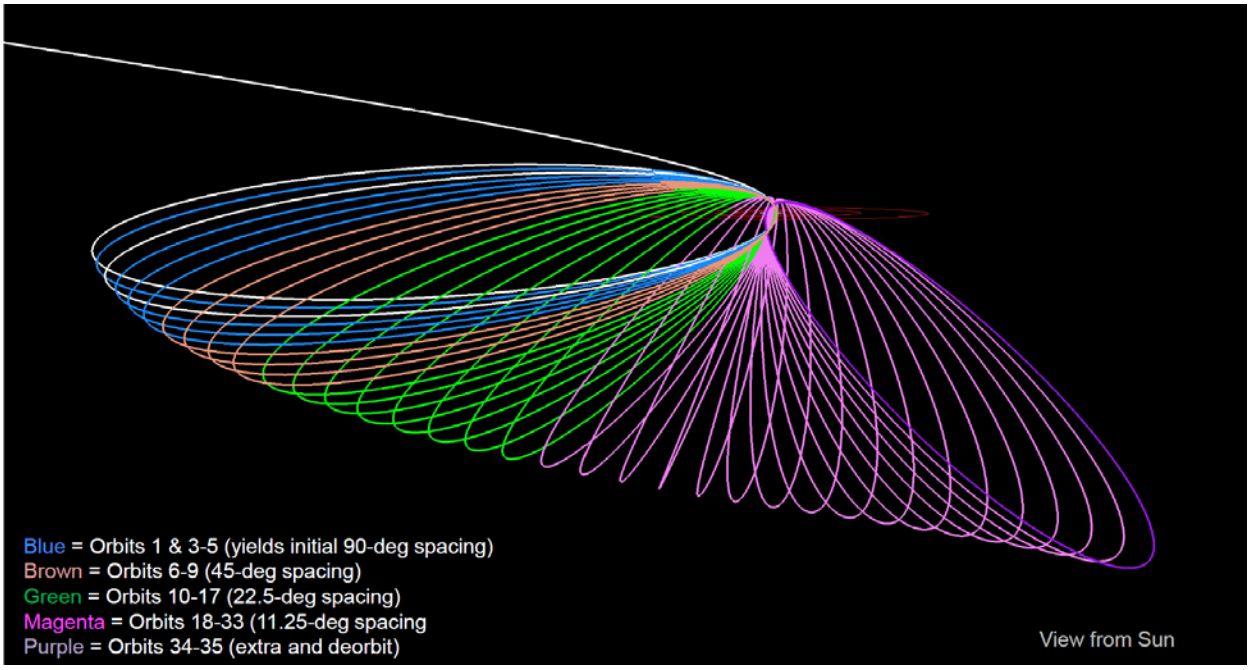


**Figure 6-2: Orbital trajectories for 53-day orbits (view from the Sun).**

Table 6-1 shows the updated Mission Plan consistent with the changes documented in Section 6.

**Table 6-1: Mission dates for 53-day orbit.**

*This document was reviewed and approved for export, see Juno-Generic-11-041.*
*This document has been reviewed and determined not to contain export controlled technical data.*

**Juno Trajectory Event Times** (for reference trajectory)

Based on **spk_ref_161212_210731_170320.bsp** (**subject to change**).
Times are in **universal time, UTC** (Spacecraft Event Time = SCET).

| Orbit | Epoch | Date/Time DOY | Date/Time Calendar |
|---|---|---|---|
| | L [1] | 217 | F 08/05/11 16:25 |
| | DSM1 | 243 | Th 08/30/12 22:30 |
| | DSM2 | 258 | F 09/14/12 22:30 |
| | EFB | 282 | W 10/09/13 19:21 |
| | PJ0 [2] | 187 | Tu 07/05/16 02:48 |
| | AJ0 | 213 | Su 07/31/16 19:46 |
| | PJ1 | 240 | Sa 08/27/16 12:51 |
| | AJ1 | 267 | F 09/23/16 03:45 |
| 2 Post-Safing | Orbit 2 | 292 | Tu 10/18/16 18:00 |
| | PJ2 [3] | 293 | W 10/19/16 18:11 |
| | AJ2 | 320 | Tu 11/15/16 05:37 |
| 3 GRAV | Orbit 3 | 345 | Sa 12/10/16 17:00 |
| | PJ3 | 346 | Su 12/11/16 17:04 |
| | AJ3 | 007 | Sa 01/07/17 03:12 |
| 4 MWR | Orbit 4 | 032 | W 02/01/17 12:00 |
| | PJ4 | 033 | Th 02/02/17 12:57 |
| | AJ4 | 059 | Tu 02/28/17 22:56 |
| 5 MWR Tilt | Orbit 5 | 085 | Su 03/26/17 08:00 |
| | PJ5 | 086 | M 03/27/17 08:52 |
| | AJ5 | 112 | Sa 04/22/17 19:15 |
| 6 GRAV | Orbit 6 | 138 | Th 05/18/17 06:00 |
| | PJ6 | 139 | F 05/19/17 06:01 |
| | AJ6 | 165 | W 06/14/17 15:58 |
| 7 MWR Tilt | Orbit 7 | 191 | M 07/10/17 01:00 |
| | PJ7 | 192 | Tu 07/11/17 01:55 |
| | AJ7 | 218 | Su 08/06/17 11:44 |
| 8 GRAV | Orbit 8 | 243 | Th 08/31/17 21:00 |
| | PJ8 | 244 | F 09/01/17 21:49 |
| | AJ8 | 271 | Th 09/28/17 07:51 |
| 9 MWR Tilt | Orbit 9 | 296 | M 10/23/17 17:00 |
| | PJ9 | 297 | Tu 10/24/17 17:43 |
| | AJ9 | 324 | M 11/20/17 05:58 |
| 10 GRAV | Orbit 10 | 349 | F 12/15/17 17:00 |
| | PJ10 | 350 | Sa 12/16/17 17:58 |
| | AJ10 | 012 | F 01/12/18 03:53 |
| 11 GRAV | Orbit 11 | 037 | Tu 02/06/18 13:00 |
| | PJ11 | 038 | W 02/07/18 13:52 |
| | AJ11 | 064 | M 03/05/18 23:56 |
| 12 MWR X-Track | Orbit 12 | 090 | Sa 03/31/18 09:00 |
| | PJ12 | 091 | Su 04/01/18 09:46 |
| | AJ12 | 117 | F 04/27/18 19:37 |
| 13 GRAV | Orbit 13 | 143 | W 05/23/18 05:00 |
| | PJ13 | 144 | Th 05/24/18 05:40 |
| | AJ13 | 170 | Tu 06/19/18 17:31 |
| 14 GRAV | Orbit 14 | 196 | Su 07/15/18 05:00 |
| | PJ14 | 197 | M 07/16/18 05:18 |
| | AJ14 | 223 | Sa 08/11/18 15:19 |
| 15 GRAV | Orbit 15 | 249 | Th 09/06/18 01:00 |
| | PJ15 | 250 | F 09/07/18 01:12 |
| | AJ15 | 276 | W 10/03/18 11:00 |
| 16 GRAV | Orbit 16 | 301 | Su 10/28/18 21:00 |
| | PJ16 | 302 | M 10/29/18 21:06 |
| | AJ16 | 329 | Su 11/25/18 07:02 |
| 17 GRAV | Orbit 17 | 354 | Th 12/20/18 17:00 |
| | PJ17 | 355 | F 12/21/18 17:00 |
| | AJ17 | 017 | Th 01/17/19 04:41 |
| 18 MWR X-Track | Orbit 18 | 042 | M 02/11/19 16:00 |
| | PJ18 | 043 | Tu 02/12/19 16:20 |
| | AJ18 | 070 | M 03/11/19 02:11 |
| 19 GRAV | Orbit 19 | 095 | F 04/05/19 12:00 |
| | PJ19 | 096 | Sa 04/06/19 12:14 |
| | AJ19 | 122 | Th 05/02/19 22:17 |
| 20 GRAV | Orbit 20 | 148 | Tu 05/28/19 08:00 |
| | PJ20 | 149 | W 05/29/19 08:08 |
| | AJ20 | 175 | M 06/24/19 18:02 |
| 21 GRAV | Orbit 21 | 201 | Sa 07/20/19 04:00 |
| | PJ21 | 202 | Su 07/21/19 04:03 |
| | AJ21 | 228 | F 08/16/19 16:01 |
| 22 GRAV | Orbit 22 | 254 | W 09/11/19 03:00 |
| | PJ22 | 255 | Th 09/12/19 03:41 |
| | AJ22 | 281 | Tu 10/08/19 13:34 |
| 23 GRAV | Orbit 23 | 306 | Sa 11/02/19 23:00 |
| | PJ23 | 307 | Su 11/03/19 23:33 |
| | AJ23 | 334 | Sa 11/30/19 07:58 |
| 24 GRAV | Orbit 24 | 359 | W 12/25/19 16:00 |
| | PJ24 | 360 | Th 12/26/19 16:59 |
| | AJ24 | 022 | W 01/22/20 05:25 |
| 25 GRAV | Orbit 25 | 047 | Su 02/16/20 17:00 |
| | PJ25 | 048 | M 02/17/20 17:52 |
| | AJ25 | 075 | Su 03/15/20 04:06 |
| 26 GRAV | Orbit 26 | 100 | Th 04/09/20 14:00 |
| | PJ26 | 101 | F 04/10/20 14:25 |
| | AJ26 | 128 | Th 05/07/20 00:35 |
| 27 GRAV | Orbit 27 | 153 | M 06/01/20 10:00 |
| | PJ27 | 154 | Tu 06/02/20 10:20 |
| | AJ27 | 180 | Su 06/28/20 20:25 |
| 28 GRAV | Orbit 28 | 206 | F 07/24/20 06:00 |
| | PJ28 | 207 | Sa 07/25/20 06:15 |
| | AJ28 | 233 | Th 08/20/20 16:09 |
| 29 GRAV | Orbit 29 | 259 | Tu 09/15/20 02:00 |
| | PJ29 | 260 | W 09/16/20 02:11 |
| | AJ29 | 286 | M 10/12/20 14:06 |
| 30 GRAV | Orbit 30 | 312 | Sa 11/07/20 01:00 |
| | PJ30 | 313 | Su 11/08/20 01:50 |
| | AJ30 | 339 | F 12/04/20 11:37 |
| 31 GRAV | Orbit 31 | 364 | Tu 12/29/20 21:00 |
| | PJ31 | 365 | W 12/30/20 21:45 |
| | AJ31 | 026 | Tu 01/26/21 07:36 |
| 32 GRAV | Orbit 32 | 051 | Sa 02/20/21 17:00 |
| | PJ32 | 052 | Su 02/21/21 17:41 |
| | AJ32 | 079 | Sa 03/20/21 03:47 |
| 33 GRAV | Orbit 33 | 104 | W 04/14/21 13:00 |
| | PJ33 | 105 | Th 04/15/21 13:36 |
| | AJ33 | 131 | Tu 05/11/21 23:31 |
| 34 Extra | Orbit 34 | 157 | Su 06/06/21 09:00 |
| | PJ34 | 158 | M 06/07/21 09:32 |
| | AJ34 | 184 | Sa 07/03/21 19:27 |
| 35 Impact | Orbit 35 | 210 | Th 07/29/21 04:00 |
| | PJ35 | 211 | F 07/30/21 04:33 |

[1] L = Launch; TIP was 08/05/11 17:25.
[2] JOI started 07/05/2016 02:30 (duration = 34:58 min = 2098 s).

Table 6-1 (53-day orbit) is similar in layout to Table 5-1 (the original mission plan with 11-day orbit). Orbits 3–33 have labels of either GRAV (gravity science) or MWR (microwave radiometer). The MWR is susceptible to radiation. A mission with 53-day orbits takes a longer time to complete a given number of orbits than one with 11-day orbits. All of the MWR orbits originally were planned for 2016 (Table 5-1) Now four of six MWR orbits are planned for 2017, the fifth in April 2018, and the sixth in February 2019 (Table 6-1).

Juno's larger 53-day orbit has an apojove of more than 110 Jupiter radii as compared with about 40 Jupiter radii for the 11-day orbit).

Figure 6-3 shows the orbital radiation environment for representative 53-day orbit. Comparing Fig. 6-3 with the superseded Fig. 5-3, the perijoves are about the same (1.06 Rj). The apojoves are much larger relative to the inner magnetosphere in a 53-day orbit than an 11-day orbit.

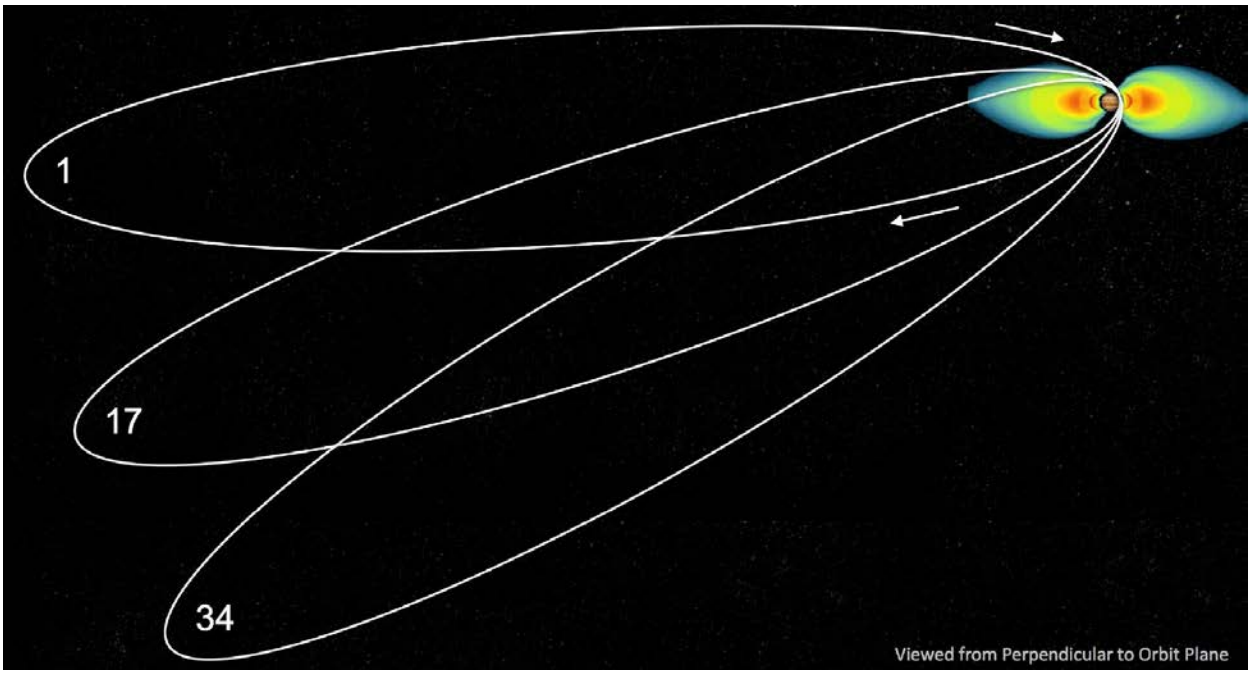


**Figure 6-3: Radiation environment for 53-day orbit periods viewed from perpendicular to orbit plane.**

Flying in a more highly elliptical orbit allows Juno to spend more time in a benign radiation environment outside the inner magnetosphere, thus slowing the build-up of cumulative dose. NASA hopes this will allow Juno to survive beyond the February 2018 primary mission end[15]. The accumulated radiation during each perijove passage is minimized by the orbit speed with respect to Jupiter. This speed ranges from 57.0 km/s for orbit 25 to 58.4 km/s for orbit 33, compared with 57.9 km/s for JOI.

Juno spends more time in the farther reaches of the Jovian magnetosphere, the region of space dominated by Jupiter's magnetic field[16]. The changed orbital design allows Juno to collect measurements outside the inner magnetosphere; these measurements are a bonus compared with the original design. At more than 110 Rj (about eight million km), Juno passes through the magnetotail and can use its particle and WAVES sensors to capture data on the structure of the planet's complex magnetic field at these greater distances. This could help scientists understand how planetary fields interact with the solar wind and what drives Jupiter's powerful auroras,

[15] Juno will continue to operate within the current budget plan through July 2018, for a total of 12 science orbits. If the spacecraft is still functioning adequately and has sufficient fuel margin, the team can then propose to extend the mission during the next science review cycle. The review process evaluates proposed mission extensions on the merit and value of previous and anticipated science returns.

[16] Jupiter's magnetosphere occupies an enormous volume of space. It extends outward around Jupiter to between 75 and 100 times the planet's width. This region includes the far magnetotail, the southern magnetosphere, and the magnetospheric boundary region called the magnetopause. The solar wind also pushes on and stretches Jupiter's magnetosphere into a shape like a fluttering windsock. This magnetotail extends as far as the orbit of Saturn, in the direction away from the Sun. Understanding magnetospheres and how they interact with the solar wind are key science goals of NASA's Heliophysics Science Division.

differentiating between those caused by the solar wind and auroral displays driven by convective processes [20].

# 7 Mission and Science Activities

## 7.1 Science Objectives and Plan Overview

Juno's science objectives go back to the beginning, to understand how the formation and evolution of Jupiter might have influenced the development of our planetary system. Juno will map the magnetic and gravitational fields of the planet to understand the interior structure and, possibly, reveal the presence of a solid core. The most favored theory of Jupiter's origin involves the accretion of a 'proto-planet' (a massive rock/ice object) before hydrogen and helium gas collapsed onto it, measurements of the internal structure hold the key to establishing whether this scenario correct.

Jupiter's composition was shaped during its early formation, with many of the 'heavier' elements (like nitrogen, carbon, oxygen, sulfur and phosphorus) expected to be delivered trapped in ices of water. Juno's microwave radiometer is designed to measure Jupiter's water abundance deep below the observable clouds to assess whether this theory is valid. Through microwave remote sensing and gravity mapping, Juno should reveal the interior structure and bulk composition of Jupiter to constrain our theories for how the giant planet formed in the first place.

Furthermore, Juno's unique orbit will allow it to access the charged environments and magnetic fields above Jupiter's poles for the first time. The unique vantage point will allow the ultraviolet and near-infrared instruments (see Section 1.1) to observe the powerful auroras that result from the magnetic field sending charged particles crashing into the planet's upper atmosphere, creating the brightest auroral emissions of any planet in our Solar System. Taken together, Juno's study of Jupiter's interior structure, atmosphere and magnetosphere will permit a comprehensive characterization of this archetypal giant planet. However, Juno's mission does not include any exploration of the satellites and rings, apart from brief glimpses early in the mission.

## 7.2 Overview of Science Activities (as of May 2017)

The remainder of this section describes science activities. Supporting that activity, the X-band receiver and transmitter provide the means by which Juno and its instruments are commanded and the science data transmitted to the Deep Space Network to carry out the intense and closely timed observations during each near Jupiter passage. The Ka-band system constitutes one of the instruments, and another investigation uses the Doppler and ranging radiometric data returned via the X-band system as well.

This section provides highlights and the most preliminary findings of Juno's planned science activities as of the American Geophysical Union conference (held December 12–16, 2016). The quoted findings in these paragraphs come from the Planetary Society website [21].

**Magnetometer.** The magnetometer observes Jupiter's dynamo, the strongest in the Solar System. Magnetometer readings suggest Jupiter's dynamo generation is closer to the surface than previously thought. Juno's first flyby measured the "greatest (magnetic) field strength any spacecraft has ever encountered," greatly exceeding predictions, according to project scientist Alberto Adriani.

**"Humidity".** From Juno's first science pass, JIRAM, the probe's infrared mapper found low relative humidity inside one of the planet's hotspots. That was expected—the Galileo mission

found the same thing—but the information can still be useful in that it gives scientists a lower limit to how dry Jupiter is. The amount of water detected in Jupiter's atmosphere will tell us how much oxygen is there. This will tell us if we are right about theories on how Jupiter—and, by extension, the Solar System—formed.

**Core accretion model.** The prevailing theory for gas giant formation, known as the core accretion model, says planets like Jupiter start out as small, rocky worlds that accumulate enough material to accrete a gaseous envelope. This suggests Jupiter's chemical composition should closely mirror that of the Suns. If we find that Jupiter is wetter than expected, we shall have cast doubt on aspects of the core accretion model.

But it is not clear how the smallest particles stick together, other than the fact that our universe is full of fully formed planets. Other theories have been proposed, like the disk instability theory, which suggests that gravitational forces bind settling nebula particles together like a collapsing balloon. However, this implies that Jupiter does not have a core, which scientists find unlikely.

Following the successful completion of the *fifth* science pass on May 19, 2017 [22], a set of early science results, from the *first* science pass (August 27, 2016) were released on May 25, 2017. These included two papers appearing in the May 26, 2017 issue of the journal Science, one describing the polar storms, the other examining the magnetic fields and auroras,. Forty-four additional papers are being published in the *Journal Geophysical Research Letters*.

## *7.3 Earth Flyby (Oct. 9, 2013)*

In this and the remaining sections, much of the information has been compiled from NASA and JPL press releases that typically follow each of the major spacecraft activities. In several of the releases, quotes from the scientists or project officials convey feelings associated at that stage of the mission. The project used some cruise activities (Earth flyby for instance) as opportunities to check the spacecraft and instrument systems, as well as the associated planning and processes for command transmission and data return during orbital operations.

When NASA's Juno spacecraft flew past Earth on Oct. 9, 2013 [23], it received a boost in speed of more than 8,800 mph (about 3.9 km/s), which set it on course for a July 4, 2016, rendezvous with Jupiter, the largest planet in our Solar System. One of Juno's sensors, a special kind of camera optimized to track faint stars, also had a unique view of the Earth–Moon system. The result was an intriguing, low-resolution glimpse [24] of what our world would look like to a visitor from afar.

"If Captain Kirk of the USS Enterprise said, 'Take us home, Scotty,' this is what the crew would see," said Juno PI Scott Bolton. "In the movie, you ride aboard Juno as it approaches Earth and then soars off into the blackness of space. No previous view of our world has ever captured the heavenly waltz of Earth and moon."

The cameras that took the images for the movie are located near the pointed tip of one of the spacecraft's three solar-array arms. They are part of Juno's Magnetic Field Investigation (MAG) and are normally used to determine the orientation of the magnetic sensors. These cameras look away from the sunlit side of the solar array, so as the spacecraft approached, the system's four cameras pointed toward Earth. Earth and the moon came into view when Juno was about 600,000 miles (966,000 kilometers) away -- about three times the Earth-moon separation.

During the flyby, timing was everything. Juno was traveling about twice as fast as a typical satellite, and the spacecraft itself was spinning at 2 rpm. To assemble a movie that wouldn't make

viewers dizzy, the star tracker had to capture a frame each time the camera was facing Earth at exactly the right instant. The frames were sent to Earth, where they were processed into video format.

“Everything we humans are and everything we do is represented in that view,” said the star tracker's designer, John Jørgensen of the Danish Technical University, near Copenhagen. [These quotes aren’t really technical details, so that gives a rationale for having them as only footnotes--no

## 7.4 Pre-JOI Trajectory Correction Maneuvers (Feb. 3, 2016 – May 31, 2016)

The Juno spacecraft successfully executed a TCM to adjust its flight path on Feb. 3, 2016 [25]. The maneuver refined the spacecraft's trajectory, helping set the stage for Juno's arrival at the Solar System's largest planetary inhabitant five months and one day later.

“This is the first of two trajectory adjustments that fine tune Juno's orbit around the sun, perfecting our rendezvous with Jupiter on July 4th,” said Juno PI Scott Bolton, with the second planned for May 31, 2016.

The Juno spacecraft's thrusters consumed about 1.3 pounds (0.6 kilograms) of fuel during the February 3 burn, and it changed the spacecraft's speed by 1 foot (0.31 meters), per second. At the time of the maneuver, Juno was about 51 million miles (82 million kilometers) from Jupiter.

## 7.5 Juno’s Entry into Jupiter’s Magnetic Field (June 25, 2016)

Juno entered Jupiter’s magnetosphere on June 25, 2016, one month after the spacecraft crossed the Jupiter–Sun gravitational boundary.)

“We’ve just crossed the boundary into Jupiter's home turf,” said Juno PI Scott Bolton. “We’re closing in fast on the planet itself and already gaining valuable data.”

Figure 7-1 presents data that the Waves investigation on NASA's Juno spacecraft recorded as the spacecraft entered Jupiter's magnetosphere on June 25, 2016, while approaching Jupiter. The figure is one frame from an animation in a JPL news web page [26]. Audio accompanies the animation, with volume and pitch correlated to the amplitude and frequency of the recorded radio and plasma waves[17].

[17] Ref. 26 links to a video with sound: “Juno Captures the 'Roar' of Jupiter,” Jet Propulsion Laboratory, https://youtu.be/8CT_txWEo5I?list=PLTiv_XWHnOZpM1iLQr95P4KDXYiYnJUOE (accessed July 27, 2017),

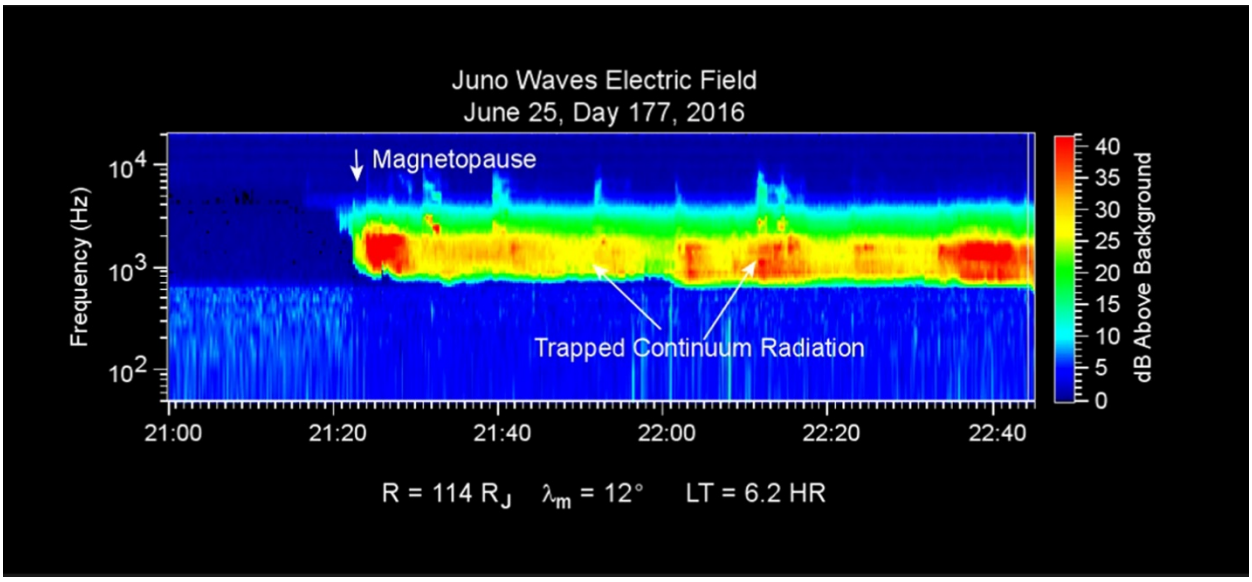


**Figure 7-1: Waves electric field profile on magnetic field entry.**

The graph uses color-coding to indicate wave amplitudes as a function of wave frequency (vertical axis, in hertz). Total elapsed time in UTC is one hour and 45 minutes. The label “Magnetopause” at just after 20 minutes into the chart marks entry into the magnetosphere, as detected by the sudden onset of a type of high-amplitude wave activity called “trapped continuum radiation.”

The trapped continuum radiation -- in the red and yellow area of this spectrogram -- consists of electromagnetic waves that are trapped in a low-density cavity in Jupiter's outer magnetosphere. The walls of the cavity are like a conductor; hence, the cavity traps these low-frequency waves. The low-frequency limit of these waves -- the lower edge of the band on the graph -- is a function of the density of particles in this outer region of the magnetosphere. The density here is roughly one electron per hundred cubic centimeters (6 cubic inches), about one percent of the density Juno detected in the solar wind just outside of the bow shock.

The vertical bar to the right of the chart indicates the color-coding of the wave amplitude, in decibels (dB) above the background level detected by the Waves instrument. Each step of 10 dB marks a tenfold increase in wave power.

When Juno collected these data, the distance from the spacecraft to Jupiter was about 4.95 million miles (7.97 million kilometers), indicated on the chart as 114 times the radius of Jupiter. Jupiter's magnetic field is tilted about 10 deg from the planet's axis of rotation. The note of 12 deg on the chart indicates that at the time these data were recorded, the spacecraft was 12 deg north of the magnetic-field equator. The “LT” notation is local time on Jupiter at the longitude of the planet directly below the spacecraft, with a value of 6.2 indicating approximately dawn.

## *7.6 Jupiter Orbit Insertion (July 5, 2016 Universal Time)*

After an almost 5-year journey from Earth, NASA's Juno spacecraft successfully entered Jupiter's orbit during a 35-minute engine burn. Confirmation that the burn had completed was received on Earth at 8:53 pm. PDT (11:53 p.m. EDT) Monday, July 4, 2016 (03:53 UTC July 5) [27].

Confirmation of a successful orbit insertion was received from Juno tracking data monitored at the navigation facility at NASA's Jet Propulsion Laboratory (JPL) in Pasadena, California, as well as at the Lockheed Martin Juno operations center in Denver. The telemetry and tracking data were received by NASA's Deep Space Network antennas in Goldstone, California, and Canberra, Australia.

Preplanned events leading up to the orbital insertion engine burn included changing the spacecraft's attitude to point the main engine in the desired direction and then increasing the spacecraft's rotation rate from 2 to 5 rpm to help stabilize it.

The burn of Juno's 645-newton Leros-1b main engine began on time at 8:18 p.m. PDT (11:18 p.m. EDT), decreasing the spacecraft's velocity by 1,212 mph (542 m/s) and allowing Juno to be captured in orbit around Jupiter. Soon after the burn was completed, Juno turned so that the Sun's rays could once again reach the 18,698 individual solar cells that give Juno its energy.

## *7.7 Instrument Turn-On (July 6 – 31, 2016)*

As planned for after JOI, the spacecraft returned to high-rate communications on July 5 and powered up five of its science instruments on July 6 [28]. Per the mission plan, the remaining science instruments were powered up before the end of July. Juno's science instruments had been turned off several days before JOI, to ensure a successful orbit insertion.

The JunoCam camera aboard NASA's Juno mission was operational and sending down data after the spacecraft's July 4 arrival at Jupiter [29]. Juno's visible-light camera was turned on 6 days after Juno fired its main engine to place the spacecraft into orbit around the planet. A post-JOI JunoCam image indicated it survived its first pass through Jupiter's extreme radiation environment without any degradation. The first high-resolution images of Jupiter, to be taken around closest approach, were still a few weeks away.

The Juno team planned and executed a short post-JOI TCM on July 13 to refine the orbit around Jupiter.

## *7.8 First Jupiter Flybys (Aug. 27, 2016 – May 19, 2017)*

On August 27, 2016, Juno successfully executed its first of 36 orbital flybys of Jupiter, a science checkout, passing Perijove 1 (see Table 6-1). The time of closest approach with the gas-giant world was 6:44 a.m. PDT (9:44 a.m. EDT, 13:44 UTC) when Juno passed about 2,600 miles (4,200 kilometers) above Jupiter's swirling clouds. At the time, Juno was traveling at 130,000 mph (208,000 kilometers per hour, km/hr) with respect to the planet. This flyby was the closest Juno will get to Jupiter during its prime mission [11].

Once every 53 days, Juno’s trajectory approaches Jupiter from above its North Pole, where the spacecraft begins a 2-hour transit (from pole to pole) flying north to south with its eight science instruments collecting data and its JunoCam public outreach camera snapping pictures. Juno’s perijove altitude and speed are similar to the JOI values to within a few percent.

On March 27 and May 19, 2017, Juno accomplished its fifth and sixth close orbital flybys of Jupiter, completing the fourth and fifth science orbits. All of Juno's science instruments and the spacecraft's JunoCam were operating during the flybys [30]. Depending on the flyby’s planned sequence and the scheduled tracking passes, the playback download of 6 megabytes of data collected during the transit can take as long as 1.5 days. “During these flybys, Juno is probing

beneath the obscuring cloud cover of Jupiter and studying its auroras to learn more about the planet's origins, structure, atmosphere and magnetosphere," NASA officials said in the statement. [31].

## 7.9 JunoCam Images

Unlike other NASA spacecraft, the JunoCam imager aboard the Juno spacecraft was added to the mission primarily for public outreach. NASA has invited the public to play a role during each perijove pass, voting on features for JunoCam to target and image on each successive flyby. These pictures have no bearing on the mission's scientific objectives, which rely on a suite of eight other instruments to study Jupiter's interior structure, its gravity and magnetic fields and its immediate environment. JunoCam is not an advanced telescopic camera. Instead, it has a relatively simple imager with what amounts to a fish-eye lens. Because Juno's elliptical orbit carries it closer to Jupiter than any other spacecraft, the wide-angle views provide exceptional detail and more context than high-power narrow-angle instruments [32].

The JunoCam detector has multiple filter strips, each with a different bandpass, bonded directly to its photoactive surface. Each strip extends the entire width of the detector, but only a fraction of its height; Junocam's filter strips are 1600 pixels wide and about 155 rows high. The filter strips are scanned across the target by spacecraft rotation. At the nominal spin rate of 2 rpm, frames are acquired about every 400 milliseconds. Junocam has four filters: three visible (red/green/blue) and a narrowband "methane" filter centered at about 890 nm. The camera provides Time-Delayed-Integration (TDI). TDI vertically shifts the image one row each 3.2 milliseconds over the course of the exposure, cancelling the scene motion induced by rotation. Junocam pixels are 12 bits deep from the camera but are converted to 8 bits inside the instrument using a lossless "companding" table, a process similar to gamma correction, to reduce their size. All Junocam products on the missionjuno website [33] are in this 8-bit form as received on Earth.

The camera's builder, Malin Space Science Systems of San Diego, first lightly processes the JunoCam images and posts them to the site [33]. What happens after that is up to the public. "We are looking forward to people visiting our website and becoming part of the JunoCam imaging team," said Candy Hansen, a senior scientist at the Planetary Science Institute and the JunoCam instrument lead. However, "once it's in their hands, we have no control, nor do we want to exert any, over what they do with the data."

The JunoCam images provide for interaction between the public and the Juno project. Each raw image includes the same view shot in green, blue and red filters and then a slightly processed color view that is a combination of all three. The public can download those images, process them in a wide variety of ways and upload the results back to the website. The uploaded processed images can be re-posted and available for anyone to download. All are in the public domain, although uploaders can opt to restrict commercial usage [32].

JunoCam's raw images are available at the Image Processing Gallery section of this site [33] for the public as "citizen scientists" or amateur astronomers. After spending most of every 53-day orbit distant from Jupiter, the spacecraft swoops from the North Pole to the South Pole in its perijove pass in just 2 hours. The Discussion and Voting sections in [33] describe the process from image receipt at one perijove to voting on JunoCam pointing for the next perijove. A Jupiter map, updated every 2 weeks, shows points of interest (POIs). Jupiter has a dynamic atmosphere where winds in the belts (brown) and zones (white) go in opposite directions. Storms develop and evolve,

and other atmospheric features come and go. With each new map, the website staff move all of the POI markers — sometimes POIs disappear, sometimes they get torn apart.

On the Voting page [33] lists which POI's are likely to be within the JunoCam field of view on a given perijove pass, and the participating citizen scientists participate in the selection of which POI's to image. “It's up to the public to determine the best locations in Jupiter's atmosphere for JunoCam to capture during (the next) flyby,” said Candy Hansen [33]. The debate is based on the threads of discussion associated with those POIs. The Juno data team sets aside data volume for two polar images at each periapsis. They will then image as many as possible of the voted priorities for that periapsis.

The Jupiter image in Fig. 7-2 is titled “Cloud Tops” with raw data taken by the JunoCam imager during Perijove 2 on February 2, 2017. Highlighting a massive counterclockwise rotating storm that appears as a white oval in the gas giant's southern hemisphere, this enhanced color image was processed and provided by citizen scientist Bjorn Jonsson. [32], [34]

Image credit: NASA/JPL-Caltech/SwRI/MSSS/Bjorn Jonsson

**Figure 7-2: “Jovian Cloud Tops” [34] processed from JunoCam data.**

## 7.10 Early Science Results (from Data-Collection Pass Aug. 27, 2016)

These early science results [22] are from the first data-collection pass. They portray Jupiter as a complex, gigantic, turbulent world, with Earth-sized polar cyclones, plunging storm systems that travel deep into the heart of the gas giant, and a mammoth, lumpy magnetic field that may indicate it was generated closer to the planet's surface than previously thought [35].

In the first pass, Juno flew within about 2,600 miles (4,200 km) of Jupiter's swirling cloud tops on Aug. 27. Since then, as Table 6-1 shows, other perijove passes have occurred. “Every 53 days, we go screaming by Jupiter, get doused by a fire hose of Jovian science, and there is always something new,” said Juno PI Scott Bolton.

Among findings that challenge assumptions are some provided by Juno's imager, JunoCam. [33].

Figure 7-3 is an image of Jupiter’s South Pole[18]. This composite image [36] shows Jupiter's South Pole, as seen by NASA's Juno spacecraft from an altitude of 32,000 miles (52,000 km). The oval features are cyclones, as large as 600 miles (1,000 km) in diameter. Multiple images taken with the JunoCam instrument on three separate orbits were combined to show all areas in daylight, enhanced color, and stereographic projection.

Both of Jupiter's poles are covered in Earth-sized swirling storms that are densely clustered and rubbing together [37].

“We're puzzled as to how they could be formed, how stable the configuration is, and why Jupiter's North Pole doesn't look like the South Pole,” said Bolton. “We're questioning whether this is a dynamic system, and are we seeing just one stage, and over the next year, we're going to watch it disappear, or is this a stable configuration and these storms are circulating around one another?”

Another surprise comes from Juno's Microwave Radiometer (MWR), which samples the thermal microwave radiation from Jupiter's atmosphere, from the top of the ammonia clouds to deep within its atmosphere. The MWR data indicates that Jupiter's iconic belts and zones are mysterious, with the belt near the Equator penetrating all the way down, while the belts and zones at other latitudes seem to evolve to other structures. The data suggest the ammonia is quite variable and continues to increase as far down as we can see with MWR, which is a few hundred miles or kilometers.

Prior to the Juno mission, it was known that Jupiter had the most intense magnetic field in the Solar System. Measurements of the massive planet's magnetosphere, from Juno's magnetometer investigation (MAG), indicate that Jupiter's magnetic field is even stronger than models expected, and more irregular in shape. MAG data indicates the magnetic field greatly exceeded expectations at 7.766 gauss, about 10 times stronger than the strongest magnetic field found on Earth.

“Juno is giving us a view of the magnetic field close to Jupiter that we've never had before,” said Jack Connerney, Juno deputy principal investigator and the lead for the mission's magnetic field investigation at NASA's Goddard Space Flight Center in Greenbelt, Maryland. “Already we see that the magnetic field looks lumpy: it is stronger in some places and weaker in others. This uneven distribution suggests that the field might be generated by dynamo action closer to the surface, above the layer of metallic hydrogen. Every flyby we execute gets us closer to determining where and how Jupiter's dynamo works.”

[18] A video that includes this image was provided by Scott Bolton, who noted it was “put out by one of our great amateur colleagues.” https://youtu.be/3kQbTBt418o

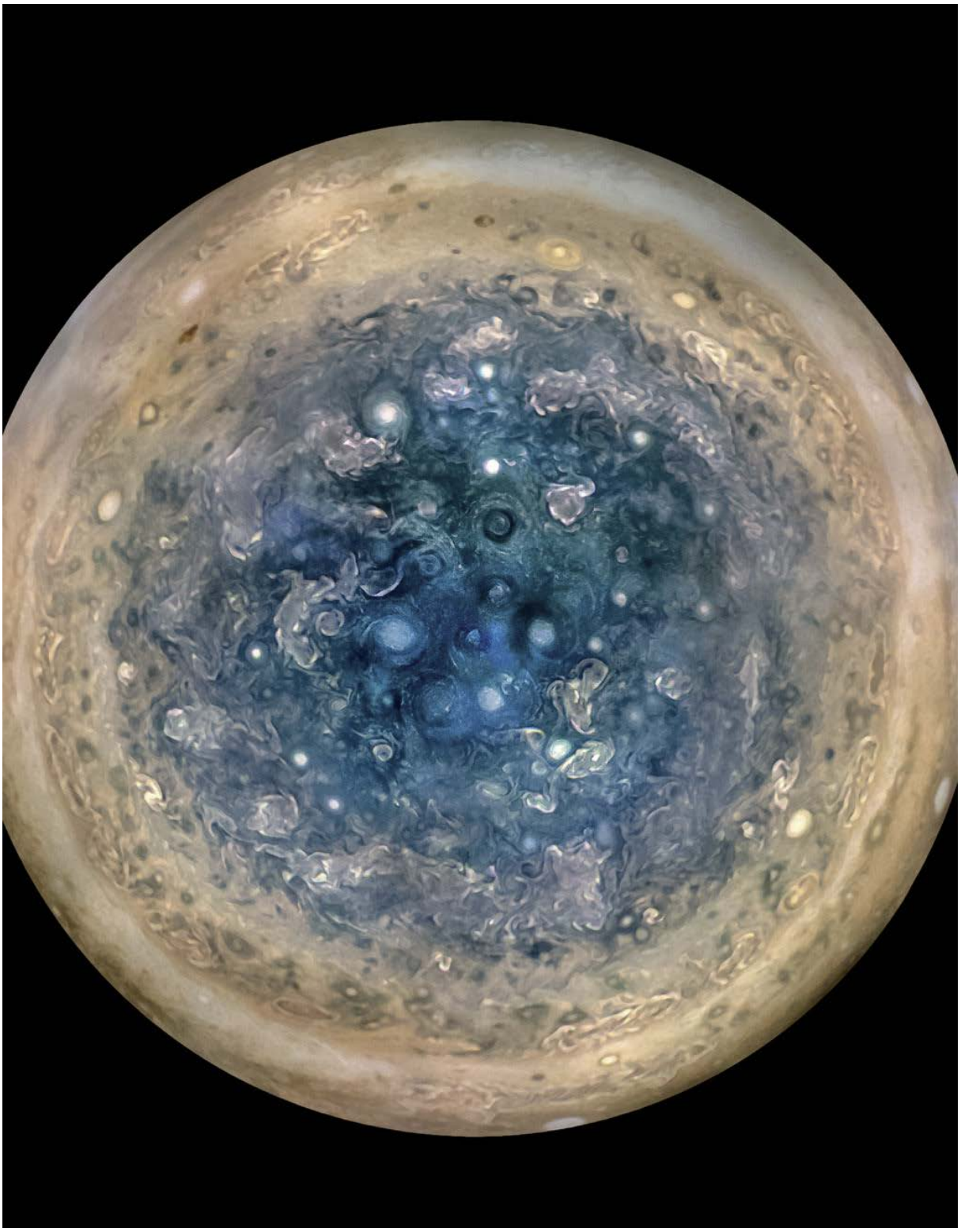

Credits: NASA/JPL-Caltech/SwRI/MSSS/Betsy Asher Hall/Gervasio Robles

**Figure 7-3: Jupiter's South Pole from an altitude of 32,000 miles (51,000 km) [36].**

Juno also is designed to study the polar magnetosphere and the origin of Jupiter's powerful auroras -- its northern and southern lights. On Earth, these auroral emissions are caused by particles that pick up energy, slamming into atmospheric molecules. Juno's initial observations indicate that the process seems to work differently at Jupiter than at Earth[19].As NASA's Juno spacecraft approached Jupiter on Aug. 27, 2016, the Jovian Infrared Auroral Mapper (JIRAM) instrument captured the planet's glow in infrared light. Figure 7-4 is derived from a video [39] composed of 580 images collected over a period of about 9 hours while Jupiter completed nearly a full rotation on its axis. An image accompanying a New York Times article about the first results [40] provides a different rendition of the JIRAM data.

The video shows the two parts composing the JIRAM imager: the lower one, in a red color scale, is used for mapping the planet's thermal emission at wavelengths around 4.8 microns; the upper one, in a blue color scale, is used to map the auroras at wavelengths around 3.45 microns.

In this case, the exposure time of the imager was optimized to observe the planet's thermal emission. However, it is possible to see a faint aurora and Jupiter's moon Io approaching the planet. The Great Red Spot is also visible just south of the planet's equator.

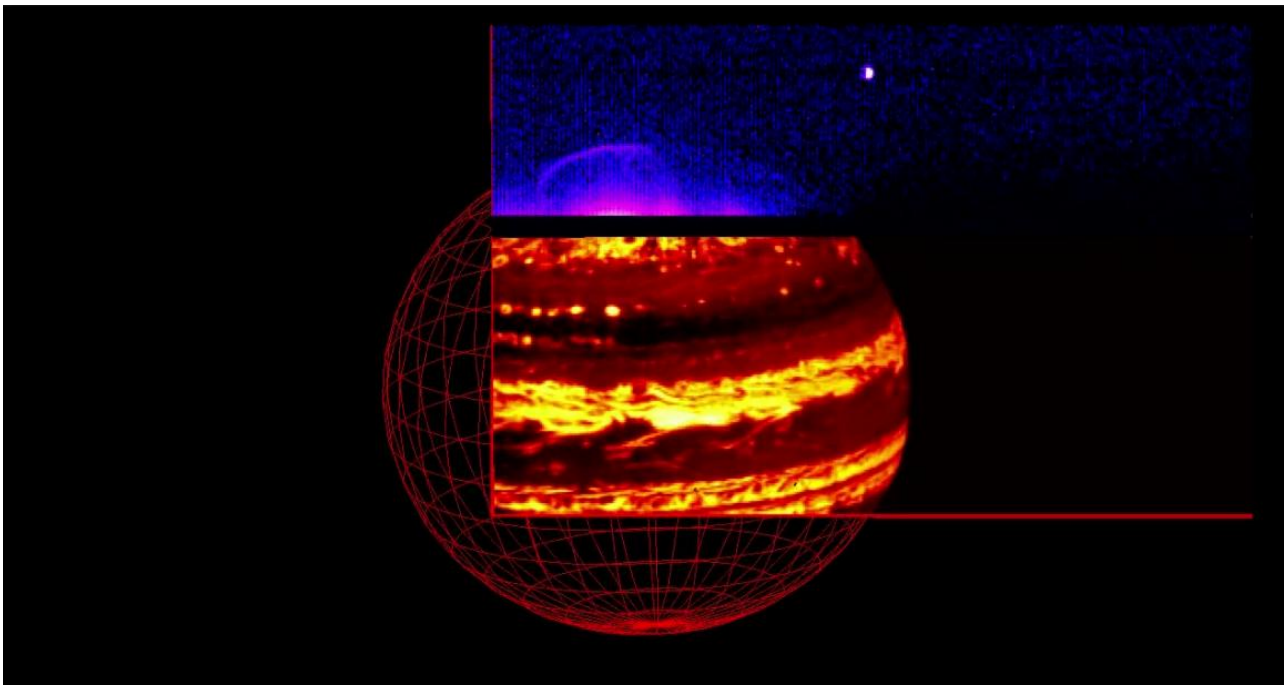

Credit: NASA/JPL-Caltech/SwRI/ASI/INAF/JIRAM

**Figure 7-4: Infrared images and spectra of Jupiter's thermal emission from the Jovian Infrared Auroral Mapper [39]**.

[19] Jupiter's magnetic field is much stronger than Earth's, producing the large radiation belt. Prior to the Juno observations, the Jovian aurora thought to be primarily powered by solar wind as on Earth. However, Jupiter's moons, especially Io, are also powerful sources of auroras. These arise from electric currents along field lines ("field aligned currents"), generated by a dynamo mechanism due to relative motion between the rotating planet and the moving moon. Io, which has active volcanism and an ionosphere, is a particularly strong source, and its currents also generate radio emissions, studied since 1955 [38].

The Figure 7-5 image below [41], titled “Approaching Jupiter” and created by citizen scientist Gabriel Fiset, uses enhanced colors to highlight the contrasting bands in Jupiter's atmosphere.

Oval storms dot the cloudscape. Approaching the South Pole, the organized turbulence of Jupiter’s belts and zones transitions into clusters of unorganized filamentary structures, streams of air that resemble giant tangled strings. The image was taken on Dec. 11, 2016 at 9:44 a.m. PST (12:44 p.m. EST), from an altitude of about 32,400 miles (52,200 kilometers) above the planet’s beautiful cloud tops.

Credits: NASA/JPL-Caltech/SwRI/MSSS/Gabriel Fiset

**Figure 7-5: “Approaching Jupiter” by "citizen scientist" from JunoCam data [41].**

**Blank**

# 8 Lessons Learned

Lessons learned are within the NASA (and JPL) knowledge management system. The Juno team benefited from lessons learned on previous NASA/Caltech Jet Propulsion Laboratory (JPL) missions, and they kept a list of lessons that were learned on Juno [42].

The Juno project has benefited from lessons learned on previous JPL missions, perhaps most notably Galileo because it was the only previous mission to orbit Jupiter, and Mars Reconnaissance Orbiter (MRO) because it was one of the more recent JPL spacecraft built by the Juno system subcontractor. The Galileo mission generated much useful data on radiation and challenges posed by the Jupiter environment. Galileo survived over 20 anomalies over the course of the mission caused by Jupiter's extreme radiation environment, and Juno's planned Jupiter orbit (Figure 6-3) would expose it over the course of the mission to a radiation dose of more than 20 million rads. The Juno flight system features avionics similar to MRO's, and they benefited from lessons that were learned by the MRO project when it overcame a variety of in-flight avionics issues.

Juno benefited from these relevant lessons learned [43] [44]; the following are representative.

**8501** Verify That Test Equipment Cannot be Interrupted by Extraneous Computer Processes

Abstract: Thermal-vacuum testing of a Ka-side frequency multiplier for the Juno Small Deep Space Transponder (SDST) was interrupted in mid-performance when a desktop computer running the test unexpectedly sought to download an update of an installed software package. While the flight hardware and test equipment were not harmed, 8 hours of test data were lost.

**16303** Juno/MSL SDRAM Vulnerability

Abstract: Both the Juno and Mars Science Laboratory (MSL) spacecraft experienced anomalies in memory devices due to single event functional interrupts (SEFIs) occurring during the cruise phase of the missions. A known problem potentially affecting other spaceflight projects, the parts' vulnerability to radiation effects was not adequately communicated. Projects need to be more penetrating in review of known part failure mechanisms.

**6169** Shaker Self-Check Unexpectedly Exceeded the Dynamic Test Limit

Abstract: Shaker system control software generates a self-check immediately prior to a test at a signal level that is normally considered to be of insignificant strength compared to test levels. During a dynamic test of the Juno high gain antenna, however, the self-check excited a response that exceeded the level from the subsequent test. In planning for dynamic testing, ensure that the self-check signal will be set lower than any test level.

**18901** Conductive Polyimide Tape and Nickel Alloy Foils Can Become Magnetized

Abstract: System testing of the Juno spacecraft's sensitive magnetometer detected an anomalous magnetic field emanating from the spacecraft. Upon investigation, the magnetic contamination was traced to tiny nickel-plated balls within the adhesive on conductive black polyimide tape. Nickel itself is normally not magnetic, and the tape was used without considering the potential for a nickel alloy to become magnetized.

**1772** Know How Your Software Measurement Data Will Be Used

Abstract: When software measurement data used to support cost estimates is provided to the NASA Independent Program Assessment Office (IPAO) by a project without an understanding of

how NASA will apply the data, discrepancies may produce erroneous cost estimates that delay project approval. The IPAO cost-estimate for the Juno ground data system did not reflect that the cost of re-integrating/re-testing inherited code had already been included in the budget for the overall JPL Multi-Mission Ground System Services (MGSS) infrastructure.

**5756** Beware of Smocks with Metal Sleeve Fasteners

Abstract: During functional test of a Juno Energetic Particle Detector (JEDI) instrument circuit board, the metal snap on the sleeve of an ESD smock caused a short circuit and damaged the flight equipment. Procure only ESD smocks with elastic sleeve closures. Remain alert to items of personal apparel that could present a safety hazard to personnel or critical equipment.

**8302** Reducing the Error Rate in Command Files Uplinked to a Spacecraft (proactive to Juno)

Abstract: A JPL Operations Working Group convened in November 2010 to review in-flight spacecraft command file errors and identify measures to mitigate the impact of such errors on mission operations. The group briefed projects entering Phase E (including Juno), or post-launch periods of increased operational tempo, to consider proactive steps to minimize command file errors.

In addition, the Juno project team defined some key project management lessons learned.

- Benefits and risks of an extended definition and planning phase. A 30-month Phase B (Preliminary Design Phase) gave the team time to complete design trades and mature requirements, but it also induced a lack of urgency that contributed to some late deliveries at the subsystem level. An article [45] in NASA's *ASK* magazine discusses how the team took good advantage of the extended Phase B.
- Early and constant focus on payload accommodation. With nine instruments on Juno, payload accommodation on the spacecraft was critical. The payload and spacecraft teams used "roadshows," multiple models, technical interchange meetings, workshops, and telecons to define and mature interfaces and build relationships that were essential to resolving integration and test problems later in the project life cycle.
- Creation of cross-project working groups. Formation of cross-project working groups brought unified focus to environment definition, design requirements, design implementation, and integration and test both horizontally with the science, spacecraft, and payload teams and vertically with the system, subsystem, box, and component teams in order to complete development within schedule.
- Maximum use of contractors' existing documentation and processes. To improve efficiency and teaming, the project made maximum use of contractor and instrument providers' existing documentation and processes that were reviewed against project requirements and implementation approaches to identify and resolve gaps.
- Use of resident engineers at contractor facility. Juno located several key JPL personnel at the contractor facility to work closely with spacecraft development and integration/test teams. They maintained an effective partnership with the contractor team and provided the needed level of insight into critical activities.

# 9 References


1. Stuart K. Stephens, *Juno Project Mission Plan*, Revision B, JPL D-35556 (JPL internal document), Jet Propulsion Laboratory, California Institute of Technology, Pasadena, CA, March 29, 2011.

2. David Hansen, *Juno Project Telecommunications Design Control Document*, Final Release, JPL D-35514 (JPL internal document), Jet Propulsion Laboratory, California Institute of Technology, Pasadena, CA, March 15, 2009.

3. Juno *Ka-band Translator (KaTS) User Manual*, BC-JUNO-00053, Thales Alenia Space, Rome, Italy, March 25, 2010.

4. *DSN Telecommunications Link Design Handbook*, DSN No. 810-005, Rev. E, Jet Propulsion Laboratory, California Institute of Technology, Pasadena, California, regularly updated. https://deepspace.jpl.nasa.gov/dsndocs/810-005/ (accessed June 2, 2017)

5. John Bordi, Ray Frauenholz, Cliff Helfrich, and Theresa Kowalkowski, *Juno Project Navigation Plan*, Rev. A (JPL Internal Document), Jet Propulsion Laboratory, California Institute of Technology, Pasadena, CA, March 10, 2011.

6. Jim Taylor, Dawn Telecommunications, Design and Performance Summary Series, Article 13, DESCANSO, Jet Propulsion Laboratory, California Institute of Technology, Pasadena, California, August 2009. http://descanso.jpl.nasa.gov/DPSummary/090924dawn-FinalCorrex--update5G.pdf; (accessed Aug. 13, 2012)

7. Deep Space Network website, Jet Propulsion Laboratory, California Institute of Technology, Pasadena, CA. http://deepspace.jpl.nasa.gov/dsn/ (accessed August 13, 2012)

8. Padma Varanasi, *DSN-Juno Mission Operations Interface Control Document*, JPL D-51062 (JPL internal document), Jet Propulsion Laboratory, California Institute of Technology, Pasadena, CA, April 2011.

9. Wolfgang Heil, *Juno Launch and Early Orbit Phase (LEOP) Implementing Agreement*, European Space Operations Center, Robert-Bosch-Strasse 5, 64293 Darmstadt, Germany, Dec. 18, 2010.

10. Gary W. Glass, *Small Deep Space Transponder (SDST) Functional Specification and Interface Control Document*, JPL D-36672 (JPL Internal Document), Jet Propulsion Laboratory, California Institute of Technology, Pasadena, CA, March 15, 2007.

11. Juno Spacecraft Information and Juno Mission and Trajectory Design, websites, Jet Propulsion Laboratory, California Institute of Technology, Pasadena, CA, http://spaceflight101.com/juno/spacecraft-information/ (accessed July 13, 2017) http://spaceflight101.com/juno/juno-mission-trajectory-design/ (accessed July 13, 2017

12. *Digital Time Division Command/Response Multiplex Data Bus*, MIL-STD-1553, U.S. Department of Defense, original release September 1978, continual updates.

13. L. Simone, F. Barletta, O. Cocciolillo, S. Cocchi, F. Diaferia, D. Gelfusa, R. Giordani, M. Maffei, M. Micaloni, R. Viola, P. Panfili, and M. C. Comparini, *A Ka-Band Translator for Radio Science Applications*, Thales Alenia Space–Italy, Rome, Italy, 2008.

14. Shanti Ancheta, Chris Leeds, Peter MacMillin, et.al, *Juno Telecom Trending Review*, (internal project document), Jet Propulsion Laboratory, California Institute of Technology, Pasadena, CA, Feb. 2017.

15. Jason Dates, *Juno Fault Protection Design Document*, Juno-ED-08-0100, Lockheed Martin Sensing & Exploration Systems, P.O. Box 179, Denver, CO, Feb. 19, 2009.

16. D. C. Agle (JPL), Dwayne Brown (NASA HQ), "Juno Spacecraft in Safe Mode for Latest Jupiter Flyby Scientists Intrigued by Data from First Flyby," 2016-271, web page, Jet Propulsion Laboratory, California Institute of Technology, Pasadena, CA, Oct. 19, 2017. https://www.jpl.nasa.gov/news/news.php?feature=6653 (accessed April 6, 2017)

17. D. C. Agle (JPL), Dwayne Brown, and Laurie Cantillo (NASA HQ), "NASA's Juno Mission Exits Safe Mode, Performs Trim Maneuver, 2016-280," web page, Jet Propulsion Laboratory, California Institute of Technology, Pasadena, CA, Oct. 25, 2016. https://www.jpl.nasa.gov/news/news.php?feature=6661 (accessed June 2, 2017)

18. Jeff Foust, "NASA investigating possible link between Juno and Intelsat thruster problems," *space.com*, Nov. 3, 2016. http://spacenews.com/nasa-investigating-possible-link-between-juno-and-intelsat-thruster-problems/ (accessed April 10, 2017)

19. D. C. Agle (JPL), Dwayne Brown and Laurie Cantillo (NASA HQ), "NASA's Juno to Remain in Current Orbit at Jupiter, 2017-043, web page, Jet Propulsion Laboratory, California Institute of Technology, Pasadena, CA, February 17, 2017. https://www.jpl.nasa.gov/news/news.php?feature=6752 (accessed June 2, 2017)

20. "Magnetosphere, Exploring Jupiter's Magnetic Field," web page, NASA Goddard Spaceflight Center, https://www.missionjuno.swri.edu/media-gallery/magnetosphere (accessed July 19, 2017)

21. Anna Scott, "Juno just flew past Jupiter for the fifth time. What have we learned from the mission so far?" The Planetary Society website, March 27, 2017. http://www.planetary.org/blogs/guest-blogs/2017/20170327-juno-early-science.html (accessed April 10, 2017)

22. D. C. Agle (JPL), Dwayne Brown, and Laurie Cantillo (NASA HQ), Nancy Neal Jones (Goddard Spaceflight Center, "A Whole New Jupiter: First Science Results from NASA's Juno Mission," 2017-153, web page, Jet Propulsion Laboratory, California Institute of Technology, Pasadena, CA, May 25, 2017. https://www.jpl.nasa.gov/news/news.php?feature=6856 (accessed June 1, 2017)

23. D. C. Agle (JPL) and Steve Cole (NASA HQ), "NASA's Juno Gives Starship-Like View of Flyby," 2013-360, web page, Jet Propulsion Laboratory, California Institute of Technology, Pasadena, CA, Dec. 9, 2013. https://www.nasa.gov/jpl/juno/juno-earth-flyby-20131210.html (accessed June 2, 2017)

24. "Earth and Moon Seen by Passing Juno Spacecraft, Music by Vangelis," Jet Propulsion Laboratory, California Institute of Technology, Pasadena, CA, Dec. 10, 2013. http://www.youtube.com/watch?v=_CzBlSXgzqI&feature=youtu.be (accessed July 27, 2017)

25. D. C. Agle (JPL), Gary Napier (Lockheed Martin Space Systems, Denver), Deb Schmid (Southwest Research Institute, San Antonio, TX), "NASA's Juno Spacecraft Burns for

Jupiter," Jet Propulsion Laboratory, California Institute of Technology, Pasadena, CA, Feb. 3, 2016. https://www.jpl.nasa.gov/news/news.php?feature=4889 (accessed July 27, 2017)

26. D. C. Agle (JPL), Dwayne Brown, and Laurie Cantillo (NASA HQ), "NASA's Juno Spacecraft Enters Jupiter's Magnetic Field," web page 2016-168, Jet Propulsion Laboratory, California Institute of Technology, Pasadena, CA, May 27, 2016. https://www.jpl.nasa.gov/news/news.php?feature=6550 (accessed July 27, 2017)

27. D. C. Agle (JPL) and Dwayne Brown (NASA HQ), "NASA's Juno Spacecraft in Orbit Around Mighty Jupiter," 2016-176, web page, Jet Propulsion Laboratory, California Institute of Technology, Pasadena, CA, July 4, 2016. https://www.jpl.nasa.gov/news/news.php?feature=6558, (accessed April 6, 2017)

28. Dwayne Brown, Laurie Cantillo (NASA HQ), and D. C. Agle (JPL), "Team Begins Powering up Science Instruments, 2016-179, web page, Jet Propulsion Laboratory, California Institute of Technology, Pasadena, CA, July 7, 2016. https://www.jpl.nasa.gov/news/news.php?feature=6563 (accessed April 6, 2017)

29. Dwayne Brown and Laurie Cantillo (NASA HQ), D.C. Agle (JPL), "NASA's Juno Spacecraft Sends First In-orbit View," 2016-185, web page, Jet Propulsion Laboratory, California Institute of Technology, Pasadena, CA, July 12, 2016. https://www.jpl.nasa.gov/news/news.php?feature=6568 (accessed April 6, 2017)

30. D. C. Agle (JPL) and Dwayne Brown (NASA HQ), "NASA Juno Mission Completes Latest Jupiter Flyby, 2016-313, web page, Jet Propulsion Laboratory, California Institute of Technology, Pasadena, CA, Dec. 9, 2016, updated Dec. 12, 2017. https://www.jpl.nasa.gov/news/news.php?feature=6695 (accessed July 27, 2017)

31. D. C. Agle (JPL) and Dwayne Brown (NASA HQ), "NASA's Juno Spacecraft Completes Fifth Jupiter Flyby," 2017-086, web page, Jet Propulsion Laboratory, California Institute of Technology, Pasadena, CA, updated March 27, 2017, https://www.jpl.nasa.gov/news/news.php?feature=6792 (accessed April 10, 2017)

32. William Harwood, "Jupiter images thrill, inspire public to participate", CBS News, July 14, 2017, http://www.cbsnews.com/news/jupiter-juno-images-thrill-inspire-public-to-participate/ (accessed August 3, 2017)

33. "Junocam", public interaction home page, Southwest Research Institute, San Antonio, TX, https://www.missionjuno.swri.edu/junocam (accessed July 27, 2017)

34. "Jovian Cloud Tops", web page, Jet Propulsion Laboratory, California Institute of Technology, Pasadena, CA, May 18, 2017. https://www.jpl.nasa.gov/spaceimages/details.php?id=PIA21391 (accessed July 27, 2017)

35. Leigh Fletcher, "Juno's Science – what do we hope to learn," in *Leicester to Jupiter: The Juno Mission*, website, June 20, 2016, http://staffblogs.le.ac.uk/leicester-to-jupiter/2016/06/20/junos-science-what-do-we-hope-to-learn/ (accessed April 10, 2017)

36. "PIA21641: Southern Storms," *Photojournal* (website), Jet Propulsion Laboratory, California Institute of Technology, Pasadena, CA, May 25, 2017. https://photojournal.jpl.nasa.gov/catalog/PIA21641 (accessed July 27, 2017)

37. S. J. Bolton, A. Adriani, V. Adumitroaie, M. Allison, S. Atreya, J. Bloxham, S. Brown, J. E. P. Connerney, et al., "Jupiter's interior and deep atmosphere: The initial pole-to-pole passes with the Juno spacecraft passes with the Juno spacecraft," *Science*, vol. 356, May 26, 2017. http://www.skyandtelescope.com/astronomy-news/juno-swoops-past-jupiters-south-pole/ (accessed May 17, 2017)

38. "Aurora," *Plasma-Universe.com*, https://www.plasma-universe.com/Aurora (accessed July 27, 2017)

39. "PIA21036: Juno Captures Jupiter's Glow in Infrared Light," *Photojournal* (website), Jet Propulsion Laboratory, California Institute of Technology, Pasadena, CA, Sept. 9, 2016. https://photojournal.jpl.nasa.gov/catalog/PIA21036 (accessed June 5, 2017)

40. Kenneth Chang, "NASA's Jupiter Mission Reveals the 'Brand-New and Unexpected'", *The New York Times*, May 25, 2017. https://www.nytimes.com/2017/05/25/science/nasa-juno-spacecraft-jupiter-storms.html (accessed June 1, 2017)

41. "Approaching Jupiter," NASA web page, May 5, 2017. https://www.nasa.gov/image-feature/jpl/pia21390/approaching-jupiter (accessed July 27, 2017)

42. Lesson Learned, "100+ Lessons Learned for Project Managers", NASA Public Lessons Learned System, https://llis.nasa.gov/lesson/1956 , lesson submitted by Jet Propulsion Laboratory, Sept. 30, 2008, site curator Michael Bell (accessed July 27, 2017)

43. *NASA Public Lessons Learned System*, website, curator Michael Bell. https://llis.nasa.gov/ (accessed June 2, 2017)

44. "Juno to Jupiter: 'A Lot of Lessons Learned," website, NASA Office of the Chief Knowledge Officer, Sept. 27, 201. https://km.nasa.gov/juno-to-jupiter-a-lot-of-lessons-learned/ (accessed June 1, 2017)

45. Rick Grammier, "Juno: Making the Most of More Time," NASA Academy of Program/Project & Engineering Leadership (APPEL) *ASK Magazine*, March 1, 2008. https://appel.nasa.gov/2008/03/01/juno-making-the-most-of-more-time/ (accessed June 1, 2017)

46. "DSN Scheduling Template," from Table 15-2, Mission Plan (JPL internal document, Juno project spreadsheet), Jet Propulsion Laboratory, California Institute of Technology, Pasadena, CA, updated June 29, 2017.

# 10 Abbreviations and Acronyms

| | |
|---|---|
| 1553 | (MIL-STD-1553) a standard for digital communications published by the United States Department of Defense |
| | |
| AA | aluminum alloy (e.g. AA6082) |
| AAC | analog acquisition card |
| A/D, ADC | analog-to-digital (converter) |
| Adv | Adverse (tolerance) |
| AGC | automatic gain control |
| AJ | Jupiter apojove (analogous to Earth apogee) |
| AJ0, AJ1, etc. | apojove number (AJ0 and AJ1 were 07/31/2016 and 09/23/2016) |
| ALGA | aft low-gain antenna |
| AOS | acquisition of signal |
| AP | activity period |
| APO | apojove OTM |
| ASC | advanced stellar compass |
| ASI | Italian Space Agency |
| AT | attenuator |
| AU | astronomical unit (149,597,871 meters (92,955,807 miles)) |
| Aux Osc | auxiliary crystal oscillator |
| | |
| BER | bit error rate |
| BLF | best lock frequency |
| BPF | bandpass filter |
| bps | bits per second |
| BPO | backup APO |
| BPSK | binary phase shift keying |
| BRM | Baseline Reference Mission |
| BTM | backup OTM |
| BW | bandwidth |
| | |
| Cam | camera (e.g. JunoCam) |
| CAN | Canberra Deep Space Communications Complex, CDSCC |
| cap | capability |
| CD | cumulative distribution (also called “percent weather”) |
| C&DH | Command and Data Handling Subsystem |
| clk | clock angle |

| | |
|---|---|
| CMD | command |
| CNR | carrier-power-to-noise ratio |
| co-pol | co-polarization, co-polarized |
| CP | circular polarization |
| CW | continuous wave |
| cx-pol | cross polarization, cross polarized |
| | |
| d | day |
| D/A, DAC | digital to analog (converter) |
| dB | decibel |
| dBc | decibels below carrier |
| dBic, dBiC | decibels relative to an isotropic circularly polarized antenna |
| dBiL | decibels relative to a isotropic linearly polarized antenna |
| dBm | decibel referenced to milliwatts |
| DESCANSO | Deep Space Communications and Navigation Systems Center of Excellence |
| DCT | design control table |
| deg | degree |
| DLLE | Downlink Loss Executive |
| DN | data number, digital number |
| DOFF | degrees off boresight |
| DOR | differential one-way ranging |
| DOY | day of year |
| DPM | digital processing module |
| DSM | Deep space maneuver |
| DSN | Deep Space Network |
| DSS | Deep Space Station |
| DSS-25 | Deep Space Station 25 (34-meter beam waveguide antenna at Goldstone, California) |
| DSS-26 | Deep Space Station 26 (34-meter beam waveguide antenna at Goldstone, California) |
| DSS-34 | Deep Space Station 34 (34-meter beam waveguide antenna at Canberra, Australia |
| DSS-63 | Deep Space Station 63 (70-meter antenna at Madrid, Spain) |
| DTCI | data command telemetry interface card |
| DV | delta-V, delta-velocity, change in velocity |
| DX | diplexer |
| | |
| $E_b/N_o$ | Energy per bit to noise spectral density ratio |

| | |
|---|---|
| EDA | entry, descent, and landing (EDL) data analysis |
| EDL | entry, descent, and landing |
| EDT | Eastern Daylight Time |
| EFB | Earth Flyby |
| EIDP | End Item Data Package |
| EIRP | equivalent isotropically radiated power |
| EM | Engineering Model |
| EOL | end of life |
| EPC | electronic power converter |
| ESA | European Space Agency |
| ESD | electrostatic discharge |
| ESTRACK | European Space Tracking (network) |
| | |
| Fav | favorable (tolerance) |
| F1 | fundamental frequency from which uplink and downlink frequencies are derived |
| $F_c$ | clock frequency |
| FEC | Front-End Controller |
| FER | frame error rate |
| FGM | Fluxgate Magnetometer |
| FLGA | forward low-gain antenna |
| FM | Flight Model |
| FOV | field of view |
| FPGA | field-programmable gate array |
| FSW | flight software |
| | |
| GDS | Goldstone Deep Space Communications Complex, GDSCC |
| GHz | gigahertz |
| GIF | guidance navigation and control interface |
| GOLD | Goldstone Deep Space Communications Complex, GDSCC |
| GRAV | Gravity Science |
| | |
| h | hour |
| HGA | high-gain antenna |
| hh:mm:ss | hour:minute:second |
| HPA | High power amplifier |
| HQ | headquarters |

| | |
|---|---|
| hr | hour |
| HY | hybrid |
| | |
| ICD | Interface Control Document |
| ICO | initial checkout |
| IF | intermediate frequency |
| IFMS | Intermediate Frequency Modem System |
| IFOC | intermediate frequency-on-chip |
| IPAO | Independent Program Assessment Office |
| | |
| JADE | Jovian Auroral Distributions Experiment |
| JEDI | Jupiter Energetic-particle Detector Instrument |
| JIRAM | Jovian Infrared Auroral Mapper |
| JOI | Jupiter Orbit Insertion |
| JPE | Jupiter–Probe–Earth (angle) |
| JPL | Jet Propulsion Laboratory |
| | |
| Ka-band | 26.5–40 GHz |
| KaTS | Ka-Band Translator |
| kbps | kilobits per second |
| kHz | kilohertz |
| km | kilometer |
| km/s | kilometers per second |
| | |
| L | launch |
| $\lambda_m$ | inclination relative to magnetic equator |
| LAN | local area network |
| LEOP | Launch and Early Orbit Phase |
| LGA | low-gain antenna |
| LHCP | left-hand circular polarization |
| LLIS | Lessons-Learned Information System |
| LNA | low-noise amplifier |
| LOS | loss of signal |
| LPF | low-pass filter |
| LT | local time (at longitude of Jupiter below the Juno spacecraft) |
| LVDS | low-voltage differential signaling |
| | |
| MAD | Madrid Deep Space Communications Complex, MDSCC |

| | |
|---|---|
| MAG | Complete Magnetometer (flux gate magnetometers and advanced stellar compass) |
| M&C | Monitor and control |
| MCM | Monitoring and Control Module (of ESTRACK) |
| MCCI | Moore Computer Consultants, Inc. (as MCCI, maker of Juno diplexers) |
| MDSCC | Madrid Deep Space Communications Complex, MAD |
| MECO | main engine cutoff |
| MER | Mars Exploration Rover |
| MES | main engine start |
| MGA | medium-gain antenna |
| MGSS | Multi-Mission Ground System Services |
| MHz | megahertz |
| MRO | Mars Reconnaissance Orbiter |
| m/s | meters per second |
| MSL | Mars Science Laboratory |
| Msps | megasymbols per second |
| MSSS | Malin Space Science Systems |
| MW | Microwave |
| MWR | Microwave Radiometer |
| | |
| NaN | not a number (may appear in some link budgets) |
| NASA | National Aeronautics and Space Administration |
| NAV | Navigation |
| NCO | numerically controlled oscillator |
| NOP | Network Operations Plan |
| NRZ-L | non return to zero – level |
| ns | nanosecond |
| | |
| OCXO | oven controlled quartz oscillator |
| OICD | Operations Interface Control Document |
| OTM | Orbit Trim Maneuver |
| OWLT | one-way light time |
| | |
| PCM | pulse code modulation |
| $P_c/N_o$ | uplink carrier power to noise spectral density |
| PDT | Pacific Daylight Time |
| $P_d/N_o$ | data power to noise spectral density |
| $P_t/N_o$ | total power to noise spectral density |

| | |
|---|---|
| PFD | phase frequency detector |
| PI | Principal Investigator (Scott Bolton of SwRI) |
| PIA | Photojournal image access |
| PJ | Jupiter perijove (analogous to Earth perigee) |
| PJ0, PJ3, … | J0 is the perijove at JOI, P3 is the perijove in Orbit 3, … |
| PLL | phase-locked loop |
| PM | phase modulation |
| Pnt | pointing (of spacecraft antenna in DCT, also called “doff”) |
| POI | point of interest |
| POR | power-on reset |
| PRM | period reduction maneuver |
| ps | picosecond |
| PSK | phase shift keying |
| $P_r/N_o$ | ranging power to noise spectral density ratio |
| $P_t/N_o$ | total power to noise spectral density ratio |
| pwr | power |
| | |
| rad | radiation absorbed dose |
| RCS | Reaction Control System thrusters |
| REM | Reaction engine module |
| RF | radio frequency |
| RFIS | Radio Frequency Instrument Subsystem |
| RFS | Radio Frequency Subsystem |
| RHCP | right-hand circular polarization |
| $R_j$ | radius of Jupiter |
| rpm | revolutions per minute |
| RS | radio science |
| RS | Reed–Solomon |
| RX | receive |
| | |
| S | Separation |
| SA | solar array |
| SA R&R | solar array restraint and release (mechanisms) |
| S/C | Spacecraft |
| SDRAM | Synchronous dynamic random-access memory |
| SDST | Small Deep Space Transponder |
| SEFI | single event functional interrupt |
| SEP | Sun–Earth–probe angle |

| | |
|---|---|
| S/N | serial number |
| SNR | signal-to-noise ratio |
| SNT | system noise temperature |
| SOHO | SOlar Heliospheric Observatory |
| SPD | sampling phase detector |
| SPE | Sun–probe–Earth angle |
| SPICE | Spacecraft Planet Instrument C-matrix (attitude) Events |
| SPK | SPICE Kernel |
| SPS | Service Preparation System (of the DSN) |
| Sps | symbols per second |
| SRU | Stellar Reference Unit |
| SSPA | solid state power amplifier |
| STM | statistical OTM |
| SwRI | Southwest Research Institute, San Antonio, TX |
| | |
| $T_1$ | integration time for the clock component |
| $T_2$ | integration time of each component |
| TAS-I | Thales Alenia Space-Italy |
| TC | Telecommand |
| TCM | trajectory correction maneuver |
| TDI | time delayed integration |
| TDL | Telecom Development Laboratory |
| Telecom | telecommunications |
| Telecom | Telecommunications (Subsystem) |
| TFP | Telecom Forecaster Predictor |
| TID | total ionizing dose |
| TIP | target interface point |
| T-LGA | toroidal low-gain antenna |
| TLM | telemetry |
| TMTCS | Telemetry and Telecommand System |
| Tol | tolerance (in DCT parameter) |
| TWTA | traveling wave tube amplifier |
| TX | transmit |
| | |
| ULDL | uplink/downlink card |
| ULLE | Uplink Loss Executive |
| USS (Enterprise) | United Star Ship or United Space Ship |
| UTC | Universal Time Coordinated (Greenwich Mean Time) |

| | |
|---|---|
| UV | ultraviolet |
| UVS | Ultraviolet Spectrograph |
| μC | micro controller |
| | |
| Var | Variance (in DCT quantity) |
| VCO | voltage controlled oscillator |
| VSWR | voltage standing wave ratio |
| | |
| W | watt |
| Waves | an instrument to measure radio and plasma waves |
| WG | waveguide |
| WR-28, WR-34 | waveguide sizes used for Juno Ka-band |
| WR-112 | waveguide size used for Juno X-band |
| WTS | waveguide transfer switch |
| | |
| X-band | 7.0 to 11.2 gigahertz |
| xpond | transponder |
| | |
| Z | load |